

UNCLASSIFIED

AD NUMBER

AD468420

LIMITATION CHANGES

TO:

Approved for public release; distribution is unlimited.

FROM:

Distribution authorized to U.S. Gov't. agencies and their contractors;
Administrative/Operational Use; APR 1965. Other requests shall be referred to Air Force Materials Laboratory, Wright-Patterson AFB OH 45433.

AUTHORITY

WL/AFSC ltr, 5 Feb 1991

THIS PAGE IS UNCLASSIFIED

UNCLASSIFIED



AD NUMBER

468 420

CLASSIFICATION CHANGES

TO

FROM

AUTHORITY

AL/AFSC 1tr

5 Feb 91

THIS PAGE IS UNCLASSIFIED

✓ 28, 324
AD-468420

AFML-TR-65-4

MATERIALS CENTRAL TECHNICAL LIB
OFFICIAL FILE COPY

ABLATIVE PLASTICS AND ELASTOMERS IN CHEMICAL PROPULSION ENVIRONMENTS

D. L. SCHMIDT

TECHNICAL REPORT AFML-TR-65-4

APRIL 1965

DDC
REFILED
AUG 23 1965
DDC-IRA E

AIR FORCE MATERIALS LABORATORY
RESEARCH AND TECHNOLOGY DIVISION
AIR FORCE SYSTEMS COMMAND
WRIGHT-PATTERSON AIR FORCE BASE, OHIO

AFML-TR-65-4

**ABLATIVE PLASTICS AND ELASTOMERS
IN CHEMICAL PROPULSION ENVIRONMENTS**

D. L. SCHMIDT

FOREWORD

This technical survey report is being made available by the Plastics and Composites Branch, Nonmetallic Materials Division, AFML. It has been documented under Project No. 7340, "Nonmetallic and Composite Materials," Task 734001, "Thermally Protective Plastics and Composites." The work was administered under the direction of the Air Force Materials Laboratory, Research and Technology Division. This report was authored during off-duty hours by Mr. D. L. Schmidt, during the period from October through December 1964.


The use of illustrative and technical information from numerous sources is gratefully acknowledged. Photographic credits are as follows: Atlantic Research Corp., Figures 2 and 30; Marquardt Corp., Figures 3, 4, and 6; Prentice-Hall, Inc., Figure 5; AIAA, Figures 8, 32, and 35; Aerojet-General Corp., Figures 9, 11, and 17; United Technology Center, Figures 10 and 23; Naval Ordnance Laboratory, Figure 12; Bendix Corp., Figure 15; Thiokol Chemical Corp., Figures 16, 19, and 25; Hughes Aircraft Co., Figure 20; Hercules Powder Co., Figures 21 and 22; Conover-Mast Publications, Inc.,

Figure 9; Koppers Chemical, Inc., Figure 26; Raybestos-Manhattan, Inc., Figure 27; Rohr Corp., Figure 28; and, H.I. Thompson Fiber Glass Co., Figure 29.

The manuscript was released by the author in January 1965 for publication as an RTD technical report.

The mention of commercially available products should not be construed in any way as an endorsement by the Government. Comparative information has been given for the purpose of illustrating the influence of environmental parameters on various materials and their variables. It should be noted that many of the commercially available materials mentioned in this report were previously developed for purposes other than those considered herein. Hence, the empirical results should not reflect unduly upon their performance in other or less severe conditions.

This technical report has been reviewed and is approved.


H. S. SCHWARTZ, Chief
Plastics and Composites Branch
Nonmetallic Materials Division
Air Force Materials Laboratory

ABSTRACT *Over)*

Plastics and elastomers possess a number of unique properties, which offer a wide range of possibilities for alteration and variation. Among these properties is the ability to absorb, dissipate, and block a large amount of environmental heat with only a small amount of sacrificial loss. This process is known as ablation, and it may serve to thermally protect chemical propulsion systems.

Ablative plastics and elastomers have been used successfully in a variety of primary and secondary liquid propellant engines. Such uses have included thrust chambers, nozzles, extension skirts, external parts, and a host of other ever-increasing number of applications. The ablators have provided a minimum-weight design when the engine thrust levels were low to moderately high (up to 20,000 pounds), firing times were short to relatively long (up to 2,000 seconds), chamber pressures were low (several hundred psia or less), or when the engine involved throttling, restarting, multiple pulses, or low propellant flow rates. The attractiveness of ablators for cooling tends to decrease with a nonoptimum propellant injector, high gasdynamic shear forces, or extremely corrosive combustion products.

Ablative organics have scored even more impressive gains in the thermal protection of solid and hybrid propellant motors. Virtually the entire motor contains ablative polymers in one form or another, including the propellant case, head-end insulator, case liner, entrance cone, nozzle, exit cone, external insulator, propellant grain supports, igniter basket, and jet vanes, as well as the ground launch equipment which is immersed in the hot exhaust for several seconds.

The interaction of propellant combustion products with plastics and elastomers results in thermal, chemical, and mechanical degradation of surface material. Thermal effects are due to the temperature level of the energetic combustion process. They are generally discernible as pyrolysis, gasification, vaporization, sublimation, melting, and thermal stress failure. The chemical corrosive effects are a function of the chemical composition, reactant concentrations, and the temperature level of the exhaust species coming in contact with the ablating material surfaces. They usually result in increased surface vaporization or fluxing (lowered viscosity) of melted components. Mechanical effects involve gasdynamic shear, erosion, particle impact, and material spallation. The net effect is to physically remove material before maximum thermal absorption can be achieved. The ability of plastics and elastomers to accommodate these destructive effects of propulsion environments is well documented in the tabulated data presented herein.

For the future, resinous and elastomeric materials will continue to serve a major role in the thermal protection of chemical propulsion systems. Significant improvements in existing materials will be necessary, however, because of the ever constant advances in propulsion design and the changing composition of propellants. To achieve this goal, future research and development will be concentrated on improving the thermal efficiency, physical properties, age-life, reliability, space environmental resistance, and cost of such polymeric materials.

Abstract

A semitechnical review of ablation and ablative materials is given, in particular where these materials must perform in the hyperenvironment produced by the exhaust gases of chemical propellants, both solid and liquid. A description of the chemical exhaust gas hyperenvironment and its interaction with ablative materials is presented. ~~Specific~~ Information is presented for the performance of various ablative materials with exhaust gases produced from specific propellant combinations. Theoretical considerations are included, as are ^{ablative material} requirements for future propellants and propulsion systems.

TABLE OF CONTENTS

	PAGE
INTRODUCTION	1
THE HIGH TEMPERATURE PROBLEM	1
COOLING TECHNIQUES	2
THE ABLATION PROCESS	3
ABLATIVE PERFORMANCE	4
Theoretical Predictions	5
Rocket Motor Firings	5
Performance Indices	5
LIQUID PROPULSION	7
Primary and Secondary Engines	7
Propellants	8
Applicability of Ablation	10
Materials Performance	11
Oxy-Acetylene	11
Oxy-Hydrogen	13
Oxy-Kerosene	15
Oxy-Ethyl Alcohol	16
Oxy-Gasoline	17
Nitrogen Tetraoxide-Hydrazine	17
Nitrogen Tetraoxide-UDMH	19
Nitrogen Tetraoxide-Hydrazine-UDMH	19
Fluorine-Hydrogen	20
Fluorine-Hydrazine	21
Chlorine Trifluoride-Hydrazine	21
Oxygen Difluoride-Diborane	21

TABLE OF CONTENTS (Cont'd)

	PAGE
SOLID PROPELLANTS	22
History	22
The Propellants	23
The Internal Environment	26
Materials of Construction	27
Materials Performance	29
Elastomeric Insulation	29
Semi-Rigid Insulation	30
Rigid Ablators	30
Environmental Effects	31
Thermal Effects	31
Chemical Effects	31
Mechanical Effects	32
HYBRID PROPELLANTS	34
THE FUTURE	34
REFERENCES	38

LIST OF ILLUSTRATIONS

FIGURE	PAGE
1. Thermal Diffusivities of Various Fiber Reinforced Phenolic Composites	88
2. Cross-Sectional Schematic and Temperature Distribution in an Ablating Charring Polymer	89
3. Equilibrium Chemical Reactions of Silica and Carbon at Elevated Temperatures	90
4. Potential Heat Absorbing Capability of an Ablative Phenolic-Silica Composite	91
5. Schematic of a Liquid Propellant Engine System	92
6. Variation in Combustion Products From N_2O_4 - N_2H_4 -UDMH as a Function of Oxidizer: Fuel Ratios	93
7. Environment and Partial Schematic of Liquid Propellant Rocket Engine Nozzle	94
8. Applicability of Cooling Techniques for Minimum Weight Space Engines	95
9. Ablative Plastic Skirt on a Nozzle of a Liquid Propellant Engine	96
10. Ablative Plastic Thrust Chamber for a 4,000 Pound Thrust Liquid Propellant Engine	97
11. Ablative Plastic Thrust Chamber and Radiative Expansion Skirt for Apollo Lunar Service Module	98
12. Experimental Arrangement for Exposing Ablative Panels in Oxy-Acetylene Combustion Products	99
13. Cross-Sectional View of a Nozzle Specimen Before and After Exposure	100
14. Effect of Chamber Pressure on the Ablation Rate of Several Fabric Reinforced Phenolics	101
15. Ablative Specimens Being Exposed to Supersonic Oxy-Kerosene Exhaust	102
16. Ablative Plastic Thrust Chamber for N_2O_4 -UDMH Engine	103
17. Ablative Plastic Thrust Chamber Installed on a N_2O_4 - N_2H_4 -UDMH Micromotor	104
18. Charring Performance of Ablative Plastic (Phenolic-Silica Fiber) Thrust Chambers Using Various Liquid Propellants	105
19. Ablative Phenolic-Graphite Thrust Chamber After Exposure to OF_2 - B_2H_6 Exhaust	106

LIST OF ILLUSTRATIONS (Cont'd)

FIGURE	PAGE
20. Advanced Guided Air-To-Air Rocket Containing Plastic Wings and Fuselage	107
21. Plastic Case and Nozzles Comprise the Third Stage Motor of the Minuteman ICBM	108
22. Plastic Retro-Rocket for the Ranger Lunar Spacecraft	109
23. Five Segment, 120-inch Diameter, Megapound Thrust Solid Propellant Motor During Test Firing	110
24. Environmental Parameters of an Advanced Solid Propellant Motor	111
25. Schematic of a Solid Propellant Motor	112
26. Elastomeric Aft Bulkhead Insulator for a Multiple Nozzle Solid Propellant Motor	113
27. A Phenolic-Asbestos Fiber Insulative Backup for a Graphite Nozzle Throat	114
28. An Ablative Nozzle Throat of Phenolic-Graphite Tape for the 156-inch Diameter Solid Propellant Motor	115
29. Tape Wrapping An Ablative Nozzle Exit Cone with Phenolic-Silica	116
30. Eight Insulative Test Specimens After Exposure to a Solid Propellant Firing	117
31. Ablation of Reinforced Plastic Throats in a Solid Propellant Motor	118
32. The Ablation Rate of Phenolic Molding Materials as a Function of the Nozzle Exit Cone Position	119
33. Influence of Exhaust Stream Oxidants on the Ablation Rate of a Charring Ablative Plastic	120
34. Schematic of a Hybrid Rocket Motor	121

LIST OF TABLES

TABLE	PAGE
1. Polymeric Materials for Propulsion Environments	47
2. Advantages and Limitations of Ablative Plastics and Elastomers	48
3. Environmental Variables Which Influence Ablative Performance	49
4. Materials Properties and Characteristics Which Influence Ablative Performance	50
5. Post-Exposure Measurements on Ablated Materials	51
6. Theoretical Performance of Liquid Propellants	52
7. Elastomeric Polymers in an Oxy-Acetylene Flame	55
8. Butadiene-NBR Composites in an Oxy-Acetylene Flame	56
9. Elastomeric Composites in an Oxy-Acetylene Flame	57
10. Thermoplastic Polymers in an Oxy-Acetylene Flame	59
11. A Phenolic Polymer and Composites in an Oxy-Acetylene Flame	60
12. Ablative Phenolic Composites in Oxy-Hydrogen Exhaust	61
13. Ablative Plastic Cones in Oxy-Hydrogen Exhaust	63
14. Ablative Plastics in Oxy-Hydrogen Exhaust	64
15. Ablative Performance of Materials in Oxy-Kerosene Exhaust	67
16. Ablation of Reinforced Plastics in Supersonic Oxy-Ethyl Alcohol Exhaust	69
17. Ablative Plastics in Oxy-Gasoline Combustion Products	70
18. Ablative Performance of Plastic Nozzles in a N_2O_4 - N_2H_4 -UDMH Propellant Environment	71
19. Performance of Ablative Plastic Thrust Chambers in N_2O_4 - N_2H_4 - UDMH	72
20. Ablative Performance of Phenolic-Silica Thrust Chambers in N_2O_4 - N_2H_4 -UDMH Exhaust Products	74
21. Ablative Performance of Plastic Thrust Chambers in a Fluorine- Hydrazine Exhaust	75
22. Ablative Performance of Plastic Thrust Chambers in OF_2 - B_2H_6 - Propellant Exhaust	76

LIST OF TABLES (Cont'd)

TABLE	PAGE
23. Solid Rocket Applications	77
24. Properties Desired in Solid Propellants.	78
25. Typical Properties of Solid Propellants	79
26. Typical Exhaust Products (%) from Solid Propellants	80
27. Important Combustion Products from Solid Propellants	81
28. Erosion Rates of Elastomeric Liners and Aft Closures	82
29. Ablative Performance of Insulative Materials in Rocket Exhausts	83
30. Thermochemical Effects of Aluminized Exhaust Products on Phenolic-Silica Ablation	84
31. Particle Erosion of Ducting Material in an Aluminized Solid Propellant Exhaust	85
32. Theoretical Performance of Hybrid Propellants	86

INTRODUCTION

Polymeric materials represent a broad class of materials with a wide range of properties and characteristics. It is to be expected, then, that numerous uses have been found for them in chemical propulsion systems. The particular polymer employed in these applications is based on the inherent properties of the polymer, or, man's ability to combine it with another component material to obtain a balance of properties uncommon to either component. Some of the important properties of polymeric materials are given in Table 1, along with a propulsion application which utilizes this property to a high degree.

Various propulsion systems have been developed over the years which are dependent upon chemical, mechanical, electrical, nuclear, and solar means for accelerating the working fluid by high temperatures. Only chemical propulsion will be further discussed, and in particular, that associated with liquid, solid, and hybrid motors and engines. These motors and engines are uniquely different from other chemical propulsion systems in that they carry on-board the necessary propellants, as contrasted to jet engines that rely on atmospheric oxygen for combustion of the fuel.

THE HIGH TEMPERATURE PROBLEM

The basic purpose of a propulsion system is to convert the thermal energy of a chemical reaction into useful kinetic energy by directed flow of the resultant products. In other words, the propulsion system is to provide thrust for the movement of a vehicle. Expulsion of material is the essence of thrust production, and without material to expel no thrust can be produced, regardless of how much energy is available. The amount of thrust generated is equal to the rate of propellant consumption multiplied by the exhaust gas velocity. To maximize the exhaust velocity, it is necessary to have the combustion process take place at the highest possible temperature and pressure. Energy is released in the process, with a major fraction appearing as thermal (heat) energy. The amount of heat released is the difference value in bond energies of the newly formed reaction products and those of the precursory reactants. The reaction products are usually energetic, and characterized as being thermally reactive, chemically corrosive, and mechanically erosive. Yet, they must be contained and controlled to achieve the desired magnitude and direction of thrust. The development of engineering materials which can accommodate the hyper-environmental conditions of chemical propulsion thus constitutes a very difficult problem.

The combustion process is carried out in a thrust chamber or a motor case, and the reaction products are momentarily contained

therein. The newly formed species are heterogeneous in composition and involve a wide variety of low molecular weight products. The temperature of these products is generally high, and it ranges from about 2,000°F in gas generators to well over 8,000°F in advanced liquid propellant engines. The combustion products leave the chamber and are directed into and expanded in a nozzle to obtain velocities from about 5,000 to 14,000 ft/sec. The mass rate of flow through the nozzle will generally vary from less than one lb/sec/in.² in small liquid space engines to more than six lb/sec/in.² in solid and liquid propellant engines (Reference 1). The firing period may last from a few seconds as in tactical missiles, to a range upwards of over 20 minutes in spacecraft engines.

Since the flow is highly turbulent and the temperature level of the reaction products and the local pressure are numerically great, heat may be transferred at a high rate to the walls of the combustion chamber, nozzle, and adjacent parts. With an increase in firing time, heat protection becomes more important and ultimately approaches the critical stage. It then becomes necessary to thermally protect or cool the exposed parts. High performance materials and cooling techniques are thus necessary to accommodate the hyperenvironmental conditions associated with rocket engines and motors.

COOLING TECHNIQUES

Various methods have been developed to cope with high temperature and heating problems, and they are based on absorptive, dissipative, and mass transfer cooling systems. More specifically, they include regenerative cooling, inert or endothermic heat sinks, ablation, and combinations of the preceding techniques.

Regenerative cooling is the most widely used form of cooling for liquid propellant engines. It is an absorptive technique in which heat transferred to the chamber wall is conducted internally to a regulated flowing fluid. This fluid is contained in cooling jackets or thin tubes affixed to the chamber wall, and it is generally composed of one or both of the propellant components. In this manner, the wall of the combustion chamber and nozzle is maintained at a safe temperature level. A modification of the regenerative cooling scheme is known as open tube cooling. A small fraction of the propellant is passed through the cooling tubes and then injected axially into the flow to produce thrust. The technique appears attractive only for large thrust engines (over 10,000 pounds) which are cooled by hydrogen.

Radiative cooling is based on the dissipation of heat by a highly emissive, high temperature surface. It offers little utility in a combustion chamber, since establishment of radiation equilibrium (heat input equal to heat output) with the combustion gases would exceed the thermostructural capability of the wall material. Radiative cooling becomes more attractive in the nozzle area where energy can be radiated out of the aft opening and into the atmosphere. Radiative cooled engines are characterized by their lightweight, simple structure, and long operating life. Such engines have been operated continuously for one hour at a thrust level of 100 pounds and a chamber pressure of 90 psi.

Transpiration cooling is another form of heat protection. It is based on either a regulated or passive mass transfer in which a solid, liquid, or gas is passed through a porous wall material. The mass is injected in a direction opposite to the incident heat flux.

Energy absorption takes place by sensible temperature rise and possibly phase changes of the mass. The surface heating is reduced by a continual mixing of the injected coolant with the high temperature combustive gases. The inherent limitations of transpiration cooling are: nonavailability of a high-temperature, uniformly porous material, pore clogging by propellant and other extraneous matter, local hot spots, high coolant weight, and great bulk.

Surface film cooling is another form of mass transfer. It involves the introduction of a coolant through a series of slots or holes and in a tangential direction to the exhaust gases. A layer of coolant is thus formed on the exposed surface adjacent and downstream from the injection slot, and serves to insulate the hot wall from excessive heating. The protective film is rapidly destroyed by the gas stream, however, due to differences in their local velocities and moments. Film cooling has been used successfully in liquid propulsion systems, but is virtually nonexistent in solid propellant motors.

Inert heat sinks are based on the storage of heat by sensible temperature rise of a large mass of material. Their service life and efficiency are thus limited by the thermophysical properties (specific heat, thermal conductivity, and melting point) of the material employed. Endothermic heat sinks also utilize the heat absorbed by a change of state. A typical system would involve an organic liquid or a metal like sodium contained in a reservoir and in contact with the heated wall.

The final form of cooling, and the one of prime interest, concerns ablative cooling. It is essentially a heat and mass transfer process in which mass is expended to achieve thermal dissipation, absorption, and blocking. The process is passive in nature, serves to control the surface temperature, and greatly restricts the flow of heat into the material substrate. As a result of these desirable attributes and those shown in Table 2, ablative cooling has been widely used for thermal protection of solid propellant motors and less extensively in liquid propellant motors.

THE ABLATION PROCESS

Since 1950, plastics have been seriously considered and under development for uses in very high temperature environments. By 1954, it was demonstrated that plastic materials were suitable for thermally protecting structures during intense propulsion heating (Reference 3). This discovery became one of the greatest achievements of modern times, because it essentially eliminated the "thermal barrier" to hypersonic atmospheric flight as well as many of the internal heating problems associated with chemical propulsion systems (References 4, 5, and 6).

Polymers in the form of rigid (thermo-setting resins), flexible (elastomers and thermoplastic resins), and semirigid materials (elastomer modified thermosets) have thus acquired a new function in the engineering world, namely that of providing thermal protection. This mode of heat protection is now known as the "ablation" or "ablative" process, and the functional materials employed are commonly referred to as "ablaters."

The process of ablation is initiated by the interaction of a material with its hyperenvironment. The net effect is to remove surface region material. This loss of mass depends upon numerous environmental (Table 3) and materials parameters (Table 4), but in all cases, it increases with the severity of the environment.

While significant progress has been made in understanding the complex nature of materials' ablation (References 8 to 17), many of the subtle aspects continue to elude the researcher. Consequently, the ablative process for a fiber-reinforced plastic or elastomeric composite will be described for the purpose of illustration. At the onset of heating, energy is absorbed at the exposed surface and then conducted internally. The rate of heat penetration is dependent upon the surface temperature (driving force), and it is diffusion-limited by the inherent properties of organic materials. Figure 1 illustrates this point, wherein it is shown that fiber-reinforced-phenolic resins have low thermal diffusivities. The containment of heat in the surface region causes its surface temperature to rise rapidly. The net heat flux to the

material surface is thus decreased continuously as the surface temperature value moves towards the radiation equilibrium temperature. Eventually the material is heated sufficiently to generate volatiles, which have varying compositions such as water, residual diluents, or polymers of low molecular weight. At higher temperatures, the polymer begins to soften and it may physically slump. Thermal agitation eventually becomes severe enough to split side groups off the polymer backbone, and finally the chemical bonds in the backbone structure are ruptured. The polymer is thus undergoing pyrolysis, which continues over a broad temperature range. The organic component of the composite is degraded into numerous gaseous products of varying molecular weights, such as water vapor, carbon monoxide, carbon dioxide, hydrogen, methane, ethylene, acetylene, and other unsaturated and saturated hydrocarbon fragments. These pyrolytic species are injected into the adjacent hot boundary layer, and they effectively lower the enthalpy (heat content) of the environment. In this manner, less heat is convected to the ablating surface.

Thermoplastic and elastomeric polymers tend to thermally degrade into simple monomeric units with the formation of considerable liquid and a lesser amount of gaseous species. Little or no solid residue generally remains on the ablating surface. On the contrary, most thermosetting and highly crosslinked polymers (especially those with aromatic ring structures) form a hard surface residue of porous carbon. The amount of char formed depends upon such factors as: the carbon to hydrogen ratio presented in the original polymer structure, degree of crosslinking and tendency to further crosslink during heating, presence of foreign elements like the halogens, asymmetry and aromaticity of the polymer structure, degree of vapor pyrolysis of the ablative hydrocarbon species percolating through the char layer, and type of elemental bonding. With the formation of a carbonaceous layer, the primary region of pyrolysis gradually shifts from the surface to a substrate zone beneath the char layer. The newly formed char structure is attached to the virgin substrate material and remains

thereon for at least a short period of time. Meanwhile, its refractory nature serves to protect the temperature-sensitive substrate from the environment. Gaseous products formed in the substrate pass through the porous char layer, undergo partial vapor-phase cracking, and deposit pyrolytic carbon (or graphite) onto the walls of the pores.

As the organic polymer or its residual char are removed by the ablative aspects of the hyperenvironment, the reinforcing fibers or particle fillers are left exposed and unsupported. If vitreous in composition, they undergo melting. The resultant molten material covers the surface as liquid droplets, irregular globules, or a thin film. Continued addition of heat to the surface causes the melt to be vaporized. A fraction of the melt may be splattered by internal pressure forces, or sloughed away when acted upon by external pressure and shear forces of the dynamic environment.

The ablation of a polymeric material thus takes place in a number of adjacent zones, as illustrated in Figure 2. Each of the reacting zones is characterized by a certain temperature distribution, which is controlled to a large degree by the chemical reactions taking place therein. These reactions and products are favored at given temperature levels, as illustrated in Figure 3. For the case presented, silicon carbide (References 14, 17, 18, and 19) is formed from the molten silica (fiber origin) and polymer carbon (resin origin) at temperatures up to about 2,800°F. At higher temperatures, equilibrium mixtures of metallic silicon and silicon monoxide gas are favored. The summation of all of these reactions is a tremendous potential for absorbing heat. Figure 4 illustrates this point, and shows the inherent heat absorption of a silica-fiber-reinforced

phenolic as a function of temperature. Naturally, only a fraction of these endothermic reactions actually take place in any given ablation situation. The objective, then, is to control the materials variables so as to maximize the heat absorbed and dissipated by any given material.

From a thermophysical point of view, ablation may be defined as an orderly heat and mass transfer process in which a large amount of thermal energy is expended by sacrificial loss of surface region material. The heat input from the environment is absorbed, dissipated, blocked, and generated by numerous mechanisms. These are (a) heat conduction into the material substrate and storage by its effective heat capacity, (b) material phase changes, (c) heat absorption by gases in the substrate as they percolate to the surface, (d) convection of heat in a surface liquid layer, if one exists, (e) transpiration of gases from the ablating surface into the boundary layer with attendant heat absorption, (f) surface and bulk radiation and (g) endothermic and exothermic chemical reactions (Reference 2). These energy absorption processes take place automatically and simultaneously, serve to control the surface temperature, and greatly restrict the flow of heat into the substrate interior.

It is apparent, then, that the performance of an ablative polymer is achieved in a manner quite unlike that for heat-resistant polymers (Reference 20). Ablators depend heavily upon the various degradative reactions to absorb, dissipate, and block a copious amount of heat. On the contrary, heat-resistant polymers must essentially remain intact during high-temperature exposure to retain a significant fraction of their room-temperature properties.

ABLATIVE PERFORMANCE

The behavior and performance characteristics of ablative plastics and elastomers in the exhaust environments of rocket engines are of great importance for (a) aiding in the selection of appropriate compositions for newly designed engines, (b) identifying unique, desirable, and undesirable properties and

characteristics of ablative compositions and constructions (c) establishment guidelines for improving the performance of available classes of ablators, and (d) generating new materials concepts which have promise for accommodating the environmental extremes of future liquid propellant engines.

Performance data are difficult to obtain on ablative materials in actual engine firings, due to (a) military security classification, (b) company proprietary rights, (c) nonrecovery of engine systems like those left in earth orbit, (d) lack of instrumentation because firings were conducted for another purpose, and (e) relatively low number of engine ground proof tests. In addition, the extremely high costs of engine firings tend to restrict the number of materials being evaluated. For these reasons, designers of ablative propulsion parts must rely upon theoretical predictions of materials performance, small rocket motor firings and attendant laboratory tests, and full-scale engine testing. Existing scaling techniques (References 21 and 22) are imperfect and full-scale firings are very expensive, however, and thus the development of appropriate theoretical ablative models and associated mathematical relationships for predicting performance must be conducted.

Theoretical Predictions

In general, the physical model is similar to that previously described. The polymeric matrix undergoes charring during the ablation process, and the various reinforcing agents and fillers contained therein experience either vaporization, melting, or sublimation. The model is generally refined to take into account all of the important physico-chemical reactions as well as the newly formed products. The laws governing the conservation of mass, chemical species, and energy are then employed in order to define what is taking place in the high-temperature boundary layer and at the material surface. These laws are stated in mathematical terms, and with the use of applicable environmental and materials data, useful solutions can be obtained. In general, ablative properties and characteristics of the following type are required: thermophysical properties (thermal conductivity, specific heat, and density) of the virgin material and resultant surface (char) layer; the weight fraction, decomposition temperature and range, and heat of decomposition of the material or composite components; the specific heat and molecular weight of the newly formed ablative gaseous species; and various erosion constants obtained experimentally from subscale firings (Reference

23). With the aid of these data and numerical values for the environmental conditions, a solution is obtained for the ablative surface temperature, temperature distribution of the substrate, and the rate of surface erosion (References 24 and 25). A solution of these equations normally involves advanced mathematics and a large amount of input data, and for these reasons, computer solutions are often required. An iteration procedure can then be followed until the optimum materials compositions and construction have been identified.

As one would expect, this analytical approach to materials ablation has its limitations. Simplifying assumptions are frequently necessary because of our incomplete state of knowledge and to limit running time on the computer. These assumptions pertain to such factors as: one-dimensional heating instead of the multidimensional case which is often involved, equilibrium conditions and infinite chemical reaction rates, and steady-state ablation whereas transient ablation may play a significant role. Materials properties up to 5,000°F may be required whereas data generally exists only up to the point of thermochemical degradation. Inspection of the equations for predicting ablative performance will also reveal that they usually do not take into account mechanical degradation (gas shear, impact erosion, and spallation) of the material. As a result of these assumptions and incomplete data, most theoretical models predict ablation rates about two to five times higher than that obtained from experimental firings (Reference 26). The converse situation, however, has also been encountered on an infrequent basis.

Rocket Motor Firings

Subsequent sections of this report will treat the detailed performance of ablative polymeric materials in laboratory and subscale rocket motor firings.

Performance Indices

The behavior and performance characteristics of ablative polymeric materials during very high temperature exposure are obtained by qualitative observations and quantitative measurements. Macroscopic physical

changes, such as spalling, flaking, delamination, particle shear, liquid runoff, vaporization, boiling, splattering, and others are observed directly on a specimen during immersion in the test medium.

The linear rate of ablation is perhaps the foremost performance index. It is the best expression of ablative performance when dimensional stability is of primary concern. By definition, the linear ablation rate is the instantaneous or average erosion per unit exposure time. A convenient means for calculating this material index (A.R.) is by the following relation:

$$A.R. = \frac{x_a + x_c}{T} \quad (1)$$

where x_a is the thickness of material physically removed, x_c is the thickness of the residual char layer or degraded zone, and T is the exposure time. An average rate of ablation may also be computed by dividing a reference thickness of material by the exposure time necessary to burn through that thickness. This performance index is commonly known as the burnthrough time T_{bt} . In cases involving a rocket nozzle, the ablative material surrounds the test medium. The linear ablation rate must therefore be obtained by other means. If the change in throat diameter during firing is neglected, the ablation of the nozzle throat (Reference 21) can be computed by:

$$A.R. = \frac{q_{t1} (P_c / P_{c1})^{0.8}}{p H_{eff}} \quad (2)$$

where q_{t1} is the initial throat heat flux, P_c is the chamber pressure at a given time, P_{c1} is the initial chamber pressure, p is the intact material density, and H_{eff} is the effective heat of ablation which is later defined. In general, ablative polymeric materials should have ablation rates less than four thousands of an inch per second to warrant further considerations.

Surface recession may also be measured by silhouette photography, thermocouple burnout, breakwire sensors, ultrasonics, radioactive absorption and backscatter, and microwaves.

The surface temperature and the distribution of heat in the reacting surface layer are also of interest. Monochromatic, bichromatic, and total radiation pyrometry are used to obtain the surface temperature, provided there is a line of sight to the ablating surface. For other cases, small diameter metallic filaments with a known melting point and at various depths from the surface, or a series of thermocouples can be used to obtain internal temperature profiles.

Since ablative polymeric materials are intended for use on aerodynamic vehicles, their performance per unit weight is of utmost importance. The most widely used materials performance index, which is based on this consideration, is the mass rate of ablation. The index is generally computed as a difference value between the initial and the final weight of the ablator divided by the exposure period. A second method for obtaining the mass rate of ablation is by computing the product of the linear rate of ablation and the intact material density. The resultant value is accurate when the ablator is noncharring. For the case of charring polymeric materials, the weight loss incurred in the thermally damaged surface regions should also be taken into account.

The insulation index (I) reflects the ability of an ablator to restrict high temperatures to the exposed surface region. It is usually based on experimental temperature data, and expressed in terms of the time necessary to achieve a preselected backwall or substrate temperature per unit thickness or weight of material. For example, I_{200} refers to the time necessary to achieve a backwall or substrate temperature of 200° (Centigrade or Fahrenheit).

The thermal insulative characteristic of an ablating polymeric material may also be expressed in terms of its thermal diffusivity value. This material property is an inverse expression of the time required for heat to diffuse through a material. By definition,

$$\alpha = \frac{k}{C_p} \quad (3)$$

where α is the effective thermal diffusivity, k is the thermal conductivity, C_p is the specific heat, and p is the material density. The thermal diffusivity of noncarbonizing polymers (like polyethylene) can be calculated with good accuracy from individually measured property values. Many polymeric composites, however, form several discrete reaction zones in the ablating surface region. The complex heat and mass transfer processes occurring in these zones greatly alter the temperature distribution (see Figure 2) and the properties of the surface residue. For this complex case, it is most appropriate to calculate a procedural thermal diffusivity value in accordance with the following relationship:

$$\alpha_p = \frac{v^2 (t_x - t_b)}{(dt/dT)_x} \quad (4)$$

where α_p is the procedural thermal diffusivity, v is the surface recession rate, t_x is the temperature at position x in the material, t_b is the temperature of the nonheated material, $(dt/dT)_x$ is the slope of the temperature versus exposure time curve at position x . Test conditions of steady-state ablation and unidirectional heating are assumed.

Another common method for expressing the performance of an ablative material is in terms of its heat of ablation. There are a number of heats of ablation used by engineers, but the effective heat of ablation H_{eff} is the most frequently used. By definition,

$$H_{\text{eff}} = \left(\frac{q_{\text{CW}}}{p v} \right) \left(\frac{H_s - H_w}{H_s - H_b} \right) \quad (5)$$

where q_{CW} is the calorimetric (cold-wall) heating rate to the surface, v is the surface recession rate, p is the intact material density, H_s is the total free stream enthalpy, H_w is the gas enthalpy at the ablative surface temperature, and H_b is the total enthalpy of the nonheated material (Reference 7).

Finally, there are several man-made ablative performance indices that reflect both the resistance to ablation and the insulative capability of materials. One such index, the A.P.I., is defined by the relationship:

$$\text{A.P.I.} = \frac{\text{A.R.} \times 200}{I_{200}} \quad (6)$$

Desirable ablative polymeric materials should have an A.P.I. of less than 20, although this limiting value is somewhat arbitrary.

The severity of the high temperature environment limits the amount of materials performance data obtained during dynamic ablation. It is therefore imperative that additional post-exposure measurements be made on the residual ablated material. Table 5 summarizes some of the conventional techniques that have been employed and the type of information obtained. Such information can be used to furnish additional insights concerning what actually took place during the ablation process.

LIQUID PROPULSION

Liquid propellant engines have been used for many years to propel aircraft, guided missiles, rockets, research devices, and other types of vehicles. They have provided thrust levels ranging from a few ounces for altitude control to several hundred thousand pounds for the earth launching of vehicles.

Liquid propulsion is characterized by its high state of development, relatively complicated systems design, capability for repeated operation, long firing times, and of

course the propellants employed. Their use has been based on a number of selection criteria, such as the operational mission, performance required, reliability, minimum weight, logistics, economics, availability, maintainability, mobility, and others.

Primary and Secondary Engines

A liquid propellant engine system usually consists of a thrust chamber (injector, combustion chamber, and nozzle), propellant

tankage, and a feed mechanism including a secondary power source, plumbing, and regulatory devices for propellant transfer (Reference 27). Figure 5 is a schematic diagram of this type of propulsion system.

Liquid propellant engines have been developed as the basic propulsion for ground launch vehicles. Their thrust levels vary from a few thousand pounds to several hundred thousand pounds. The engines generally burn a liquid oxygen and RP-1 bipropellant because it is inexpensive, widely available, nontoxic, relatively easy to handle, and has a high specific impulse. Recent developmental efforts, however, have been centered on engines which are capable of using nitrogen tetroxide and hydrazine-unsymmetrical dimethyl hydrazine (-UDMH) at room temperature, hence the name "earth storable." The propellants can be contained in the tankage for long periods of time, and thus provide a quick launch capability. Meanwhile, research engines employing other higher energy storable propellants are being developed. These engines are to utilize oxidizers of nitrogen-fluorine compounds and oxygen difluoride, fuels like hydrazine and other amines, and various additives of the light metals, aluminum borohydride, diborane, and decaborane (Reference 29). These advanced propellants are more corrosive than the conventional cryogenic fuels, and thus added materials problems will be encountered in their use.

Primary propulsion is also required for upper-stage vehicles. These liquid propellant engines utilize many of the propellants employed for large boosters, and in addition, fuels like inhibited red fuming nitric acid (IRFNA) and UDMH. Since the propellants and engine must be transported to a great altitude before being used, performance and weight become critical criteria. For that reason, engines are being developed which will burn liquid oxygen and liquid hydrogen. Greater performance can be achieved with other propellants in terms of specific impulse, but their production and use have been tempered by higher propellant costs, more difficult engineering problems, and increased severity of the exhaust environment. Nevertheless, some attention is also being given to oxidizers of liquid fluorine

and oxygen difluoride, because in combination with hydrogen, they yield the highest possible performance in a bipropellant combination. Adding light metals such as lithium to hydrogen fuel offers possibilities for achieving even greater specific impulses (Reference 30).

Thrust chambers used for secondary propulsion constitute a second major class of liquid propellant engines. The thrust chamber is an integral unit consisting of a cylinder, a throat, and a nozzle. The liquid oxidizer and fuel are injected into the cylinder and then combusted with the aid of an igniter, or burned spontaneously in the presence of each other (hypergolically). Engines of this type have been built with variable thrust levels from a few pounds up to 22,000 pounds, and as a result, they cover a wide spectrum of applications. Their current and projected uses may possibly include gas generation, altitude control and stabilization of flight vehicles and satellites (Reference 31), coplanar and interplanar orbit changes, trajectory corrections, rendezvous, docking, lunar and planetary landings, retrofiring for re-entry or stage separation, and mission abort (Reference 32). Engines for secondary propulsion employ many of the same cryogenic and storable bipropellants previously mentioned, but in addition, they sometimes burn a liquid monopropellant like 90-percent hydrogen peroxide.

Propellants

Chemical propulsion can be effected with a wide variety of liquid propellants. To be useful, they must be a good source of energy, release energy during combustion to produce a suitable hot-working substance, and convert as much thermal energy as possible into kinetic energy of the products. In other words, liquid propellants must generally possess the following attributes: a high numerical value for its latent chemical energy, specific impulse, bulk density, specific heat, thermal stability, reaction rate, storability; a low numerical value for its vapor pressure and freezing points; and be nontoxic, chemically noncorrosive, and able to undergo stable combustion over a wide range of pressures. Each propellant combination has its advantages and

limitations, and numerous tradeoffs must be made in selecting a propellant. High specific impulse is often sacrificed in primary propulsion to achieve high bulk density and thus less tankage, low combustion temperatures to obtain a lighter cooling system, and less corrosion for fewer material container problems. High propellant performance, however, is of paramount importance in upper-stage engines.

Liquid propellants have been classified according to composition and storability. Monopropellants contain an oxidizer and a combustible substance within a single compound (nitromethane), or they are a mixture of several substances (hydrogen peroxide and alcohol). A bipropellant is composed of an oxidizer and a fuel. They are stored separately and then brought together in the proper mixture ratio to achieve maximum thrust. A tripropellant has three components, such as beryllium, oxygen, and hydrogen. The beryllium is reacted with oxygen to release energy and generate a high temperature. The propulsive substance (hydrogen) is then added to the systems, and after mixing, it is energized prior to passing through the nozzle (Reference 33).

A second major class of liquid propellants, and one of current technical interest, is the thixotropic (gelled) propellants. They are unique in that they only flow under the influence of an applied force, i.e., a shearing force is necessary to progressively break down the gel structure and reduce the apparent viscosity until it behaves as a Newtonian (liquid) propellant. The thixotropic propellants are gellants containing ultrafine particles, which gel through the mechanism of interparticulate forces. The particles have a diameter in the micron range, a very large surface energy, and a composition like aluminum, beryllium, boron, magnesium, or a metallic hydride (Reference 34). Liquid fuels and oxidizers have also been gelled by colloidal particles of silica and carbon. Chemical gels are randomly oriented polymeric (long-chain macromolecules) swelling agents which have trapped the liquid within a molecular network. A typical material of this type is polyvinyl chloride. Chemical gels are well suited to holding metal additives, and thus appear to have the best overall

potential for future uses. It is thus apparent that the gelled propellants are similar in some respects to the conventional liquid propellants, yet exhibit certain differences and advantages. Their principal attributes include densities as much as five times higher than available liquids, increases in specific impulses up to 20 percent, lack of propellant sloshing during lift-off and small applied forces, less boil-off or vaporization losses during storing, less stringent requirements for low propellant tank porosity, and possibly a reduced explosion and fire hazard (Reference 35). The disadvantages of the propellant system are that they require special pumping, gel thinning, and metal separation at elevated temperatures, and that there is a possibility of chemical reaction of the liquid and gelling agent during storage.

Liquid propellants may also be classified according to the temperature at which they can be stored. There are the cryogenic propellants like liquid hydrogen (which is stored at a temperature of -423°F), earth storable propellants like RP-1 (stable at 77°F), and space storable propellants like oxygen difluoride (boiling point greater than -238°F). Table 6 lists a number of propellants being used in operational engines as well as others of current interest. Note that a high combustion temperature is characteristic of all the propellants, and varies over a temperature range of $4,012^{\circ}$ to $7,298^{\circ}\text{F}$.

High temperature combustion of a liquid propellant produces a variety of products of low molecular weight. The composition of these exhaust species depends upon the specific fuel and oxidizer employed and their ratio, as well as the local temperature and pressure conditions. The exhaust products created by various propellants will be given in detail later in this report. In Figure 7, the influence of the oxidizer to fuel ratio on the composition and quantity of combustion products is illustrated for the widely used nitrogen tetroxide and hydrazine-UDMH propellant. The theoretical data presented in Figure 6 was based on a combustion chamber pressure of 100 psia. Last, the exhaust species may change significantly as they flow from the combustion chamber out of the nozzle. This situation is illustrated

in Figure 7, which gives the varying environmental conditions of temperature, pressure, velocity, wall shear stress, and heating rate in the different locations of a typical liquid propellant rocket nozzle.

Applicability of Ablation

Ablative cooling has been used in a number of liquid propellant engines. The materials employed are generally of an oriented fiber-reinforced resin, and they are used in direct contact with the exhaust products. A thin layer of elastomeric material may also be used to insulate the outer structure from the inner ablating plastic. Fibrous oxides (in particular, silica and quartz) have consistently shown superior performance in oxidizing environments. This desirable performance has been attributed to their inherently high heat absorbing capability (see Figure 4). By realizing a significant fraction of the theoretical heat absorption, high ablative cooling is insured. Another reason for the desirable performance of silica fibers is their ability to reinforce the char layer, and to form a viscous melt during intense heating. This molten layer covers the thermally degrading resin surface, and acts as an oxidation barrier for the charred residue. In fluorine environments, however, oxide reinforcements experience increased vaporization (References 38, 39, and 40). But, carbon and graphite reinforcements exhibit greater chemical inertness in fluorine-containing products of combustion, and thus have been used exclusively. With respect to resins, only the high char-yielding phenolics and epoxy novolacs have been employed.

The utility of ablative cooling for liquid propulsion has been critically reviewed (Reference 30), and its general area of applicability can be inferred from Figure 8, which indicates that minimum weight engines should use ablative cooling when the thrust is moderately low and the firing times are not comparatively long. Ablators are particularly attractive when the engine performance characteristics involve throttling, restarting, multiple pulse or low propellant flow rates. Ablative cooling becomes essential when the engine must be partially or entirely recessed into the vehicle's interior.

Ablative plastics have certain limitations in the liquid propellant exhaust environments. Their service life is time dependent, and varies with the firing time to about the one-half power. Firing times in excess of 310 seconds have been obtained, however, with a low thrust (150 lb) and low chamber pressure (130 psia) engine. At lower chamber pressures, engine operation up to about 1,980 seconds have been achieved. Ablative polymeric composites are generally not used in the throat region of liquid propellant engines, unless the total erosion can be maintained at five percent or less at the end of the firing period. Very high mass-flow rates of exhaust products, extremely long firing times, and small diameter nozzle throat regions tend to decrease the attractiveness of ablative polymeric cooling. Ablators are somewhat sensitive to the propellant injector performance. Poorly designed injectors have been noted to cause recirculation hot spots at the chamber wall, which resulted in a nonpredictable, nonuniform, and excessive localized erosion. Some residual thrust may also be encountered in liquid propellant engines that utilize ablative cooling. During engine cool down, gaseous products may be formed by continued resin vaporization in the partially degraded resin layer.

With respect to the high thrust engines of launch vehicles, ablative materials have only been used sparingly. The frequent need for proof testing, availability of cryogenic propellants for cooling, and the previously mentioned long firing durations and high mass-flow rates of exhaust products tend to favor other forms of cooling.

Many liquid propellant engines employed on upper-stage vehicles are pressure-fed and use ablative cooling. Such engines generally have a very high expansion ratio nozzle (diameter of aft opening divided by throat diameter) to achieve high thrust efficiency in the vacuum of space. At nozzle expansion ratios greater than about 10 to 1, the wall heating rate decreases to a point where regenerative cooling is no longer optimum. Instead, a passively cooled extension skirt provides greater efficiency per unit weight. The second-stage engine of the Titan launch vehicle, which is fueled by kerosene (RP-1)

and liquid oxygen, utilizes this concept of cooling (Reference 41). The nozzle is shown in Figure 9, and it is comprised of both regeneratively cooled and ablatively cooled sections. The ablative skirt is on the aft end of the nozzle. It was constructed of an asbestos fiber-reinforced phenolic, with an outer structural member of plastic honeycomb sandwich. An additional feature of the ablative skirt is that it permits a dry jacket altitude start and thus minimizes the possibility of fuel leakage during first-stage missile operation. Similar ablative extension skirts are presently under development for engines approaching the megapound thrust level. One such skirt has been successfully tested in five successive firings for a total accumulated time of 300 seconds, using a propellant of liquid oxygen and RP-2 hydrocarbon fuel.

Ablative plastic chambers have been built and successfully used on liquid engines having small to moderately high thrust levels (References 1,18,23,25,30,31,32,37, 39, 42 to 50). A typical thrust chamber is shown in Figure 10, which is a cross-sectional photograph of an ablative plastic chamber after firing. The 4,000-pound engine was run for 300 seconds at a chamber pressure of 100 psia, and with a propellant combination of nitrogen tetroxide and hydrazine-UDMH. Ablative chambers have been operated for longer periods of time. The record to date is a 33-minute firing of a 1,000-pound thrust, flight-weight thrust chamber. It was operated with storable propellants and chamber pressures from 60 to 300 psia. Ablative chambers have also been successfully tested on liquid propellant engines having a thrust of 30,000 pounds. A chamber in this thrust class is scheduled for the Apollo lunar service module (Figure 11). It has a diameter of 17 inches, vacuum thrust level of 21,900 pounds, a total firing time of 900 seconds, and it can be restarted more than 50 times (Reference 51). In this particular application, the aft end of the nozzle is exposed and experiences heating of a very low magnitude. It thus can be radiation cooled with a skirt of silicon-coated columbium and titanium which has a thickness of 0.025 and an expansion ratio of 40 to 1.

Materials Performance

The ablative performance characteristics of various polymeric materials, which are presented in the following sections, have been carefully selected from those available in the literature. The performance of one material could be directly compared with another, but only if both materials were evaluated in the same propulsion environment. Any attempt to correlate the performance of a given material in two different environments will be very difficult because different flame temperatures, combustion products, and other variables are involved. Hence, the data are intended primarily to illustrate the hyperthermal effects of propulsion exhausts on polymeric materials. They should not be used for design purposes, although the choice of materials for any given design can be greatly narrowed in number by careful consideration of the data presented herein.

Oxy-Acetylene

Ablative polymeric materials intended for use in propulsion environments are evaluated first in the combustion products from an oxy-acetylene torch. The purpose of this materials screening test is to identify polymers and composites which exhibit desirable ablative characteristics and thus warrant further refined evaluation. Secondly, it will permit the rejection of other undesirable materials early in the evaluation and development cycle.

The oxy-acetylene torch has gained favor because it is readily available (References 52 to 62), relatively inexpensive, easy to operate, yields reproducible results, and generates reaction products of interest. These products in molecular and radical forms are H_2O , CO , CO_2 , O , H_2 , OH , and H , and, they can be varied in concentration by adjusting the ratio of fuel to oxidizer. In this manner, chemically oxidizing, reducing, or neutral gaseous environments are made available. Surface heating rates up to about 700 Btu/ft²-sec at stagnation pressures of slightly more than one atmosphere can be generated on a near-continuous basis. Other performance features of importance include flame temperatures up to about 5,700°F, gas

enthalpies of about 1,600 Btu/lb, mass-flow rates up to about 0.02 lb/sec, and subsonic exhaust velocities of 100 to 300 ft/sec.

The evaluation method and equipment for oxy-acetylene screening of ablative polymers has now been standardized, as a result of the pioneering efforts of the U.S. Naval Ordnance Laboratory with cooperation from other government organizations, the aerospace industry, and the American Society for Testing Materials (Reference 63). A typical facility (References 64 and 65) is shown in Figure 12, which is an oxy-acetylene torch with a Victor Type 4, No. 7 tip. The gas flow rate is 225 standard ft³/hr, with an oxygen to fuel volume ratio of 1.20. The combustion flame has a temperature of about 5,500°F and is essentially chemically neutral in composition. The tip orifice is placed at a distance of 0.75 inch from the test specimen, and at an angle of 90 degrees with respect to the specimen. The overall dimensions of the specimen are 4 inches by 4 inches by 0.25 inch, although any specimen size many diameters larger than the flame would be satisfactory. A water-cooled holder is used to contain the specimen. The exposure period is initiated and continued until the flame penetrates the entire thickness of material. The test data measured and calculated include a record of the backface temperature, burnthrough time t_{bt} , an insulation index based on the time to achieve an arbitrarily selected temperature, average rate of ablation, and an overall ablation performance index (API).

The performance of several major types of elastomeric polymers is given in Table 7. The epoxy-based and silicone elastomers are noted to have a lower rate of ablation and higher insulation index than the well known butadiene-acrylonitrile (NBR) and polyurethane materials. In spite of their desirable performance, epoxy-based and silicone elastomers have not been widely used for ablative propulsion cooling. This situation exists because the elastomers must be used in a composite form to achieve an acceptable ablation rate, and, other selection criteria must also be considered. The data in Table 8 illustrate one of these points. It is shown that the ablative characteristics of butadiene-acrylonitrile can be altered significantly by

the addition of various fillers and reinforcing agents. Phenolic resin powder is noted to greatly affect the ablation rate, because it yields a large amount of residual char and thereby improves the erosion resistance. Fibrous asbestos contributed to the composite performance by virtue of its reinforcing action, low thermal conductivity, and its water-of-hydration and transpiration cooling effect. The presence of finely divided silica powder also influenced the ablative characteristics, because they formed a viscous melt during heating and covered the surface with a protective film. In this manner, the rate of oxidation of the char layer was minimized. Endothermic fillers such as boric acid may also be beneficial. They tend to restrict high temperatures to a narrow zone by the heat absorbing phase changes that are taking place, and furnish gaseous species for transpiration cooling of the char layer and adjacent boundary layer.

Additional performance features of elastomeric polymers in oxy-acetylene combustion products are given in Table 9. Data are reported for virtually all of the major types of elastomers, which were evaluated in composite form. The results clearly show that the elastomeric component had a pronounced effect on the ablative characteristics, and that it serves as more than just a binder for the reinforcing agents and fillers. The elastomeric silicones looked universally good, although considerable promise was also demonstrated by the polysulfides. In almost all of the cases, the presence of oxidizing species in the exhaust products resulted in a higher rate of ablation. Some of the non-charring polymers were somewhat insensitive to the gas chemistry, and yielded about equal performance in an oxidizing, reducing, or neutral flame.

While the screening information presented in Tables 7 to 9 is useful in assessing potential utility in ablative applications, many selection criteria must be considered. These include such factors as the: costs, compatibility with propellant and motor case, adhesive bonding characteristics, elongation, elastic modulus, strength properties, thermophysical properties, availability, reproducibility, performance reliability, ease of processing and fabrication, aging stability,

gas permeability, and possibly others. Based on all of these considerations, the NBR-elastomeric composites have generally been found to exhibit the best balance of properties and characteristics.

Thermoplastic polymers had ablative characteristics similar to the previously described elastomeric polymers. This fact is readily apparent by comparing the data presented in Table 10 with that of Table 7. The polyamide nylon possessed the lowest rate of ablation, whereas polyethylene had the highest ablation rate. In general, the thermoplastic polymers tended to depolymerize during oxy-acetylene heating. A large quantity of liquids and gases were formed, with only a minor amount of residual char. In contrast to this type of performance, the thermosetting resins formed a large amount of polymer carbon during ablative heating. Aromatic polymers like phenol formaldehyde were particularly effective because of the structural char obtained, which serves as a refractory barrier for the virgin substrate material. Even in a nonreinforced composition, the phenolic resin may have an erosion rate less than one-half that of steel. This is shown in Table 11, which contains the ablative characteristics of a variety of powder- and fiber-filled phenolic resins. The graphite-fabric-reinforced phenolics exhibited a phenomenally low ablation rate of only one mil/sec. Bulk graphite exhibited a lower rate of ablation, but its effective thermal conductivity was at least an order of magnitude greater than the reinforced plastic ablators. Because of these characteristics, graphite-fabric-reinforced phenolics have been widely used in reducing or low-oxidizing exhausts from propellants. The vitreous- and oxide-fiber-reinforced phenolics had ablation rates several times higher than that of the nonmelting graphite-fabric-reinforced ablator. Their insulative characteristics were much better, however, and they were more attractive for use in oxidizing environments. In contrast, the nylon-fabric-reinforced phenolic exhibited an ablation rate of 15.6 mil/sec. This was due to high vaporization of the nylon component, which incidentally, provided considerable transpiration cooling and a good insulative index.

Oxy-Hydrogen

The oxy-hydrogen rocket motor has been of particular interest to the propulsion industry, because of its utility as a materials screening device, as a simulation capability for subscale nozzle testing, and because of its availability at a number of different organizations (References 67 to 75). The motor (Reference 67) used in this study was operated at a chamber pressure of 275 psia, an oxygen-hydrogen volume ratio of 3.97, and a total propellant flow rate of 45 standard ft³/min. The motor generated exhaust products having a stagnation temperature of about 5,500°F and a velocity of 7,966 ft/sec (Mach 2.5). The equilibrium molar composition of the exhaust stream was H₂O, H₂, H, OH, O, and O₂ in that order of decreasing concentration. The flame was directed at an angle of 45 degrees to the specimen surface, which was six inches from the exit plane of the nozzle. The specimen was thereby heated at a calorimetric rate of about 450 Btu/ft²-sec. The test specimens were generally rectangular in shape, with 6 inches by 2 inches by 0.25 inch thickness being a representative configuration. The material exposure was initiated and continued for a preselected arbitrary time, or until specimen burnthrough had occurred. A spring-loaded thermocouple was affixed to the back side of the specimen for temperature sensing throughout the exposure period. Data obtained in this manner are presented in Table 12.

The phenolic, elastomer-modified phenolic, and silicone resins in composite form were found to have comparatively low linear rates of ablation. Their performance in terms of the mass ablation rate indicated that the rigid phenolics were superior in erosion resistance, followed by the silicone and elastomer-modified phenolics in that order of decreasing performance. The composition and percentage of filler or reinforcement in the ablative composite exerted a profound influence on the ablation rates. Fibrous silica containing ablators were the only types to survive the full firing of sixty seconds duration. Asbestos fibers with their relatively low melting point and low viscosity in the molten state were apparently eroded at a

rapid rate. The nonmelting carbon fibers provided good reinforcement to the surface char layer during ablation, but they were rapidly oxidized by the reactive species in the exhaust stream.

A cursory examination was also conducted on the influence of fabrication variables on ablative performance. It was found that the molding pressure and post curing conditions had little effect on the linear ablation rate of a silica-fabric-reinforced phenolic composite. The mass ablation rate and backface temperature of these composites, however, were significantly altered by specimen preparation conditions. High pressure (1,000 psi) molded specimens had the lowest mass ablation rates, but they also experienced greater internal heat transfer. High pressure moldings are denser and thus have an improved erosion resistance. Post curing, however, releases some volatiles with an attendant decrease in the transpiration cooling capability.

The oxy-hydrogen motor has also been found to be a useful tool in determining the mechanically destructive effects of high stagnation pressures on ablative performance. One of the available motors (Reference 70) was employed in this study, and operated at a chamber pressure of 700 psia, a propellant mass-flow rate of 0.194 lb/sec/inch², and a thrust level of 180 pounds. The combustion products were expanded into a two-inch diameter stream having a recovery temperature of 5,870°F, a velocity of 7,440 ft/sec or Mach 1.82, and a stagnation enthalpy of 3,603 Btu/lb. The exhaust stream was directed onto the ablative materials, which were at a distance of two inches from the aft end of the nozzle. The materials were in the form of 45-degree-angle cones having a nose radius of one-half inch. The stagnation point of the test models were exposed to six consecutive firings of two-seconds duration each, and the experimental data obtained are given in Table 13.

The superiority of silica-fiber-reinforced phenolic composites was again demonstrated in these oxy-hydrogen exhaust tests. The erosion resistance of the ablative plastics varied with the resin type and percentage. Resin content should be a minimum (without

introducing resin starved areas) in order to achieve a minimum ablation rate. The silica-fiber-reinforced phenolics formed a coherent surface char, which greatly influenced the erosion rate and high thermal shock resistance. The char structure on these models was not spalled off by the multiple firing sequence of the test. On the contrary, the organic-fabric-reinforced phenolics formed structurally weak char layers. These chars were continuously removed during firing by mechanical fracture, shearstress failure, or thermal shock. The remaining traces of the char structure were oxidized by the test environment. Noncharring resins, like polytetrafluoroethylene, exhibited very high ablation rates. They are thus unsuitable for use in high stagnation pressure, high mass-flow environments.

The oxy-hydrogen motor (71 to 75) has also been used for evaluating ablators in the form of small nozzle specimens. One of the most extensively used facilities (References 71, 72, 74, and 75) employs a low thrust (130 pound) motor of conventional design, but one which contains elaborate instrumentation for closely monitoring and controlling the environmental parameters. The motor was operated at a chamber pressure of 500 psia and an oxidizer to fuel weight ratio of 4.65. The propellant flow rate was 0.39 lb/sec, or about 2 lb/inch²/sec for a throat of one-half inch diameter. This high mass-flow rate produced high shear stress at the wall of the nozzle throat which is believed to be on the order of 100 lb/ft². The temperature of the exhaust gases was about 5,464°F, which is sufficient to heat the nozzle wall at a very high rate. The initial calorimetric heating rate was about 544 Btu/ft²-sec, and decreased to about 310 Btu/ft²-sec at a wall temperature of 4,300°F.

Each candidate material was prepared in the form of a subscale nozzle specimen, and bolted to the aft end of the motor combustion chamber. Material exposure was then accomplished by exhausting the hot gaseous products through the test nozzle. Interaction of the combustion products with the ablator resulted in material ablation, which was most pronounced in the throat region. This is illustrated in Figure 13. As the throat enlarged due to material ablation,

the motor chamber pressure decreased accordingly. The firing was terminated when the chamber pressure fell to 200 psia. Linear and area ablation in the throat was then determined by correlating the chamber pressure with firing time. Char depths were measured from a cross-sectioned piece of the ablated nozzle. In addition, a relative performance index was computed, using the firing time of a silica fabric phenolic specimen as the standard. Experimental results obtained in this manner are shown in Table 14.

The thermal and mechanical severity of the test environment greatly exceeded the capability of the nonfilled plastics, thereby resulting in very high ablation rates and short firing times. The charring epoxy resin was only slightly better than the noncharring polyethylene, and this was apparently due to the continuous removal of the surface char layer during test. The char layer could therefore not perform its function as a refractory barrier between the virgin plastic and the high temperature environment. In an attempt to improve the erosion resistance, various powdered fillers were added to the ablative plastics. Little or no improvement in performance was obtained, however, as evidenced by the high mass-flow rate of ablation. On the contrary, fibrous reinforcing agents exerted a pronounced effect on the ablation rate and on the retention of char contained on the ablating surface. Fibers which had a low melting point and low viscosity in the molten state, like asbestos and glass, gave results inferior to the silica and quartz reinforcements. Furthermore, the oxide melting reinforcements were noted to be superior to the nonmelting carbonaceous types. As previously noted, the fibrous oxides form a protective film over the oxidation-susceptible char layer. In addition, the melt flowed under the influence of the gasdynamic shear forces and tended to heal (fill) surface defects (spallation, delamination) produced during ablation. Short fibers or powdered oxides may also be added to fabric reinforced resins. The addition of silica fabric to the phenolic-graphite fabric composite increased its ablative performance and lowered its thermal conductivity, with only a small increase in density. Zirconia powder

was also shown to significantly improve the erosion resistance of phenolic-graphite fabric composites. The best erosion resistance was obtained by fibers oriented normal to the gas stream followed by chopped fabric and fibers in that order of decreasing performance.

While the phenolic polymers have looked universally good in the oxidizing turbulent exhaust streams from liquid propellants, other charring resins with aromatic or ring structures have also demonstrated acceptable performance. These plastics include the silane-modified phenolics (phenyl silanes), epoxy novolacs, and furfuraldehydes. The epoxy novolacs in particular warrant further consideration since they generally entail fewer fabrication problems in the manufacture of end items.

The ablative performance of reinforced plastics at varying chamber pressures is a matter of practical importance in the design of throttleable motors. Figure 14 is a plot of the initial rate of ablation of several fabric-reinforced phenolics at chamber pressures up to 450 psia. The silica-fabric-reinforced phenolics exhibited increasing erosion rates with the chamber pressure, although the material performance was almost insensitive to the throat diameter. On the contrary, the ablation rate of the graphite-fabric-reinforced phenolic was very sensitive to the chamber pressure and the nozzle throat diameter. Higher chamber pressures apparently increased the concentration of the oxidizing species at the ablating wall, which for the case of graphite-fiber-containing composites, led to increased oxidation and vaporization of the material.

Oxy-Kerosene

A large family of rocket motors, which burn the oxygen-kerosene propellant, have been used for characterizing ablative polymeric composites. These motors range in size from the small jet piercing torch (References 58, 76, and 77) having an exhaust diameter of 0.5 inch to the launch vehicle engines with exhaust diameters of several feet (Reference 3).

The jet piercing torch was originally developed for blasting holes in naturally occurring ceramics (rock formations), but more recently, it has economically provided rocket exhaust products at very high pressures, mass-flow rates, and with a chemical composition of H_2O , CO , CO_2 , OH , H_2 , H_2O_2 , and O . In normal operation, the test device (Reference 77) was as shown in Figure 15. It was usually run at the following approximate conditions: chamber pressure of 105 psia, an oxidizer to fuel ratio of 3.22, a fuel flow rate of 36 lb/hr and an oxidizer flow rate of 116 lb/hr. The combustion stream formed was about six inches in length, 0.5 inch in diameter, chemically oxidizing, had a temperature of 4,800°F, an enthalpy of 3,450 Btu/lb, and a velocity of Mach 1.7. The principal combustion products are usually CO , H_2O , and CO_2 , with minor amounts of H_2 , OH , H , O_2 , and O . The exhaust jet was directed at an angle of 30 degrees onto a rectangular test specimen and thereby imparted a stagnation pressure of 53 psia and a calorimetric heating rate of 770 Btu/ft²-sec to it. The ablative material was in the form of a specimen 2 inches by 3 inches by 3/8-1/2 inch.

The ablative performance of various plastics, elastomers, and ceramics in oxy-hydrogen exhaust products are given in Table 15. The high temperature behavior and performance trends obtained were in general similar to those already reported. The ablation rates obtained with the phenolic resin and the filled acrylonitrile-butadiene agents were reduced up to one-half of the values obtained on nonreinforced polymers. With respect to oxide-fiber-containing composites, the ablation rate decreased with increasing melting point and viscosity in the molten state. The addition of an oxide powder filler to an oxide-fiber-reinforced plastic did not greatly change the ablative characteristics, but the influence of graphite powder was significant. The presence of graphite in the aluminum-silicate-fiber-containing composite apparently increased the emissivity of the molten layer, and thereby reduced the amount of material necessary to expend heat by other thermal protective mechanisms.

Ceramic materials exhibited a comparatively low rate of ablation in the oxy-hydrogen exhaust stream, as compared to ablative

plastics and elastomers. Bulk graphite had a linear rate of ablation slightly better than the graphite-fabric-reinforced phenolic. The lowest rate of material removal during exposure was obtained with magnesia. This ablative ceramic, like other oxide ceramics, invariably exhibited thermal shock failure with observed spalling and cracking of the surface. Crack propagation was successfully restricted in these materials by the use of a metallic honeycomb (References 78 and 79). The ablation rates of such reinforced ceramics, however, were invariably higher than those of the nonreinforced types.

Oxy-Ethyl Alcohol

In the mid-1950's, subscale rocket engines were used extensively for the characterization of reinforced plastics intended for both re-entry heat shields and rocket exhaust applications. In one of these programs (Reference 80), a number of fiber-reinforced phenolics and silicones were exposed to supersonic combustion products and found to have a surprisingly low rate of ablation. The rocket engine employed a propellant combination of oxygen and ethyl alcohol in a mixture ratio of 2.08, and yielded oxidizing exhaust products having a temperature of about 5,390°F, and a velocity of approximately 6,900 ft/sec. The motor chamber pressure was 300 psia and the nozzle exit diameter was four inches. One-inch diameter hemispherical models of the reinforced plastics were exposed within the first shock diamond of the high pressure exhaust stream. Material ablation commenced almost immediately with specimen exposure, and within one-tenth of a second, a steady-state rate of ablation was achieved. After about five-seconds exposure, the plastic models were removed from the test medium. The important environmental parameters of the rocket exhaust and the ablative materials information obtained are presented in Table 16.

The ablative performance of the reinforced plastics in the high pressure rocket exhaust is shown to be affected by the type of polymer employed. In general, phenolics were found to be superior, followed by silicones and melamine in that order of decreasing performance. The strong char layer formed by the phenolic-containing composites obviously

contributed to the erosion resistance. The composition of the reinforcing agent exerted a strong influence on the ablation rate, although the physical type used (fiber versus fabric) did not appear to be important. The outstanding performance of the silica reinforcement may be attributed to the high gas-shear resistance of molten silica, formation of an oxidation-resistant surface film, and cooling effected by partial vaporization of the oxide.

The rate of heat penetration into the reinforced plastic models during exposure was unusually low, as evidenced by their low thermal diffusivities. Significant differences in values for the various ablators, however, were not discernible. This was due primarily to the difficulties associated with temperature measurements in ablating zones having high thermal gradients, which are characteristic of low thermal conductivity materials in thermally and mechanically severe environments. In other words, the thermal layer thickness on the ablating models (char layer) decreases with an increase in the heating rate and/or mechanical erosion.

Oxy-Gasoline

In the search for an ablative radome coating, a number of homogeneous and composite plastics were evaluated in the exhaust from an oxy-gasoline rocket motor (Reference 81). This test facility was operated at a chamber pressure of 300 psi, and with a propellant mass flow of about 0.5 lb/sec. The exhaust stream generated had a diameter in excess of three inches, a temperature of about 5,700°F, and a velocity of Mach 4. The high temperature jet was exhausted into an evacuated chamber, which was maintained at a pressure of 0.15 psia (simulated 100,000-ft altitude). The test models were prepared in the form of a one-inch diameter cylinder having a hemispherical tip. These specimens were immersed in the exhaust stream for a nominal period of ten seconds, during which time the surface temperature was measured with a total radiation pyrometer. The performance data obtained are presented in Table 17.

The superior erosion resistance of silica- and quartz-fiber-reinforced phenolics was

again demonstrated in the oxy-gasoline exhaust environment. Nonfilled plastics had erosion rates about an order of magnitude higher than the fiber-reinforced composites. Powder fillers were found to be detrimental in that the erosion rate increased with their presence. The causative factor(s) was not isolated, but it is believed that the particle filler was forcibly ejected from the ablating surface by the continuously generated ablative gases.

Nitrogen Tetraoxide-Hydrazine

The performance of ablative polymeric materials in the combustion products of nitrogen tetraoxide and hydrazine propellant is of considerable importance to the propulsion industry. Materials data obtained in this exhaust environment are being utilized in the design of both experimental and operational ablative thrust chambers.

In one laboratory program conducted to date, a small rocket engine was employed to generate the test environmental conditions. The motor (Reference 82) was operated at an initial chamber pressure of 150 psia, an oxidizer to fuel ratio of 1.0, a sea level thrust of 85 pounds, and a propellant combination as previously mentioned. The combustion chamber was water cooled to insure a long firing time. The oxidizing exhaust products had a theoretical flame temperature of about 4,850°F, an average gas temperature of 3,560°F, and a composition of N_2 , H_2O , H_2 , OH, and H.

Initial efforts were expended in studying the performance of a radiation-cooled thrust chamber. The unit was constructed of a disilicide-coated spun tungsten having a wall thickness of 0.036 inch. Two of these chambers were tested and both of them ruptured within two seconds of firing. Somewhat better results were obtained with free standing pyrolytic graphite. One of the units survived a total of 81 seconds and a second chamber lasted through 44 seconds of firing prior to completely shattering. In view of the disappointing results obtained with the refractory metal and pyrolytic graphite materials, further efforts were directed to the ablative cooling approach. Integral thrust chamber and nozzle units were constructed of

silica-fabric-reinforced phenolics, and evaluated in the $N_2O_4 - N_2H_4$ environment. Firing times up to 235 seconds were obtained, at which time the engine failed due to a joint separation between the nozzle and the thrust chamber. No net erosion was experienced in the throat region, but a char depth of 0.55 inch was recorded in this region.

In view of the initial successes with ablative thrust chambers, further tests were scheduled with ablative nozzle sections and a water-cooled combustion chamber. The ablative plastic throat sections were fabricated in the form of small convergent-divergent units having a 0.75-inch diameter opening. These test nozzles were affixed to the combustion chamber, and the hot exhaust stream was directed through the specimen with an initial throat heating rate of 720 Btu/ft²-sec. The chamber pressure was monitored continuously during firing, which permitted a correlation of the throat area erosion with decreasing chamber pressure. The firing was continued for a period of 300 seconds, or until the throat increased in diameter by about 0.088 inch to drop the chamber pressure to 120 psia (80% of initial value). Experimental data obtained in this fashion are reported in Table 18.

The fibrous silica-reinforced-phenolic composites exhibited excellent erosion and charring characteristics in the oxidizing environment of nitrogen tetroxide and hydrazine. One of these materials survived a full firing period of 300 seconds duration for which the initial chamber pressure was maintained and from which a char depth of only 0.42 inch resulted.

During the initial stages of exhaust heating, the phenolic resin expanded and then charred. This resin bloating action produced a minor increase in the motor chamber pressure, which subsequently decreased in value with char maturity and partial vaporization of the molten silica fibers. The molten silica provided superior oxidation protection for the resin char, and thereby minimized dimensional ablation. The asbestos-fiber-reinforced-phenolic composite experienced excessive erosion, which was attributed to its relatively low melting point, low boiling point, and low viscosity in the melted state.

High erosion rates were also experienced with the graphite-fiber-reinforced phenolics. The causative factor was apparently a rapid oxidation of the susceptible char structure and reinforcing agent. With respect to the fiber orientation, it was found that the shingle orientation (60-degree angle to the gas stream) was better than the end-grain orientation (90-degree angle to the gas stream). The shingle layout reduced the internal heat-transfer rate, and in the case of the graphite-fabric-reinforced phenolic, minimized the erosion rate. The physical form of the reinforcing agent was also noted to be important. Fabric constructions were superior, followed by chopped fabric and fibers in that order of decreasing performance. The use of volcanic ash as a filler in the phenolic resin tended to slightly increase the erosion rate and lower the effective thermal conductivity. Last, some delamination was noted in all of the ablative plastic chambers which is somewhat typical for motor firings of long duration.

The charring of ablative plastics in the exhaust of nitrogen tetroxide and hydrazine has been analyzed (Reference 47) for thrust chambers operating between 50 and 200 psia. From these results, a mathematical relationship has been developed for expressing the materials performance. The thickness of ablator $x_{500^\circ F}$ required to maintain a limiting backwall temperature of 500°F is equal to:

$$x_{500^\circ F} = A(P_c)^x (T)^y \quad (7)$$

where A is a constant between 0.0028 and 0.0036, P_c is the chamber pressure in psia, superscript x is a constant between 0.2 and 0.4, T is the firing time in seconds, and superscript y is a constant between 0.45 and 0.77. The exact values of the constants have to be determined from data obtained on specific thrust chambers and propellants, but considerable experience has shown that the numerical range is small.

Although graphite was susceptible to oxidative attack, certain grades exhibited good performance in the exhaust products of storable propellants. The best performance was obtained with a pyrolytic graphite coated ATJ-graphite nozzle. It successfully

withstood the entire 300-seconds firing with only 0.040-inch ablation in the nozzle throat. The bulk graphite experienced considerably more oxidation during engine firing, and as a result, lasted only 160 seconds of the firing time. The rate of heat penetration into the graphite interior was very high, which is undesirable from the standpoint of requiring additional insulation backup material.

Nitrogen Tetraoxide-UDMH

Thrust chambers have been designed, built, and successfully fired for a total of 880 seconds while employing a propellant combination of N_2O_4 -UDMH. A photograph of one of these chambers is shown in Figure 16. It was constructed of a preferentially wound, bias-cut phenolic-impregnated-silica fabric, with an inside diameter of 8.65 inches, a nozzle throat diameter of 6.13 inches, and a length of 23.3 inches. The thrust chamber was overwound with an epoxy resin and glass fiber to increase its structural properties. The total thrust-chamber weight was 98 pounds. The engine was operated at a thrust level of 1,900 pounds, a chamber pressure of 92 psia, a propellant flow rate of 16 lb/sec, and an oxidizer to fuel ratio of 1.58. The exhaust gases had a theoretical combustion temperature of about 4,482°F, and a composition of H_2O , N_2 , H_2 , CO , H , and CO_2 . No throat erosion was encountered even after five successive firings totalling 880 seconds (Reference 46).

Nitrogen Tetraoxide-Hydrazine-UDMH

The majority of ablative thrust chambers used in liquid propellant engines have employed the fuel to oxidizer combination of N_2H_4 -UDMH and N_2O_4 . A strong preference has been shown for this propellant because it is relatively inexpensive, available in large quantities, earth storable, and it generates combustion products of only moderate reactivity. The propellant gaseous species vary somewhat with the mixture ratio, as shown in Figure 6. They generally include H_2O , N_2 , CO , H_2 , CO_2 , OH , H , O_2 , NO , and O .

A subscale rocket engine (Reference 83) was used to determine the behavior of ablative plastics in the combustion products

of N_2O_4 - N_2H_4 -UDMH. This reduced scale motor was incapable of simultaneously reproducing the heating rate, shear forces, and combustion chemistry of full-scale motors. Nevertheless, it provided a convenient means for conducting ablative materials investigations. Figure 17 is a photograph of this motor. It was operated at a propellant mixture ratio of 2.5, a chamber pressure of 115 psia, a thrust level of 25 pounds, and a theoretical flame temperature of 5,158°F.

The test ablative materials were compression molded in the form of a conical thrust chamber, with the major fiber orientation perpendicular to the gas flow. The plastic chambers were then impregnated with an epoxy resin to make them gas tight. In certain thrust chambers, a refractory throat insert was adhesively bonded into the test assembly to obtain performance data on more dimensionally stable materials. The initial throat diameter was 0.531 inch, and the nozzle had an expansion ratio of four to one. During motor firing, the throat region was exposed to a calorimetric heating rate of about 495 Btu/ft²-sec with a lesser thermal rate at other areas of the chamber. The duration of firing was continued until a 50-percent reduction in chamber pressure was encountered.

The experimental data obtained on the ablative plastic thrust chambers are given in Table 19. From these data, it is apparent that various ablative plastics are ideal materials of construction for liquid propellant thrust chambers. The phenolic and silicone polymers exhibited excellent ablative performance. It is noted that the performance of the phenolic was altered considerably by the use of various polymeric modifiers. The polyamides and silicones appeared promising in this respect. The presence of a polyamide modifier lowered the thermal conductivity of the intact plastic composite and the newly formed char structure. The major influence of the silicone resin was apparently to increase the oxidation resistance of the phenolic char by forming a molten liquid surface layer during heating. The elastomer-modified phenolic had poorer performance, which may be attributed to the lower char yield obtained with this material. A low resin content was

optimum, but a 25 weight percent appeared to be necessary to insure a low composite thermal conductivity, adequate char, and to avoid resin starved areas. The composition and physical construction of the reinforcing agent was also found to be very important. Plastic composites containing asbestos fibers, which liberate water during pyrolysis, exhibited very low charring rates. The more conductive silica fibers, however, had the lowest rate of vaporization. Both graphite and carbon reinforcements oxidized at a relatively high rate, and consequently, they should generally not be used in this type of environment. Last, the type of ablative materials employed in the chamber region appeared to influence the performance of the throat region material.

As expected, the use of a dimensionally stable refractory permitted the longest firing times. The pyrolytic-tantalum-carbide-coated-graphite throat exhibited the lowest rate of radial increase, followed by pyrolytic graphite, bulk graphite, and the carburized 90-tantalum/10-tungsten composition in that order of decreasing performance. Ablative plastics were also shown to have some utility in the throat region of thrust chambers. Their erosion rates were about twice as great as the coated graphite and pyrolytic graphite throat. Nevertheless, the silica-fiber-reinforced phenolic did out perform bulk ATJ-graphite. The ablator not only had a lower erosion rate, but exhibited far superior insulative characteristics.

Theoretical analyses have also been conducted on the performance characteristics of ablative plastics in the exhaust products of nitrogen tetroxide, hydrazine-UDMH. An analytical method was developed (Reference 23) wherein the ablation process was described using finite differences (Dusinberre) for multicomponent transient conduction and the endothermic decomposition of the resin at a given temperature. This approach was used to examine the influence of materials variables on the durability of ablative plastic thrust chambers. It was found that variations in the thermal and physical properties of the ablator strongly influenced the performance of a charring ablator. Their importance tended to decrease, however, as erosion (physical removal) became more and more

the controlling ablative process. For a given ablator, the wall thickness had the strongest influence on the charring rate. Thermal conductivity of the surface char and density of the virgin material were also important materials variables, but were of less significance. The analytical results of this program were later verified by ablative thrust chamber firings. The performance data obtained are given in Table 20. The prediction of materials performance in the low thrust engine was between one and 15 percent, and, the predicted erosion losses in the high thrust chamber were within 22 percent of the actual values.

The design of ablative plastic thrust chambers for liquid propellant engines is rapidly approaching sophistication, because of the many firings conducted with subscale engines. Some of the materials performance data obtained in these firings is given in Figure 18. The total materials degradation (charring and erosion) of silica-fiber-reinforced phenolics is given as a function of the firing time. The scatter in the data is considerably less than one would expect, and for that reason, the design curve may serve as a first approximation of the performance of future thrust chambers operating with the listed chamber pressures, firing times, and propellants.

Fluorine-Hydrogen

Liquid fluorine and fluorine-containing compounds are receiving an increasing amount of attention as oxidizers for liquid propellant systems. These materials are among the most reactive, highest energy oxidizers known, and when in combination with current fuels, they produce a very high specific impulse. Unfortunately, they produce attendant thermal protection problems due to their extremely high flame temperatures and corrosive exhaust products. Species such as HF, H, H₂, and F are common in the exhaust flow from F₂-H₂ engines.

A laboratory rocket motor (Reference 39) was used to evaluate several ablative plastic chambers in a fluorine-hydrogen engine. The motor was operated at a chamber pressure of 256 psia, an oxidizer to fuel weight mixture ratio of 8.1 to 1, and a flame temperature of 6,500°F. Plastic thrust chambers were

prepared in the form of simple cylinders having an internal diameter of two inches, and outside diameter of four inches, and a length of eight inches. Chambers were prepared of both silica-fabric-reinforced phenolic and nylon-fabric-reinforced phenolic. Following exposure for a nominal 22 seconds, the chambers were sectioned and examined. It was found that the charred surface region was relatively inert to the fluorine-containing products. Ablation was primarily a result of hydrogen attack by the very high temperature. In contrast, the silica fibers were melted and rapidly vaporized by high temperature interaction with the fluorine exhaust species. This is the well known formation of silicon tetrafluoride from silicon dioxide and fluorine or a fluorine-containing product. Further details of ablative plastics performance in fluorine-hydrogen motors are classified.

Fluorine-Hydrazine

Liquid fluorine in combination with hydrazine is another high energy propellant of considerable technical interest. It produces a reactive exhaust stream having a temperature of about 7,770°F, and a composition of HF, H, H₂, F, and other trace elements.

A laboratory rocket engine (Reference 84) was used to evaluate a number of plastic materials in the F₂-N₂H₄ combustive environment. The 60-pound motor was operated at a fuel mixture ratio of 2.13, a propellant flow rate of 0.24 lb/sec, and a chamber pressure of about 94 psia. The thrust chambers were composed of various charring resins reinforced with either asbestos, silica, or carbon fabrics. They were eight inches long and two inches in diameter. The nozzle was composed of ATJ-graphite and backed up with an asbestos fiber furfuryl resinous insulator. It had a diameter of 0.78 inch and an expansion ratio of 5.1 to 1. These chambers were exposed for a period of 45 to 58 seconds and then carefully examined. The data obtained is reported in Table 21.

At the extremely high temperatures imposed by the gas stream, the molten silica was likely very fluid and easily removed by the dynamic shearing forces of the environment. The near absence of molten silica on the specimen surface after testing indicated

that hydrogen fluoride reaction and vaporization was also a mechanism of silica removal. The low erosion rate of the asbestos containing composites was unexpected. A partial explanation may be advanced on the basis of a greater phase stability of solid MgF₂ in the exhaust stream.

The potential of polymeric materials in the fluorine-hydrazine propellant exhaust is not clearly evident from the data in Table 21. Additional testing will be necessary to identify the best resinous matrices and reinforcing agents.

Chlorine Trifluoride-Hydrazine

The propellant ClF₃-N₂H₄ is presently being investigated for future spacecraft propulsion needs. Laboratory investigations are thus underway to determine the suitability of ablative cooling for the thrust chamber and nozzle of the engine. The motor (Reference 82) employed in these tests was operated at a chamber pressure of 150 psia, a propellant mixture ratio of 2.2, and a theoretical combustion temperature of 5,771°F. It generated exhaust species of HF, N₂, HCl, H₂, H, and Cl.

Thrust chambers including a nozzle section were prepared of phenolic resin and silica fabric. They were successfully fired for periods up to 267 seconds, with the firing times cut short by failures at the butt joint of the chamber and nozzle. An increase in throat area of 30 percent, a char depth of 0.60 inch, and an average erosion rate of 0.21 mil/sec was noted for the throat region of the maximum duration specimen indicated. Post firing examination of the ablative chamber and nozzle revealed considerable chemical corrosion of the molten silica surface by the hydrogen-fluoride exhaust products.

Oxygen Difluoride-Diborane

Propulsion for deep space missions requires a propellant having a very high specific impulse, high bulk density, space storability, and hypersonic velocity. Oxygen difluoride and diborane satisfy these requirements, and have been under development (Reference 85) since about 1960. Unlike many of the boron hydride propellants, the OF₂-B₂H₆

combination burns without the troublesome residual deposits of boron and boron hydride products. The propellant and oxidizer have poor coolant properties, however, and thus regeneratively cooled engines cannot be used. For this reason, ablative cooling is used in such engines.

In the experimental program (Reference 45) which was conducted on the ablatively cooled engine, the subscale motor employed was operated at the following nominal conditions: a chamber pressure of 150 psia, a thrust level of 150 pounds, a propellant flow rate of 0.57 lb/sec, mixture ratio of 3.00, and a theoretical flame temperature of 6,650°F. Thrust chambers of ablative plastics were prepared in the form of cylinders, with an outside diameter of about 4 inches and a length of approximately 10 inches. The monolithic ablative chambers were fabricated with a nominal 60-degree wrap angle to the specimen axis. Chambers containing a refractory nozzle section had their reinforcement at a 90-degree angle to the gas stream. The ablative chambers were bonded in a steel structural shell, and exposed to the combustion products for the time specified in Table 22. These exhaust species included major amounts of HF, H, BOF, and H₂, with minor amounts of BO, H₂O, BOH, H, OH, O, F, BF, and BOH₂.

A graphite-fabric-reinforced-phenolic thrust chamber after firing is shown in Figure 19. The experimental data obtained on this ablated chamber is given in Table 22, along with performance information on other ablative thrust chambers. Both phenolic-graphite-fabric and phenolic-silica-fabric composites were satisfactory when used in the thrust chamber barrel. The former material, however, exhibited a lower erosion rate and a higher rate of char. In the throat section, the silica fabric proved to be greatly inferior to the more inert graphite fabric. Firing durations up to three times longer were achieved with the phenolic-graphite throat material as compared to the phenolic-silica composite. The graphite-fabric-reinforced precharred-epoxy-novolac material, with its laboratory preformed char structure, proved to be an interesting material. Its erosion and char rate were somewhat higher than that obtained on phenolic-graphite-fabric composites, but further improvements could conceivably make it competitive with the best ablaters. In summary, the test data indicate that an ablative thrust chamber of phenolic-graphite fabric with a throat insert of a refractory material (and backed up with a plastic insulator) will likely be optimum in liquid propellant engines burning OF₂-B₂H₆ propellant.

SOLID PROPELLANTS

The evolution of propulsion for ordnance purposes, weapon delivery systems, ballistic and space vehicles, and scientific exploration suggests an ever-increasing role for solid propellant motors. Unlike the previously discussed liquid propellants, the solid rocket fuels are characterized by their obvious solid phase propellants, lower specific impulse (about 8 to 20% less), higher densities, fixed fuel to oxidizer ratios, and higher costs (about 0.80 per pound). Motors employing the solid propellants exhibit certain performance traits, which include simplicity, compactness, safety, instant firing readiness, short developmental times, reduced developmental costs, greater reliability, shorter firing times, storability, ease of maintenance, and a passive thermal protection system (References 86, 87, and 88). Other motor

characteristics that were once exclusive to liquid propellant engines, such as throttling and restarting, have now been achieved in certain rocket engines (Reference 89).

History

Solid propellants date back to at least the 13th century. The Chinese are known to have prepared gun powder by grinding potassium nitrate, sulfur, and charcoal. They then packed the mixture in a cylindrical paper container. The energy content of these first generation propellants was low, i.e., about 70 to 100 lb (force)-sec/lb (mass). The next major advancement in solid propellants was the discovery of cellulose nitrate (gun cotton)

in 1845 and glyceryl trinitrate (nitroglycerin) in 1846. The combination of these two ingredients by Nobel resulted in the first double-based propellant, and, a great acceleration in the technology of explosives. In the succeeding years, performance increases in solid propellants were relatively slow. Then in the early 1940's, solid rocketry began to be recognized as a means for accomplishing a variety of propulsion missions. A number of motors were therefore designed and built, but the results left much to be desired. The motors had a low mass fraction (inefficiently loaded with propellant), poor ballistic properties (low specific impulse and burning rate, unsatisfactory mechanical properties (hard and brittle). The JATO (jet assist take-off) units (Reference 90), which were developed for aircraft, were somewhat typical. The motor container was essentially a metal cylinder into which was molded a modified black powder, using a 22-step pressing operation and 40,000 psi. Six of these units, each weighing 12.7 pounds, were used in August 1941 for this country's first aircraft jet assist take-off and acceleration (Reference 91).

Perhaps the real breakthrough in the state-of-the-art came in June 1942 with the development of a rubber-based fuel, case bonded, internal burning propellant grain encased in a metal motor case having a thin wall and high strength. The propellants were composed of an oxidizer salt, like potassium perchlorate, dispersed in an amorphous binder of asphalt. In 1945, elastomeric-base matrices with improved physical properties and burning characteristics were used in place of asphalt binders. Ammonium perchlorate was also substituted for potassium perchlorate with a 13-percent increase in the propellant performance. New additives, modifiers, and catalysts were developed to alter the propellant ballistic characteristics and alleviate inherent property limitations of the binders and oxidizers.

The early solid propellant motors were of the end-burning type, as in a lighted cigarette. Since an increasing amount of chamber was exposed with the firing time, design of the thermal protection system was difficult and often inefficiently used. In March 1957, the internal core-burning grain was introduced

to solid rocketry with outstanding success. This type of grain design permitted the propellant to serve as its own insulator, and thus reduced the thermal requirements on the case materials (Reference 92).

The solid propellant rockets being used today or under development vary greatly in application, propulsion features, size and sophistication. This is illustrated in Table 23, which reports nine major uses for solid propellant motors along with their range of firing durations, thrust levels, chamber pressures and mass ratios. Most of the uses serve ordnance purposes, such as antisubmarine torpedoes, air defense (like the guided air-to-air rocket shown in Figure 20), tactical defense (like the bazooka antitank rocket), strategic weapons delivery (like the motor employed in the Minuteman intercontinental ballistic missile shown in Figure 21), and the high acceleration anti-missile rocket. Solid propellant motors have many space and scientific missions, such as the launching of space vehicles and interplanetary probes, retro-rockets for spacecraft like that shown in Figure 22, and sounding rockets for upper atmospheric research. Solid propellant motors also aid in the safety of vehicles, such as the emergency escape from aircraft and launch vehicles and gas generation for emptying submarine ballast tanks. To accommodate these various mission requirements, the size and sophistication of solid propellant motors must also vary greatly. Perhaps the smallest rocket being used today is the Marc 3, which provides spin control of the Tiros cloud cover satellite. It is only 0.75 inch in diameter 2.79 inches long, weighs 0.085 pound, contains less than three grams of propellant, has a chamber pressure of 300 psi, delivers five pounds of vacuum thrust, and fires in 0.3 second. This motor is in great contrast to that shown in Figure 23, which is a five-segmented launch vehicle. It delivers over a million pounds of thrust over a firing period of 112 seconds (Reference 93).

The Propellants

The solid propellant is a composition of matter, which serves as the precursor for the propulsive medium. It is stable at room temperature, and once ignited, evolves gas

continuously at high temperatures without any dependence on the atmosphere.

The solid propellants may be classified as being mainly of two types, homogeneous and composite. Homogeneous propellants are composed of single molecules or colloidal mixtures. The former material is a single-based propellant, like cellulose trinitrate. Double-based propellant consists of an oxidizer (usually an inorganic salt) bound within an organic fuel matrix. These propellants are cast, extruded, or machined into various geometric shapes, which are known as grains.

To obtain high performance, a solid propellant should satisfy the following criteria: (a) have a high heat of reaction per unit volume, (b) generate reaction products of low molecular weight, (c) take part (all propellant ingredients) in the combustion reaction and contribute to the available energy, (d) form a minimum amount of liquid or solid particulate matter during combustion, and (e) burn in a predictable, stable, and reproducible manner to form nonluminous, noncorrosive, and nontoxic gases. Available solid propellants are limited in at least one of these ballistic requirements. Propellants generating all gaseous products have relatively low heats of reaction and contain elements (like nitrogen) that contribute little or no energy. Propellant exhaust containing entrained particles have a lower weight percentage of gases available for expansion through the nozzle (Reference 94).

In addition to the performance criteria already discussed, a solid propellant must possess certain other physico-chemical, mechanical, and permanence properties to enhance its utility. Many of these important characteristics are given in Table 24. As expected, no single propellant rates close to the ideal. The selection of a propellant for a specific mission must therefore involve a careful consideration of the ballistic characteristics, properties of available propellants, and other trade-offs in arriving at the optimum propellant.

A solid propellant is a mixture of an oxidizing and a reducing material that can coexist in the solid state at ordinary temperatures. It is generally composed of three

elements, the oxidizer, fuel or binder, and various additives. Some typical formulations of available solid propellants are reported in Table 25 along with the generalized properties for each type.

The oxidizer of a solid propellant may be an integral part or a discernible phase of the propellant mixture. It is generally composed of an organic nitrate or an inorganic compound such as the perchlorates and nitrates of ammonia and potassium. The organic nitrates are basically solid monopropellants, relatively unstable, and capable of oxidizing the organic material contained in its molecule. The most commonly used organic nitrates include glyceryl trinitrate, diethylene glycol dinitrate, and cellulose trinitrates. The crystalline inorganic nitrates are also used in certain solid propellants. Nitrates of sodium, potassium, and ammonia have been employed, and of these, ammonium nitrate has likely been used the most. It contains 20 weight percent of oxygen, has a density of 119 lb/ft³, and generates a smokeless, relatively nontoxic exhaust. Since its oxidizing potential is low, it has been used primarily for the slow burning, gas generator propellants. The best available oxidizers being employed today are of a perchlorate composition. Their available oxygen contents range from 34 weight percent for ammonium perchlorate to 66 weight percent for nitronium perchlorate. A strong preference has been shown for ammonium perchlorate because it is relatively insensitive to moisture, and it forms an exhaust that is not highly visible. This oxidizer, like all of the perchlorates, combusts with the fuel to produce chlorine-containing gases that are toxic and corrosive.

The fuels utilized in solid propellants have been composed of hydrocarbons or hydrocarbon derivatives, such as elastomeric polymers, synthetic resins, and cellulose-based materials. The selection criteria is generally based on their ability to be polymerized from a liquid to a semi-solid via catalysts or heat, oxidized to form a large volume of low molecular weight gases, impart desirable mechanical and processing properties; and their composition, mechanical and processing properties, low cost, and availability. The early cottonseed oil, modified asphalt fuels were inferior with respect to satisfying these

requirements. Such bituminous hydrocarbons had to be heated to obtain a liquid phase which was suitable for blending with the solid oxidizer. Upon cooling, the propellant became brittle and subject to cracking. Asphalt also contains a high percentage of aromatic rings, which limits the amount of available hydrogen working fluid. Elastomeric polymers were subsequently developed to alleviate these problems, and for the first time, a large family of suitable binders having dissimilar properties were made available. The use of elastomers also simplified the processing conditions in that they were available in liquid monomeric form. These unpolymerized materials were first mixed with the oxidizer, and with the aid of a catalyst (like sulphur) transformed to a high molecular weight, cross-linked, rubbery semi-solid. Cross-linking of the polymer was effected through the functional groups (hydroxyl, carboxyl, epoxy, or mercapto) contained on the hydrocarbon polymer structure. The first elastomer to find widespread use was ethyl formal polysulfide. Its thermosetting characteristic permitted it to be used as a case-bonded propellant. Its performance was not as good as the asphalt base binder, because of the high concentration of disulfide linkages and resultant high molecular weight, sulphur-containing exhaust products. Replacing the ethyl formal group with hydrocarbon linkages significantly increased the ballistic and physical properties. The next elastomeric binder to be investigated was the polyurethanes, which are the condensation product of polyols with isocyanate. They contained a higher percentage of oxygen in their polymeric structure, and thus less oxidizer was necessary for complete combustion. They also formed exhaust products of lower molecular weight. Unfortunately, the uncured polymer was so viscous it restricted the amount of additives that could be incorporated into the system. Additional limitations have been a tendency to crystallize at low temperatures, and a sensitivity to moisture in processing and storage, although marked improvements have recently been made. Polybutadiene acrylic acid was the next major advancement. Liquid prepolymers with lower viscosities were thus made available, which permitted higher solid loading of the propellant. Most of these hydrocarbon resin binders are

actually copolymers, such as butadiene-acrylonitrile, buta styrene, and buta methyl-vinyl pyridine. Although the performance of these matrices were superior to that of the polyurethanes, their physical properties were not as good. Further improvements were made, however, by placing the carboxy group on the terminal butadiene molecules. The resultant binder has exhibited good mechanical properties over an extremely wide temperature range and a capability of extremely high loadings (References 96 and 97). The chief problem with the carboxyl-terminated polymers are their sensitivity to composition and processing variables. Other polymeric binders are also under investigation for possible future uses. These include various epoxy resins and more recently the fluorocarbons and fluorohydrocarbons. The chief advantage in using fluorine in solid propellants is the resultant formation of high energy, gaseous metal fluorides as exhaust products. The impact of these recent developmental efforts has yet to be described in the open literature.

Solid propellants generally contain one or more additives, modifiers, inhibitors, plasticizers, or catalysts to impart certain ballistic or mechanical properties to the material. They have been used for increasing the specific impulse, diffusing radiant heat, improving the binder flexibility, increasing storability, altering the burning rate, enhancing combustion stability, increasing the wettability of the oxidizer, and a variety of other purposes. The use of metallic inclusions in solid propellants is well known (Reference 98). Their physical condition is generally that of micron-size particles, and more recently, of a filamentous nature for increased propellant strength (Reference 99). The chemical composition of these inclusions are highly purified aluminum, beryllium, magnesium, boron, and lithium. Up to 18-percent aluminum powder is generally used in a composite propellant to achieve an increased grain density, higher combustion temperature, and to alleviate certain types of unstable combustion conditions. Beryllium forms an oxide exhaust product of lower molecular weight, increased toxicity, and higher combustion temperature. Metal hydrides are also under consideration as

propellant additives, since they contain the highly desirable, low molecular weight hydrogen. Their stability is somewhat unpredictable, and they are chemically reactive with many propellant ingredients. Further research and developmental efforts will thus be necessary to exploit the utility of the metal hydrides. Perhaps the most troublesome problem associated with the metal additives is their condensed phase (liquid or solid) in the exhaust species. Added problems are thus encountered in higher heat transfer rates to the nozzle walls, and particle erosion of the thermal protection materials (References 100, 101, and 102).

The Internal Environment

The internal environment of a solid propellant motor is likened to that of a high temperature, high pressure vessel. Within its walls are the energetic products of chemical reactions, which must be contained and controlled to obtain thrust. The environmental variables within a solid rocket vary appreciably in magnitude and position. This fact is readily apparent from Figure 24, which is a schematic of the aft end of a core-burning, high performance motor.

The forward section and the cylindrical body of the motor case are subjected to full pressure forces developed by the hot gases. Heat transfer to some portions of the head-end insulator and the case liner is virtually nonexistent during the initial firing period because the propellant serves as an insulative barrier. Eventually the propellant burns through to the thermal insulator and thereafter, it is exposed directly to the hot exhaust gases. The time at which this occurs varies with the particular core geometry employed and the variability in propellant burning rate. Ideally, the flame front should not contact the insulator until the motor has served its intended purpose. As the combustion products move toward the aft end of the motor, they increase in velocity and decrease in pressure and temperature. These gases eventually come in contact with the thick insulator, which is located just aft of the propellant grain. Gases moving subsonically across the insulator's surface exert a shearing action at the gas-solid interface. The surface also experiences considerable heating and

thermochemical ablation during the motor firing, and some additional degradation during propellant burnout or tail-off. The exhaust stream then moves into the diverging entrance section of the nozzle, also known as the entrance cone. Thermal and mechanical aspects of the environment increase significantly, as evidenced by the higher surface heating rate and erosive forces. The flow undergoes maximum constriction in the throat region of the nozzle, and as a consequence, exposes the walls to the highest level of heating (2,000 Btu/ft²-sec or more), gas shear (600 lb/ft² or higher), and particle erosion (due to the metal content). As the gases leave the throat and pass into the exit cone, they undergo high expansion and a large increase in velocity. Heating rates to the exit cone walls decrease with distance from the throat, and in all cases, is of a relatively low magnitude. Nevertheless, the exit cone experiences added structural stresses because of high gas turbulence, shock wave interactions and effects, and acoustical vibrations.

From a chemical point of view, the internal environment of a solid propellant motor is composed of a wide variety of chemically active products of combustion and their dissociated species. A high degree of variance is also noted for the amount of any given specie at a particular location within the motor.

In Table 26, the major reaction products are given for six types of solid propellants. While these propellant gases may contain an appreciable amount of hydrogen, their overall composition is essentially chemically oxidizing. Certain components of the solid propellant are noted for greatly altering the equilibrium composition of products. For example, the presence and subsequent oxidation of aluminum to alumina resulted in a greatly reduced water content and a significant increase in the amount of available hydrogen. Modern day propellants generate significant quantities of other gaseous and condensed species which are reported in Table 26. Gaseous combustion products of importance are given in Table 27, along with the maximum volume percent concentration noted in any propellant investigated. At temperatures above 5,800°F, it is believed

that significant quantities of CN, C₂H₂, free radicals of C₂H, C₃H, and C₄H, and polyatomic gaseous carbon can exist in the exhaust stream. In addition to the gaseous species given, the combustion stream may contain entrained matter like alumina, beryllia, beryllium, carbon, aluminum nitride, and possibly others.

Materials of Construction

Rocket motors are constructed of composite materials (References 104 to 107) with each component material performing a specific function depending on its location. This type of construction is optimum, since the environmental conditions and hence the materials requirements vary greatly with motor position. With the aid of Figure 25, the materials requirements for different parts of the solid propellant motor shall be given. Typical material compositions shall be discussed.

The forward bulkhead (No. 1) of the motor case is exposed to stagnant but hot gases, and thus must be lined with an insulative material. The modulus of this insulator is low enough to transmit the chamber pressure into the external structural member. Insulators that are brittle tend to crack during the initial pressurization, with possible catastrophic burnthrough of the motor case wall. Insulators are composed of an elastomer-modified charring resin (like a copolymer of butadiene-acrylonitrile and phenolic) with various reinforcements and/or low conductivity fillers. The bulkhead insulator is generally premolded in segments and then adhesively bonded in place (Reference 57). In the cylindrical portion of the motor, a case liner (No. 2) is required to prevent corrosion of the structural case during storage and overheating during motor firing (Reference 109). Since the liner must transmit the chamber pressure forces into the structural case, it must possess flexibility, an elongation greater than the propellant, and high tensile strength. Optimum performance also requires that it have a low thermal conductivity, some erosion resistance, low density consistent with ablative and mechanical properties, low gas permeability, good bonding characteristics, compatibility with the propellant and the case, and a resistance to long-time aging effects (Reference 110). This

demanding combination of requirements along with a need for ease of fabrication and low cost are difficult (if not impossible) to achieve in a single material. The elastomers, by far, have been found to be most suitable. They are flexible and have elongations up to several hundred percent. As a result, they will follow (without cracking or bond separation) the shrinkage of a solid propellant during curing as well as the compressive loading during motor firing. The liner material is frequently very similar to that employed as the propellant binder, and is generally composed of a nitrile, urethane, butyl, or polysulfide rubber. To these elastomeric polymers are added various particulate and fibrous matter, such as powders of boric oxide, potassium oxalate, silica, alumina, carbon, or phenolic, and long fibers of asbestos, silica, or possibly carbon. These liners are applied to the motor case by conventional spray or centrifugal sling methods, or by hand rolling solid sheets to the interior of the case. In the aft end of the motor case, sidewall insulation (No. 3) is necessary in those areas exposed throughout the motor firing and those locations left exposed by recession of the propellant grain front. The materials used in these areas must have performance capabilities similar to the insulator in the forward bulkhead, except that improved erosion resistance is required because of the moving gas stream. In general, the sidewall insulator is composed of an elastomeric resin copolymer or charring rubber reinforced with various fibrous compositions. The external case (No. 4) of the rocket motor supports the mechanically and thermally induced stresses, which are due to internal gas pressure, vibration, acceleration, thrust vector control and differential thermal expansion of component materials. To accommodate these factors, the structural material should have high strength, adequate modulus, and resistance to buckling. Either a continuous glass-filament-wound epoxy plastic (Figures 21 and 22) or a high temperature metal (steel, titanium, or aluminum) case serves as the exterior structural member. Material requirements become more demanding as the gases move into the aft bulkhead section (No. 5) of the nozzle. Increased material rigidity, resistance to erosion, and thermal insulations are required. Some degree of surface recession is permitted, since its

influence on thrust is small. The aft bulkhead insulator is usually composed of a material similar to that employed in the case sidewall. Both elastomer-modified, thermosetting resins and heavily loaded rubber compositions have been employed with success. Figure 26 is an example of a filled elastomeric insulator for the aft bulkhead of a four nozzle solid propellant motor. The insulator was matched metal molded using a hydraulic press, and then bonded in the motor case. The divergent entrance cone (No. 6) of the nozzle must exhibit even greater erosion resistance because it is redirecting the propellant gases at a relatively steep angle. Refractories like metals, ceramics, and graphites are unsuitable for use in this section because of certain property limitations, and the configuration and size of the part. Instead, ablative plastic composites which form a surface char and possibly a viscous melt during heating appear to be optimum. They are composed of either phenolic or epoxy resins reinforced with fibers or fibrous constructions of asbestos, glass, silica, quartz, carbon, or graphite. The latter material in the form of a woven fabric or tape impregnated with phenolic resin has shown exceptionally good performance. Undoubtedly the most critical materials requirements are those of the nozzle throat. Its configuration and dimensions must remain essentially unchanged throughout motor firing to insure constant chamber pressure and thrust conditions. Small diameter throats (five inches or less) generally require the use of steel, molybdenum, tungsten, a high density graphite, with or without an oxide coating (No. 7) a metal carbide, a highly crystalline pyrolytic graphite (Reference 111), or a metal infiltrated porous refractory. Nozzle throat inserts (No. 8) of molybdenum and steel are most frequently used for short duration firings, while bulk graphite is much better for longer duration operations. When it is critical to maintain throat dimensions, a metal (like silver) infiltrated porous refractory (such as tungsten) is employed (References 112, 113, and 114). All of these materials are heavy, however, and possess certain other limitations. Molybdenum and tungsten are inherently brittle below their ductile to brittle transition temperatures (Reference 115). Graphites and carbides are brittle because their crystallographic

structures preclude plastic flow at low temperatures. Moreover, the carbides are very sensitive to thermal shock (Reference 89). The use of thermally conductive throat materials necessitates the addition of an insulative backup (No. 9) material. An example of this type of construction is shown in Figure 27, wherein a phenolic-asbestos fiber insulator has been molded around a graphite throat insert. The insulator should have a high thermal stability, little or no gasification at temperature, high strength, moderate to high modulus, high heat capacity, and moderate thermal conductivity. Asbestos- and silica-fiber-reinforced phenolics have many of these attributes, and thus have been used in virtually every application. Resin gasification at high temperatures presents a potential problem, and when encountered, a thin layer of fibrous oxide insulation is placed between the throat and the backup material. Ablative plastics are also used in the throat region of solid propellant motors when the firing duration is short, the chamber pressure is relative low, or the throat diameter is quite large (References 116 and 117). Such a throat section is shown in Figure 28 prior to machining. It is a phenolic-resin-impregnated-graphite tape, which has been wrapped on a mandrel and cured. It has a thickness of over five inches and a throat diameter of over three feet. An ablative nozzle throat of this type was successfully fired on a 1.2-million-pound thrust solid propellant motor. The test motor was 156 inches in diameter, burned 650,000 pounds of propellant, and operated 155 seconds. The firing demonstrated that a single or segmented bulk graphite throat is not required nor desired. Consequently, ablative plastic throats will be used on future three-million-pound thrust developmental engines (References 118 and 119).

Ablative plastics are also employed in the divergent exit cone region (No. 11 and 12). The material adjacent to the throat insert must have a high erosion resistance. It is therefore composed of a graphite- or carbon-fabric-reinforced-phenolic resin backed up with an insulative phenolic, silica-fabric laminate. The exit cone is usually prepared by a tape wrapping operation, as shown in Figure 29. Reinforcing fibers are oriented normal to the nozzle centerline or canted downstream (shingle layup). In the smaller

nozzles, compression-molded parts are generally adequate. Diced fabric (one-half-inch impregnated fabric squares) or chopped fibers are compacted by means of matched metal molding, autoclaving, or hydroclaving. Since the thermal severity of the exhaust stream decreases with distance from the nozzle throat, ablative materials having a good balance of insulative and erosion characteristics are employed. These materials are of a phenolic-resin composition with either silica-, glass-, or asbestos-fiber reinforcements. The fabrication process used is identical to that previously noted for the forward exit cone section, but in some cases, many involve a filament-wound plastic.

Jet vanes (Reference 120) and tabs (Reference 121) are sometimes employed in solid rocketry for thrust vector control. They are normally located behind the nozzle and protrude into the exhaust stream. Their basic purpose is to provide directional control at low missile speeds following launch, and at very high altitudes where air vanes become less effective. They offer the advantages of being reliable, simple in design, low in cost, and produce less than one percent thrust loss. Since the jet vanes and tabs are subjected to highly erosive environmental conditions, their service lives are generally short. Nevertheless, reinforced plastics have been found suitable for use in certain solid propellant motors. For other designs, alloys of tungsten and molybdenum are more promising.

Structural parts and control accessories in the aft region of a solid propellant motor may be overheated by thermal radiation from the exhaust gases and nozzle, recirculation of the combustion products, and afterburning of the fuel-rich gases. This base heating problem has been solved by the use of heat barriers in the aft end of the motor. They are generally constructed of a rigid plastic sandwich material overcoated with a metallic reflective film or an elastomeric coating. Heat barriers in the region of movable or gimballed nozzles require both flexibility and thermal protection, and for these areas, asbestos blankets coated with an elastomeric material has proved to be adequate.

In addition to the ablative materials employed in the primary propulsion systems, specialty purpose ablators are also required in the launching area of rocket motors. During ignition and take-off of the solid propelled vehicle, the launch equipment may be immersed in the exhaust plume for up to five seconds. Severe damage by heat and blast may result unless suitable thermal protection is afforded to the exposed areas. A number of ablative elastomeric coatings have been developed which exhibit a high degree of transient thermal protection, good adhesive properties, permanence characteristics, and ease of application. Millions of dollars of cables, hoses, umbilical cords, piping, electronic equipment, etc. have been saved from destruction by these coatings.

Materials Performance

The ablative performance of polymeric composite materials is generally obtained in subscale solid propellant motors. The motors are usually of the end-burning type, and offer considerable versatility with respect to length of firing period and the gas, chemistry, temperature, and pressure. Such motor evaluations are preferred in the industry because of their environmental simulation fidelity and their ability to scale-up test results to anticipated full-scale hardware. The subscale motor firings tend to be expensive, however, and frequently to reduce costs one must employ a simulator motor. Such motors closely simulate the exhaust of actual solid propellants by means of liquid, gaseous, and slurry (unpolymerized propellant) systems (Reference 122).

Elastomeric Insulation

A small evaluation test motor (ETM) was used to determine the ablative characteristics of a number of promising elastomeric composite materials. The propellant was an uncured mixture of polybutadiene, ammonium perchlorate and aluminum, weighing 32 pounds, which generated a theoretical flame temperature of 5,800°F. The motor was operated at a chamber pressure of 580 psig, for a duration of 45 seconds, at a mass flow rate of 3.5 lb/inch²-sec through the throat region. A forged tungsten throat insert was used to minimize loss of chamber pressure with firing time.

Table 28 gives the performance data obtained for a variety of commercially available, elastomeric insulators. The erosion rate of the liner material varied with both material composition and motor position, although the differences were small. Much higher erosion rates were obtained on these materials in the aft closure of the motor. In addition, a greater spread was obtained in the materials performance values. In view of the comparable erosion rates obtained, it appears that the choice of a case insulator or aft closure bulkhead material will be primarily based on considerations other than solely the erosion rate of the material.

Semi-Rigid Insulation

An end-burning solid propellant motor has been employed to determine the ablative characteristics of fiber-reinforced thermosetting polymers and filled elastomer-modified polymeric composites. A double based propellant of ammonium perchlorate, plasticized polyvinyl chloride, and different amounts of additives (such as aluminum) were employed to generate combustion products of varying chemical reactivity and a temperature range from 4,700° to 6,640°F. Eight test specimens having a 3 inch by 2 inch by 0.50 inch size were mounted around the inside face of an octahedral cylinder, and positioned within the rocket motor so that the hot propellant gases flowed parallel to the material surface. In this manner, direct comparative results on the various polymeric insulators were obtained with economy of operation. The experimental arrangement is shown in Figure 30, which is a post-firing photograph of some currently used case insulative materials. Note the differences in surface char retention, uniformity of ablation, and other discernible features. Additional performance features are given in Table 29 for selected compositions. In general, the performance of the insulator was significantly affected by the chemistry and constituents of the exhaust stream. Charring polymeric materials were the most sensitive to gas chemistry, while the silicone elastomer appeared to be little affected. The concentration of oxidizing species, which varied greatly in the propellant exhaust, apparently was the main contributory factor involved. With respect to the charring rate of the insulators,

a threefold difference was obtained. Char rates varied, from 1.9 to 5.9 mil/sec.

Rigid Ablators

As previously pointed out, fiber-reinforced plastics are seldom used in the throat region of small diameter solid propellant motors. Nevertheless, subscale motors are useful evaluation tools for determining the erosion and gas shear resistance of candidate ablaters. In a laboratory program (Reference 123) recently completed, a number of plastic composites were exposed in an end-burning, 8-inch-diameter, case-bonded, solid-propellant motor. Test specimens were fabricated in the form of a small nozzle, using various phenolic resins and carbon or graphite-fabric-reinforcements. The fabric was oriented perpendicular to the gas stream for maximum erosion resistance. The 5,560°F propellant gases were exhausted through a 0.6-inch-diameter-specimen throat for a firing period of 60 seconds. From the test data obtained, instantaneous surface regression rates were computed from the initial chamber pressure to the end of test. Data obtained in this manner are presented in Figure 31.

Erosion rates between 8 and 12 mils per second were obtained during the initial firing period and a chamber pressure of about 600 psia. At lower chamber pressures, the regression rate decreased accordingly. The polyamide modified phenolic reinforced with graphite fabric exhibited the best performance, followed by a substituted-phenolic-carbon-fabric, a phenolic-graphite-fabric, and a phenolic-carbon-fabric material in that order of increasing surface ablation rates.

While carbon- and graphite-fiber-reinforced phenolics generally exhibit the best performance in the throat region of solid propellant nozzles, the oxide-fiber-reinforced plastics also have utility. Reinforcing agents like silica are more resistant to oxidation, have a lower thermal conductivity, are less expensive, and more readily available in a variety of physical forms. Considerable information thus exists on the behavior of silica-fiber-reinforced-phenolic composites, and some representative data are shown in Table 30. The test specimens

were prepared in the form of a subscale nozzle configuration. It had a 30-degree half-angle entrance cone, a one-inch-diameter throat, and a 15-degree half-angle exit cone. The throat insets were fabricated of 25 weight percent phenolic resin and 75 weight percent silica fabric. They were compression molded under high pressure, with the reinforcement in an end-grain orientation. The remainder of the specimen was composed of a glass-fabric-reinforced-phenolic resin. After exposure of the nozzle specimens to the hot propellant exhaust, the average throat ablation rate was determined from direct linear measurements. The data given in Table 30 indicate that the ablation rate increases with the aluminum content of the propellant, the temperature and oxidant concentration of the exhaust products, and the motor chamber pressure. The specific influence of each of these factors will be discussed later.

Rigid thermosetting resins reinforced with various fibrous materials are also widely used in the exit cone of solid propellant nozzles. In laboratory tests conducted with subscale nozzle specimens, it has been found that either carbon- or graphite-fabric-reinforced phenolics exhibit the highest dimensional stability near the throat region. Conventional design is to use the more thermally stable graphite reinforcement in the throat region where dimensional stability is of paramount consideration. Carbon fabric is generally specified for the divergent and convergent areas adjacent to the throat, because its lower thermal conductivity (compared to graphite) coupled with adequate erosion resistance leads to a minimum weight design. Silica-fiber reinforcements are usually not used near the throat section because of shear removal of molten surface material. At nozzle area ratios of about 11 to 13, silica-fabric-reinforced phenolics exhibit the lowest ablation rate. This is shown in Figure 32.

Environmental Effects

Thermal Effects

All ablative materials undergo thermal degradation at elevated temperatures. The rate of material degradation depends strongly upon the surface temperature assumed, which

in turn is largely dictated by the incident heat flux. The surface heating rate, of course, is governed primarily by the flame temperature and the local pressure.

Polymeric materials may experience a number of thermally induced changes of state during ablation, such as melting, sublimation, gasification, or pyrolysis. Reinforcing agents or fillers present in an ablative composite may undergo similar reactions. The surface temperature of an ablating organic material is generally low, and its rate of ablation is usually high. The surface temperature of an ablator containing a melting component (like an oxide) will generally be much higher, and depending upon the heating rate, will plateau at a temperature slightly above its melting point. Once the melting point is exceeded, large increases in the heating rate have little influence on the surface temperature. Charring ablators can achieve the highest surface temperatures, often in excess of 5,000°F. Their surface temperature quickly adjusts in accordance with the incident heat flux.

Thermal stress failure is another possible effect of propulsion heating. It appears in the form of surface cracking during initial exposure of a material, or upon refiring of a previously exposed ablator. Confinement of high environmental temperatures to the surface region of the ablator results in very high thermal stresses, which may exceed the ultimate strength of the material. Thermal stress failure is seldom experienced in ablative polymeric materials, although it may be encountered in the newly formed surface char region of the ablator. Cracking due to high thermal stresses, however, is frequently noted in ablative ceramic and refractory compositions.

Chemical Effects

All propulsion materials are chemically reactive with the high temperature combustion products from solid propellants. While the chemical effects can not be separated from the previously described thermal effects in order to study them independently, it is clear that gas chemistry plays an important role in the ablation of materials.

As the temperatures encountered in solid propellant exhaust increases virtually all of the chemical species given in Table 27 are capable of reacting with the surfaces of ablating polymers. Past experience has shown, however, that the various oxidants present in an exhaust stream are particularly detrimental.

There is generally a limit as to the amount of oxidizer that can be combined with the fuel of a solid propellant. The mixture is thus fuel rich, and a considerable amount of hydrogen from the organic binder may appear in the exhaust products. This condition has led to the popular misconception that the exhaust products from solid propellants are chemically reducing. On the contrary, they generally contain a high percentage of oxidizing species (water vapor and carbon dioxide) as shown in Table 26.

At very high combustion temperatures, the chemical nature of the exhaust products increases in complexity. Dissociated products are formed, which are capable of both "reducing and oxidizing" (redox) reactions. Moreover, recombination of these highly reactive species at the wall is a possible source of intense and localized heating (due to the heat of recombination).

Most polymeric materials used in ablative propulsion composites will form a surface char during heating. This char structure is susceptible to thermochemical oxidation, which proceeds in a series of five steps: the convection or diffusion of oxidants to the surface, physical and chemical adsorption of reactants on the surface, gas-solid reaction, desorption of reaction products, and counter-diffusion and convection of the newly formed products into the exhaust stream. The slowest of these chemical and gas dynamic processes limits the rate of reaction. At temperatures below about 940°F, the process is usually limited by the rate of chemical reaction. Between about 940° and 2,740 F, the overall process is in a transition regime and none of the steps appear to be dominating. At higher surface temperatures, the gas dynamic processes overshadow the thermochemical oxidative processes. The reaction is then known as a diffusion controlled reaction.

Concentration of the oxidants in the exhaust stream will thus influence the surface regression rate of a charring ablator. The magnitude of this effect cannot be determined deductively, and hence laboratory studies and subscale firings are necessary. In one study conducted to date, several solid propellants were used to generate exhaust products having different concentrations of oxidizing species. The effect of these exhaust streams on the ablation rate of a graphite-fabric-reinforced phenolic-resin composite is shown in Figure 33. The surface regression rate increased with the concentration of oxidants, which is in accordance with theory. The effect was most pronounced at high chamber pressures. It is believed that water vapor exerted the major oxidative effect on the carbonaceous surface, and to a lesser degree, the carbon dioxide.

Chemical reactions at the ablating surface may also be significantly influenced by the presence of entrained matter in the exhaust stream. Particulate aluminum, for example, is converted to the corresponding oxide during propellant combustion, and thus reduces the concentration of available oxidants at the ablating wall. The aluminum particles may also interact with the ablating surface to form less desirable products. To illustrate, alumino-silicate has been detected in the exposed surfaces of an ablated silica-phenolic nozzle. This newly formed product is undesirable since it has a viscosity lower than that of the molten silica, and is therefore more susceptible to gas shear removal.

Mechanical Effects

Exhaust gases moving over an ablating surface produce a shear stress at the gas-solid or gas-liquid interface and a shear stress gradient in the surface material. These interface shear levels may range upwards to about 600 lb/ft² or more, thus imposing a severe mechanical force on the material. Microscopic pieces of the surface may thus be sheared away in what is commonly known as physical erosion. Heat contained in the eroded material is removed in the process, but this beneficial effect is counterbalanced by a number of unwanted features. First, the ablative material is inefficiently utilized since it is not in a

gaseous form when leaving the surface. Secondly, the particles or droplets sheared from the surface may impact on an ablating surface downstream and produce additional damage. Third, surface discontinuities are created which disturb the gas flow and alter the environmental parameters.

Spallation is the macroscopic loss of ablating surface material, due to mechanically induced failure, the combined action of mechanical and thermal stresses, or particle impact. This type of physical damage is most likely to occur in ablative polymers that form structurally weak surface chars, highly porous interface regions between the char and virgin material, or those devoid of a reinforcing agent. Material failure generally occurs at the char, virgin material interface, since this is the region of highest stress and greatest pore volume. Loss of material performance caused by spallation effects can be minimized, however, by adding a melting component (preferably a fiber) to the composite. Surface defects are thus continually filled with the flowing molten material, thus eliminating localized turbulence and excessive heating. This is not the case with charring ablaters like phenolic-graphite or epoxy-carbon. Surface defects produced during ablation tend to increase in size with exposure time.

Ablative gases trapped in the substrate of an ablator may produce still another form of spallation. Fillers like flakes or tightly woven fabric tend to induce spallation, whereas continuous filaments to the ablating surface provide a ready made path for the escape of substrate volatiles. If the latter approach is inadequate, one may resort to two different techniques. The first involves the use of low melting point fibers which will be preferentially ablated and thereby form the desired porosity in the composite. The second approach involves the drilling of holes of very small diameter perpendicular to the surface.

When the ablating surface contains a liquid phase, some of the material may be physically detached by spattering (Reference 126). Gas bubbles are formed in the liquid layer by material degasification, decomposition, or vaporization. If the bubbles burst violently,

droplets or irregular globules may be ejected into the boundary layer.

The presence of particles or entrained matter in the exhaust stream of a solid propellant are known to have important effects on the performance of ablative polymers. These effects include possible chemical reactions, surface fluxing, and added heat transport as previously noted, but in addition, may involve particle impact (Reference 127). The amount of erosion produced by the particles is a function of the flux density, mass, velocity, and angle of contact. The nature of the ablating surface is also important, particularly its roughness, strength, and ductility. The presence of a melt layer is especially helpful in dissipating the impact energy and thereby lowering abrasive damage.

Particle impact damage has been encountered in solid propellant nozzles, manifolds, thrust vector control systems, elbows, and bends. The damage has been attributed to alumina particles contained in the exhaust stream. In order to study the mechanism and magnitude of damage incurred by such materials, a small rocket motor was employed to evaluate various classes of materials. The end-burning motor (Reference 128) consisted of a high strength steel case, with an attached blast tube, elbow, and nozzle. It was operated at a chamber pressure of 1,300 psia for a period of 14 seconds. The propellant weighed about 26 pounds, contained two-percent aluminum, and burned at a flame temperature of 4,913°F. Candidate materials were evaluated in the elbow section of the motor just upstream from the nozzle throat. After exhausting alumina through the 45-degree elbow at a rate of 0.40 lb/sec inch², it had a characteristic gouge. Additional performance data on other classes of materials are given in Table 31. The refractory tungsten material had the lowest erosion rate, followed by graphite, phenolic-graphite, and phenolic-silica in that order of decreasing performance. The poor performance of the silica-containing phenolic was apparently due to rapid removal of the molten surface film during formation, thereby permitting considerable particle damage to the rigid surface material.

HYBRID PROPELLANTS

The hybrid propellant is a unique combination of a combustible liquid and solid phase material. It offers certain advantages of both the conventional liquid and solid rockets, such as: a wider selection of propellant combinations, thrust modulation in the range of 10 to 1, simple stop-start capability, specific impulse higher than that of existing solids, better mechanical properties in the solid fuel, impulse efficiencies over 93 percent, improved safety, regenerative cooling with the liquid phase, simpler logistics, and possibly others. Hybrid motors require additional developmental efforts, however, to improve their fuel utilization, loss of performance during throttling, and low fuel burning rates (References 129 to 132).

Although both solid and liquid fuels have been used in hybrid motors, better performance is generally obtained with a liquid oxidizer and a solid fuel. This type of hybrid motor is illustrated schematically in Figure 35.

The theoretical performance capabilities of hybrid propellants are apparent from the data presented in Table 32. The mass mixture ratio, specific impulse, bulk density, and combustion temperature are reported for a number of liquid oxidizers and solid fuels. Note that a high hydrogen content is characteristic of all of the fuels. Furthermore, all of the fuels may be classified as hydrides of carbon or a metal. The metal hydrides

are shown to be highly energetic, and because of their reactivity and poor mechanical properties, must be encapsulated within an organic binder. The presence of a hydrocarbon binder lowers the specific impulse of the fuel. As a first approximation, one may subtract one second of impulse for every weight percent of binder employed. Additional features of the hybrid propellants become evident by contrasting them with available solid propellants. Some of the hybrid propellants have a specific impulse value comparable to high performance solids, but in general, the former propellants are vastly superior. This is due to a more efficient oxidizer used in the hybrid propellant. The densities of the two propellant classes are similar. Flame temperatures, however, are markedly different. Some hybrid propellants have theoretical combustion temperatures up to 9,136°F.

While ablative polymeric materials appear to have considerable potential for the thermal protection of hybrid motors, related engineering experience has been limited to date. Satisfactory performance of ablative plastics has been obtained, although the reactivity of the fuel suggests future chemical corrosion problems for the elastomeric liner. The extremely high flame temperatures also indicate severe thermochemical ablation. Further research is obviously required to define the materials problems involved, and to formulate technical approaches for overcoming existing limitations of the ablaters.

THE FUTURE

The rate of technical progress precludes an accurate prediction of the potential of polymeric materials in future chemical propulsion systems. Certain conjectures and speculations can be made, however, from a knowledge of the past (Reference 134) and a consideration of the current research (References 135 and 136), new trends, and future possibilities. This approach is conservative by nature, since it can not account for the material breakthroughs which are sure to come. Perhaps if no other useful purpose is

served, the following predictions will help stimulate the thinking of others and possibly lead to new and unique approaches for solving the problems at hand.

As in the past, polymeric materials will continue to serve a major role in the thermal protection of chemical propulsion systems. Significant improvements in existing materials will be necessary, however, because of continuing advances in propulsion design and the ever-changing composition of

propellants. To achieve this goal, future research will be concentrated on improving the thermal efficiency, physical properties, age-life, reliability, space environmental resistance, and cost of polymeric materials.

Considerable potential still exists for improving the ablative efficiency of polymers. Advances beyond the current state-of-the-art will be achieved by synthesis of new structural units, modification of existing polymers, and through the use of fillers and reinforcing agents to compound and formulate until the desired balance of properties is achieved. Continued emphasis will be placed on the highly aromatic polymers, like the polyimides, polyphenylenes, polybenzimidazoles, and others. These resinous materials yield a very high percentage of residual char having good structural properties, and thus provide a high resistance to pressure forces and erosion by gas shear. New semi-organic, inorganic, and organo-metallic polymers will emerge from the research phase, and provide properties undreamed of heretofore. These polymers will likely be of the polyborazole (boron-phosphorous), phosphonitrilic (phosphorous-nitrogen), carborane, polyphosphoamides (phosphorous-carbon-phosphorous), polysiloxanes, triazines, phthalocyanine, ferrocene, and possibly others. It is anticipated that these materials will exhibit the thermochemical stability and oxidative resistance necessitated by future energetic propellants. Many of the newly prepared polymers will be infusible, insoluble, and difficult to work with. For that reason, they will have to be further modified with well known polymeric structures to obtain the necessary processibility, fabricability, and permanence features. New high temperature organic and refractory reinforcing agents will also become available to increase the strength, modulus, and erosion resistance of ablative composites. Refractory filaments will be produced by the chemical vapor plating process in compositions of carbon, graphite, metallic carbides, nitrides and borides. Whisker reinforcements with extraordinary mechanical properties will also be produced in pyrolytic graphite, alumina, boron carbide, silicon carbide, and similar refractory compositions. These specialty reinforcing agents should prove to be exceptionally useful in volume-limited applications, and where the ultimate in

materials performance is required. Other filler materials will be discovered or synthesized for use in resinous or elastomeric composites. Weight reductions up to 50 percent have been achieved with recently developed elastomeric case insulations, and similar performance increases can be expected by proper filling of future polymeric materials.

Reliability in materials performance has always posed problems for polymers and other organic materials. The problem is basically a need for complete familiarity with the material and its performance, and knowledge and ability to exactly reproduce it for each use. Technological needs, however, have generally forced the use of polymeric materials before adequate knowledge and design data were acquired. Moreover, the increased complexity of the propulsion thermal protection systems and the extreme operating conditions of temperature, vibration, and acceleration have tended to degrade reliability. The last few years, however, have produced a new breed of evaluative engineers and designers who are skilled in obtaining reliable design data, developing acceptance criteria, and utilizing this information in optimum designs. Ablative polymers thus have a bright future in military and manned systems wherein the utmost in reliability is demanded. To illustrate, the large solid propellant boosters being developed will employ plastics even in such critical areas as the nozzle throat.

Another important property of polymeric materials is their resistance to long-time storage here on earth and in space. During storage, they may experience the high temperatures of solar heating, the low temperatures of the arctic, the humidity of underground silos, the particle erosion of the desert, and other terrestrial factors. A satisfactory five years storage is difficult to obtain at the present time, but increased knowledge of the degradation mechanisms of polymeric materials should point the way to development of superior materials. With respect to the space environment, we note that some polymeric materials have faithfully served for several years in orbit. Interplanetary flights will require even longer periods of time and polymeric materials will

have to be made more resistant to high vacuum and space radiation through the use of newly developed additives. Atmospheric entry and landing of space probes on other planets will expose polymeric materials to a new environmental chemistry. Simulation studies are already underway to determine the suitability of polymers in these planetary gases, and from the information obtained, it appears that polymers will be one of the family of future space materials.

Chemical propellants will continue to serve as the work horse of the propulsion systems. Undoubtedly, there will be widely diversified efforts to improve the technology, extend the capability, and increase the technical understanding of chemical propellants and related engine systems. There are indications that the specific impulse level of liquid propellants has reached a plateau, and further improvements will be difficult, costly, and technically limited by the chemical binding energies of the propellants and exhaust products. The theoretical impulse level of present day cryogenic and storable propellants is about 350 (see Table 6). The propellants being considered in future high performance engines have specific impulses of about 450, although a value of 536 is possible in the tri-propellant class. Solid propellant technology has also entered a phase of consolidation rather than discovery (Reference 137). The sea level specific impulse of available solid propellants is somewhat lower than that of the liquids, e.g., about 250 for an aluminized composite material (see Table 24). Improved solid propellants under development will deliver up to about 265 seconds impulse, and, for the far future, impulse levels up to about 340 seconds are theoretically possible. Hybrid propellants currently being developed have a sea level specific impulse of about 300 seconds, with increased performance to about 400 seconds (see Table 31) in the far future. Their efficiency will undoubtedly be tempered by the progress made in developing more energetic liquid oxidizers and solid fuels. These developments in propellant technology will undoubtedly create new problems of chemical corrosion, thermochemical ablation, and mechanical erosion of the container

and inert parts employed in propulsion systems. Nevertheless, the development of polymeric materials having chemically non-reactive surfaces, the utilization of the environment to create inert refractory surfaces, and the combination of ablative cooling with other forms of thermal protection will provide the necessary solutions. A second engineering approach toward the achievement of higher propellant efficiency is the use of higher chamber pressures. This trend will increase the demand for propulsion materials having higher strength, lower gas permeability, and a higher resistance to thermal radiation. These problems are not insurmountable, and as we have witnessed in the past, new polymeric matrices and composite materials will be developed to meet the challenges posed. A third and highly promising approach for increased propulsion performance is the use of materials of lighter weight. In this respect, plastics and elastomers with their inherently low densities will provide new opportunities for the engine designers. Perhaps a good illustration is the plastic skirt with the high-expansion ratio which is being developed for future magapound thrust engines.

Not all of the chemical propellants employed in the future will generate hot exhaust products. Small control rockets are being developed, which exhaust a sublimed vapor through a nozzle. The rate of gas generation would likely be controlled by solar or thermoelectric heating of the solid propellant to give up to 0.1 pound thrust under start-stop and throttleable conditions. Control rockets of this type could be constructed almost entirely of reinforced plastics and elastomeric materials.

While the previously mentioned basic approach will yield higher performance ablative polymers and composites thereof, additional engineering approaches will also be pursued. It appears highly likely that ablative cooling can be combined with other forms of thermal protection to yield a highly efficient system. For example, ablative coatings could provide transient protection for refractory metal tubing used in regeneratively cooled liquid

propulsion engines. Film cooling of refractory metal inserts in solid propellant nozzles could be accomplished by upstream degradation of some ablative polymer. Forced transpiration cooling of a porous pyrolyzed plastic suggests still a third feasible example.

In summary, polymeric materials have solved critical engineering problems associated with chemical propulsion systems. With continued development of new polymers and their use, we can look forward with confidence to new vistas in propulsion.

REFERENCES

1. C. Lyons and D. Lawson, "Ablative Characteristics of Reinforced Plastics in Nozzles and Thrust Chambers for Varying Environments," Applications of Plastic Materials in Aerospace, D. Simkins, Ed., Chem. Eng. Prog. Symp. Series No. 40, Vol. 59, Amer. Inst. of Chem. Eng., New York City, 1963, pp. 33-38.
2. D. Schmidt, "Ablation," Engineering Design for Plastics, E. Baer, Ed., Reinhold, New York City, 1964, pp. 815-868.
3. W. Lucas and J. Kingsbury, "The ABMA Reinforced Plastics Ablation Program," Modern Plastics 38, 135 (1960).
4. D. Schmidt, "Ablative Rocket Cooling," Space/Aeronautics 39, 94 (June 1963).
5. D. Schmidt, "Ablative Re-Entry Cooling," Space/Aeronautics 37, 64 (February 1962).
6. I. Gruntfest and L. Shenker, "Ablation," Intern. Sci. and Techn. 19, 48 (July 1963).
7. D. Schmidt and H. Schwartz, "Evaluation Methods for Ablative Plastics," SPE Trans. 3, 238 (October 1963).
8. S. Scala, "A Study of Hypersonic Ablation," Proceedings of the Xth International Astronautical Congress, F. Hecht, Ed., Vol. 2, Springer Verlag, Vienna, 1960, pp. 790-827.
9. L. Roberts, "A Theoretical Study of Stagnation-Point Ablation," NASA TR R-9, 1959.
10. L. Lees, "Ablation in Hypersonic Flows," Seventh Anglo-American Aeronautical Conference, V. Tavtlian, Ed., Inst. Aero. Sci., New York City, 1959, pp. 344-362.
11. H. Meyers and D. Harmon, "Energy Transfer Processes in Decomposing Polymeric Systems," High Temperature Resistance and Thermal Degradation of Polymers, S. C. I. Monograph No. 13, MacMillan, New York City, 1961.
12. D. Spalding, "Heat and Mass Transfer in Aeronautical Engineering," Aeron. Quart. XI, 105 (May 1960).
13. S. Scala and L. Gilbert, "Thermal Degradation of a Char-Forming Plastic During Hypersonic Flight," ARS J., 32, 917 (June 1962).
14. R. Rosensweig and N. Beecher, "Theory for the Ablation of Fiberglass-Reinforced Phenolic Resins," AIAA J., 1, 1802 (August 1963).
15. K. Kratsch, L. Hearne, and H. McChesney, "Thermal Performance of Heat Shield Composites During Planetary Entry," Engineering Problems of Manned Interplanetary Exploration, Vol. of Tech. Papers, AIAA, New York City, 1963.
16. H. Hurwicz, "Aerothermochemistry Studies in Ablation," Combustion and Propulsion Fifth AGARD Colloquium, R. Hagerty, A. Jaumotte, O. Lutz, and S. Penner, Ed., Pergamon Press, Oxford, 1963, pp. 403-455.
17. S. Ruby, J. Cohen, and F. Ward, "Behaviour of Plastic Laminates at Elevated Temperatures," Planetary and Space Sci. 3, 68 (February 1961).

REFERENCES (Cont'd)

18. M. Carey "Experimental Chemical Kinetic Effects in Ablative Composites," C. Coulbert, 6th Liquid Propulsion Symposium, Los Angeles, Calif., 23-25 Sept 1964.
19. N. Beecher and R. Rosensweig, "Ablation Mechanisms in Plastics With Inorganic Reinforcements," ARS J. 31 532 (April 1961).
20. G. Ehlers, "Thermal Stability," Engineering Design for Plastics, E. Baer, Ed., Reinhold, New York City, 1964, pp. 400-436.
21. H. Hoercher and B. Mitchel, "The Development of Ablative Nozzles, Part II. Ablative Nozzle Concept, Scaling Law, and Test Results," Proc. of the IAS National Meeting on Large Rockets, Inst. Aerospace Sci., New York City, 1962, pp. 106-116.
22. T. O'Connor and H. Hoercher, "Prediction of Ablative Behavior in Rocket Nozzles," 5th Liquid Propulsion Symposium, Tampa, Fla., 13-15 (November 1963).
23. S. Tick, G. Huson, and R. Griese, "Design of Ablative Thrust Chambers and Their Materials," Paper No. 64-261, 1st AIAA Annual Meeting, Washington, D. C., 29 June-2 July 1964.
24. W. Kuby, "The Internal Environment of a Solid Propellant Rocket Nozzle," No. 64-158, AIAA Solid Propellant Rocket Conference, Palo Alto, Calif., 29-31 January 1964.
25. S. Lafazan and B. Siegel, "Ablative Thrust Chambers for Space Applications," Applications of Plastic Materials in Aerospace, D. Simkins, Ed., Chem. Eng. Prog. Symp. Series No. 40, Vol 59, Amer. Inst. of Chem. Eng., New York City, 1963, pp. 39-50.
26. R. Kendall and R. Rindal, "Analytical Evaluation of Rocket Nozzle Ablation," Paper No. 64-101, AIAA Solid Propellant Rocket Conference, Palo Alto, Calif., 29-31 Jan 1964.
27. G. Sutton, Rocket Propulsion Elements, 3rd ed., Wiley, New York City, 1963, p. 181.
28. C. Thalen, "Materials Requirements for Storable Liquid Propellant Rocket Motors," Materials Science and Technology for Advanced Applications, D. Mash, Ed., Prentice-Hall, Englewood Cliffs, N. J., 1962, p. 29.
29. Anon., "U. S. in Space," Chem. & Eng. News, 41, 70 (30 September 1963).
30. C. Coulbert, "Selecting Cooling Techniques for Liquid Rockets for Spacecraft," J. of Spacecraft and Rockets, 1, 129 (March-April 1964).
31. M. Cardullo, "Chemical Rocket Engines for Altitude Control of Space Vehicles," Paper No. 2701-62, ARS 17th Annual Meeting and Space Flight Exposition, Los Angeles, Calif., 13-18 Nov. 1962.
32. O. Romaine, "Secondary Rockets," Space/Aeronautics, 39, 83 (May 1963).
33. H. Burlage, "Liquid Propulsion," Space/Aeronautics, 41, 60 (February 1964).
34. E. Haberman, "Liquid Rocket Propellant Technology Moves Forward," CEP 60, 72 (July 1964).

REFERENCES (Cont'd)

35. R. Beichel, "Liquid Rockets," *Space/Aeronautics*, 42, 39 (September 1964).
36. Anon., Rocket Engine Liquid Propellants, Rocketdyne-NAA Publication 573-A-2, Rev. 3-64, 1964.
37. R. Fio Rito, "Engine Design Aspects for Ablatively Cooled Hypergolic Pulse Rockets," 5th Liquid Propulsion Symposium, Tampa, Fla., 13-15 Nov 1963.
38. E. Bartlett, "A Systematic Method for Determination of Ablation Rates in a Corrosive Environment," Ballistic Missile and Aerospace Technology, Vol. III, Propulsion, Space Science, and Space Exploration, C. Morrow, L. Ely, and M. Smith, Ed., Academic Press, New York City, 1961, pp. 103-119.
39. W. Kaufman, W. Armour, and L. Green, "Thermal Protection of Fluorine-Hydrogen Thrust Chambers by Carbonaceous Materials," *ARS J.* 32, 1600 (October 1962).
40. E. Bartlett, "Thermal Protection of Rocket-Motor Structures," *Aerospace Eng.* 22, 86 (January 1963).
41. W. Boam, "Fabricating the Titan Propulsion System," *Metal Progr.* 79, 83 (March 1961).
42. Anon., "Ablative Thrust Chamber Technology," *Reinforced Plastics* 6 (November-December 1963).
43. D. David, "A State-of-the-Art Report on Ablative Thrust Chamber Technology," *Plastics Design & Processing* 3, 20 (August 1963).
44. W. Lehman and I. Glick, "Uncooled Thrust Chambers for Liquid Prepackaged Propulsion System," 5th Liquid Propulsion Symposium, Tampa, Fla., 13-15 November 1963.
45. J. Lovingham and M. Luperi, "Injectors and Combustion Chambers for $OF_2-B_2H_6$," 6th Liquid Propulsion Symposium, Los Angeles, Calif., 23-25 September 1964.
46. Anon., "Thiokol Fires Throttleable, Ablative Motor," *Aviation Week and Space Techn.*, 77, 91 (26 November 1962).
47. R. Osborn, "Effect of Chamber Pressure on Ablation Rate of a Packaged Liquid Thrust Chamber," Packaged Liquid Propulsion Symposium, Washington, D. C., 16 October 1962.
48. J. Lee and J. Hahn, "Regression Rate of Char Front in Ablative-Cooled Rocket Motor Under Pulse Operation," Paper No. 64-262, 1st AIAA Annual Meeting, Washington, D. C., 29 June - 2 July 1964.
49. R. Fio Rito, "Ablatively Cooled Pulse Rocket Engine Design," Paper No. 64-260, 1st AIAA Annual Meeting, Washington, D. C., 29 June - 2 July 1964.
50. S. Tick and G. Huson, "Analytical Study of Ablative Thrust Chambers with Pulsing," 6th Liquid Propulsion Symposium, Los Angeles, Calif., 23-25 September 1964.
51. C. Plattner, "Apollo Service Module Engine Beginning Pre-Qualification," *Aviation Week & Space Techn.* 81, 42 (27 July 1964).

REFERENCES (Cont'd)

52. I. Grunfest and L. Shenker, "Behavior of Reinforced Plastics at Very High Temperatures," Modern Plastics **35**, 155 (June 1958).
53. D. Wizansky and E. Russ, "An Oxyacetylene Flame Apparatus for Surface Ablation Studies," U. Calif. Tech. Report HE-150-167, 28 January 1959.
54. D. Wizansky, E. Russ, and W. Gledt, "An Oxyacetylene Flame Apparatus for Surface Ablation Studies," U. Calif. Tech. Report HE-150-171, 26 May 1959.
55. H. Perry, H. Anderson, and F. Mihalow, "Behavior of Reinforced Plastics Surfaces in Contact with Hot Gases. Part III: Experiments," Technical Papers of the 15th Annual SPE Technical Conference, C. Rhine and J. Day, Ed., Vol. V, SPE, New York City, 1959, p. 70-1.
56. H. Plant and M. Goldstein, "Plastics for High Temperature Thermal Barriers," Preprint Book of the 15th Annual SPI Technical and Management Conference, SPI, New York City, 1960, Section 18-D.
57. S. Prosen, M. Kinna, and R. Barnet, "The Development of a Reliable Insulation for Solid Propellant Rocket Motors," Technical Papers of the 17th Annual SPE Technical Conference, Vol. VII, SPE, New York City, 1961, p. 26-4.
58. C. Whipple, D. Peper, and F. Smith, "Silicones for Ablative Applications," Preprint of the Seventh National SAMPE Symposium on Adhesives and Elastomers for Environmental Extremes, Section 16, Los Angeles, Calif., 20-22 May 1964.
59. W. Bobear and T. Gair, "Thermal Insulative Features of Silicone Rubber," Preprint of the Seventh National SAMPE Symposium On Adhesives and Elastomers for Environmental Extremes, Section 18, Los Angeles, Calif., 20-22 May 1964.
60. M. Schwartz, W. Bandaruk, and G. Mills, "Evaluation of Ablation Materials for High Temperature Application," SAE Preprint No. 98T, SAE National Aeronautic Meeting, Los Angeles, Calif., 5-9 October 1959.
61. W. Bobear and T. Gair, "Thermal Insulative Tests for Silicone Rubber," Rubber World **150**, 35 (July 1964).
62. S. Herzog and W. Donaldson, "Ablation and Erosion in the Missile Environment," Presented at the Third Pacific Area National Meeting of the ASTM, San Francisco, Calif., 11-16 October 1959.
63. H. Perry, "Reinforced Plastics Pierce Heat Barrier," Materials Res. & Std., **1**, 122 (February 1961).
64. A. Fisher, M. Kinna, F. Koubek, and R. Barnet, "The Performance of Selected Plastics Materials in a High Temperature Environment," NAVWEPS Report 7390, 1 March 1962.
65. F. Koubek, "High Temperature Resistant Materials for Missile Propulsion Systems," NOL TR 63-3, 30 January 1963.
66. R. Headrick, "Ablative Elastomeric Insulation Materials," ASD TDR 62-400, August 1962.

REFERENCES (Cont'd)

67. J. Walton and M. Bowen, "The Evaluation of Ceramic Materials Under Thermal Shock Conditions," Mechanical Properties of Engineering Ceramics, W. Kreigel and H. Palmour, Ed., Interscience, New York City, 1961, p. 157.
68. C. Murray, "Ablation of Phenolics in Oxygen-Hydrogen Exhaust," Technical Report No. 90, Western Plastics, 23, (November 1962).
69. G. Sherrard and C. Murray, "The Materials Used In Aerospace Applications for Plastics," SAE Paper 684A, SAE-Amer. Soc. of Naval Eng., National Aero-Nautical Meeting, Washington, D. C., 8-11 April 1963.
70. F. Baltakis, D. Hurd, and R. Holmes, "Effects of High Temperature, High Velocity Gases on Plastic Materials," WADC TR 59-459, June 1960.
71. G. Epstein and H. King, "Plastics for Rocket Motor Nozzles," Ind. Eng. Chem. 52, 764 (September 1960).
72. G. Epstein and J. Wilson, "Reinforced Plastics for Rocket Motor Applications," SPE J. 15, 473 (June 1959).
73. J. Rollbuhler, "Experimental Investigation of Rocket-Engine Ablative Material Performance After Postrun Cooling at Altitude Pressures," NASA TN D-1726, June 1963.
74. D. Robbins and R. Kremith, "Thermal Erosion of Ablative Materials," AST TDR 63-254, March 1963.
75. D. Robbins and R. Kremith, "Thermal Erosion of Ablative Materials, Part II," ASD TDR 63-254, July 1963.
76. G. Boyd and K. Hoffman, "Simulated Rocket Environments for Materials Screening," Technical Papers of the Annual SPE Tech. Conf. Vol. VIII, SPE, Stamford, Conn., 30 January-2 February 1962, p. 1-1.
77. J. Vogan, "Thermal Protective Surfaces for Structural Plastics," WADD TR 60-110, July 1960.
78. M. Adams and E. Scala, "The Interaction of High Temperature Air with Materials During Re-Entry," International Symposium on High Temperature Technology, McGraw-Hill, New York City, 1960, pp. 54-60.
79. M. Adams and E. Scala, "Ceramic Heat Shielding for ICBM Re-Entry Vehicle," Ceramic Industry 74, 128 (April 1960).
80. G. Sutton, "Ablation of Reinforced Plastics in Supersonic Flow," J. Aero/Space Sci. 27, 377 (May 1960).
81. J. Cavanaugh and J. Sterry, "Heat Protective Ablative Coatings for Radomes," WADD TR 60-507, August 1960.
82. R. Rowley, "An Experimental Investigation of Uncooled Thrust Chamber Materials For Use in Storable Liquid Propellant Rocket Engines," JPL TR 32-561, 15 February 1964.

REFERENCES (Cont'd)

83. T. Hughes, "Ablative Thrust Chamber Feasibility," Aerojet-General Corp. Report 652/SA4-2.2-F-1, Vol. 1, 28 June 1963.
84. H. Blaes, et al., Unpublished data, Philco Research Laboratories, Newport Beach, Calif., 1964.
85. B. Dawson and R. Schreib, "Investigation of Advanced High Energy Space Storable Propellant Systems, OF_2/B_2H_6 ," Reprint 63-238, AIAA Summer Meeting, Los Angeles, Calif., 17-20 June 1963.
86. A. Zaehring, "Plastics for Solid Propellants," *Modern Plastics* 38, 225 (May 1961).
87. R. Geckler and K. Klager, "Solid-Propellant Rocket Engines," Handbook of Astronautical Engineering, H. Koelle, Ed., 1st ed. McGraw-Hill, New York City, 1961, p. 19-2.
88. H. Ritchey and J. McDermott, "Solid Propellant Rocket Technology," Advances in Space Science and Technology, F. Ordway, Ed., Vol. 5, Academic Press, New York City, 1963, p. 47-86.
89. E. Kirchner, "Solid Rockets," *Space/Aeronautics* 42, 44 (September 1964).
90. A. Jaumotte, "Rocket Propulsion Elements," Rocket Propulsion, M. Barrere, A. Jaumotte, B. de Veubeke, and J. Vandekerckhove, Elsevier, New York City, 1960, p. 7.
91. J. Shafer, "Solid Rocket Propulsion," Chapter 16, Space Technology, H. Seifert, Ed., Wiley, New York City, 1959, p. 16-05.
92. M. Summerfield, J. Shafer, H. Thackwell, and C. Bartley, "Applicability of Solid Propellants to High-Performance Rocket Vehicles," *Astronaut.* 7, 50 (October 1962).
93. I. Stone, "Five-Segment Motor Tested Successfully," *Aviation Week & Space Techn.* 79, 52 (29 July 1963).
94. M. Farber, "Fluorine Solid Propellants," *Astronaut.* 5, 34 (August 1960).
95. G. Sutton "Solid Propellants," Rocket Propulsion Elements, 3rd. Ed., Wiley, New York City, 1963, p. 336-337.
96. C. Herty, "Making Solid Propellants," *Chem. Eng.* 71, 85 (February 1964).
97. J. McDermott, "The Role of High Polymers in Composite Solid Rocket Fuels," *Rubber Age*, 83, 807 (August 1958).
98. S. Blackman and D. Kuchl, "The Use of Binary Light Metal Mixtures and Alloys as Additives for Solid Propellants," Preprint 1595-61, ARS Solid Propellant Rocket Conf., Salt Lake City, Utah, 1-3 Feb. 1961.
99. Anon., "Wire-Reinforced Solid Rocket Test-Fired," *Aviation Week & Space Techn.* 81, 58 (26 October 1964).
100. S. Morizumi and H. Carpenter, "Thermal Radiation From the Exhaust Plume of an Aluminized Composite Propellant Rocket," Preprint No. 64-61, AIAA Aerospace Sciences Meeting, New York City, 20-22 January 1964.

REFERENCES (Cont'd)

101. S. Colucci, C. Gracey, and R. Fairall, "Experimental Determination of Nozzle Heat Transfer Coefficients With Aluminized Propellants," Preprint 1606-61, ARS Solid Propellant Rocket Conf., Salt Lake City, Utah, 1-3 February 1961.
102. D. Kurtovich and G. Pinson, "How to Find the Exhaust Heat Radiation of Aluminized Solid Rockets," Space/Aeronautics **36**, 66 (July 1961).
103. J. Batchelor, J. Simmons, and W. West, "Chemical Reactions Between Plastic Composite Materials and Propellant Exhaust Products," ASD TDR 63-737, Volume 1, August 1963.
104. W. Hourt, "Plastics as Heat Insulators in Rocket Motors," Ind. Eng. Chem. **52**, 761 (September 1960).
105. D. Rosato, "Plastics in Missiles: Part I. An Introduction to Current Uses of Plastics," British Plastics **33**, 348 (August 1960).
106. D. Rosato, "Non-Metallic Composite Materials and Fabrication Techniques Applicable in Present and Future Solid Rocket Bodies," Preprint No. 1613-61, ARS Solid Propellant Rocket Conference, Salt Lake City, Utah, 1-3 February 1961.
107. E. Gilchrist, "Plastics in Missiles. Part 5: Materials for Nozzle Insulation," British Plastics **33**, 359 (August 1960).
108. G. Fust and A. Kays, "Low Cost Insulation for Rocket Motors," Proceedings of the 19th Annual SPI Technical and Management Conference, SPI, New York City, 1964, Sec. 20-D.
109. R. Jones and S. Eglin, "Solid Rocket Liner and Insulation Materials," ARS Paper No. 2244-61. October 1961.
110. G. Epstein and E. Jaffe, "Materials for Internal Thermal Protection of Rocket Motor Cases - A State-of-the-art," Preprints of the 17th Annual Tech. and Management Conf., SPI, New York City, 1962, Sec. 7-C.
111. J. Campbell and C. Coulbert, "Pyrolytic Refractories for Rocket Thrust Chambers," 5th Liquid Propulsion Symposium, Tampa, Fla., 13-15 November 1963.
112. S. Baranow and R. Hiltz, "The Application and Performance of Infiltrated Tungsten Structures as Inserts in Solid Propellant Rocket Nozzles," Paper No. 2413-62, ARS Launch Vehicles: Structures and Materials Conference, Phoenix, Arizona, 3-5 April 1962.
113. F. Gessner, J. Seader, R. Ingram, and T. Coultas, "Analysis of Self-Cooling with Infiltrated Porous Tungsten Composites," J. Spacecraft and Rockets **1**, 643 (November-December 1964).
114. P. Schwarzkopf and E. Weisert, "Self-Cooled Rocket Nozzles," Paper No. 64-129, AIAA Solid Propellant Rocket Conference, Palo Alto, Calif., 29-31 Jan. 1964.
115. E. Olcott and J. Batchelor, "Failure Mechanisms in Dense Tungsten Alloy Rocket Nozzles," J. Spacecraft and Rockets **1**, 635 (November-December 1964).
116. I. Stone, "HITCO Producing 120-In. Motor Nozzles," Aviation Week & Space Techn. **81**, 66 (20 July 1964).

REFERENCES (Cont'd)

117. Anon., "Huge Hydroclave Works on Massive Titan III Exit Cones," *Missiles and Rockets* 13, 28 (23 September 1963).
118. Anon., "New LPC 156-In. Test Succeeds," *Missiles and Rockets* 14, 11 (5 October 1964).
119. C. Plattner, "Subscale Motors to Verify 260-In. Design," *Aviation Week & Space Techn.* 80, 40 (22 June 1964).
120. R. Ahearn, "Development of Jet Vanes for Solid Propellant Missiles," SAE Paper 520D, SAE National Aeronautic Meeting, New York, N. Y., 3-6 April 1962.
121. H. Hohlstein, "Jet Tab Thrust Vector Control," AIAA Solid Propellant Rocket Conference, Palo Alto, Calif., 29-31 January 1964.
122. W. Jones, "Solid Propellant Exhaust Simulation," *AIAA J.* 1, 721 (March 1963).
123. Unpublished data, Aerojet-General Corp., 1964.
124. J. Batchelor, N. Vasileff, S. McCormick, and E. Olcott, "Insulation Materials for Solid Propellant Motors," WADD TR 60-109, Part II. August 1961.
125. J. Wilhelm, "Ablation of Refrasil-Phenolic Nozzle Inserts in Solid Propellant Exhaust Environments," Paper No. 64-223, 1st AIAA Annual Meeting, Washington, D. C., 29 June-2 July 1964.
126. B. Steverding, "Theory of Liquid Ablation," USAMC Report No. RR-TR-63-24, 22 October 1963.
127. E. Ungar, "Particle Impacts on the Melt Layer of an Ablating Body," *ARS J.* 30, 799 (September 1960).
128. L. Cothran and S. Barnes, "Behavior of Plastic and Refractory Materials in the Particle-Impingement Areas of Solid Propellant Ducting Systems," Paper No. 64-224, 1st AIAA Annual Meeting, Washington, D. C., 29 June-2 July 1964.
129. D. Ordahl, "Hybrid Propulsion," *Space/Aeronautics* 41, 108 (April 1964).
130. D. Ordahl and W. Rains, "Hybrid Propulsion for Advanced Missions, Recent Developments, Current Status, and Future Outlook," Paper No. 64-226, 1st AIAA Annual Meeting, Washington, D. C., 29 June-2 July 1964.
131. A. Wahlquist and G. Panelli, "Some Aspects of the Applications of Hybrid Propulsion Systems," Paper No. 64-225, 1st AIAA Annual Meeting, Washington, D. C., 29 June-2 July 1964.
132. J. Gustavson, "The Hybrid Rocket Motor and Its Unique Capabilities," Paper No. 1167-60, ARS Semi-Annual Meeting, Los Angeles, Calif., 9-12 May 1960.
133. R. Kraemer, "Liquid-Propellant Propulsion Systems," Handbook of Astronautical Engineering, H. Koelle, Ed., 1st Ed., McGraw-Hill, New York City, 1961, p. 20-47.
134. D. Schmidt and R. Tomashot, "Aeronautics and Rocketry," *Reinforced Plastics* 3, 12 (November-December 1964).

REFERENCES (Cont'd)

135. H. Schwartz, "New Materials and Physical Constructions for Ablative Use," High Temperature Technology, Butterworths, Washington, D. C., 1964, p. 447-469.
136. D. Schmidt, "Advances in Ablative Plastics and Composites Research," AIAA Sixth Structures and Materials Conference, Palm Springs, Calif., 5-7 April 1965.
137. I. Silver, "Solids → A New Challenge," Astronautics & Aeronautics 2, 60 (December 1964).

TABLE 1

POLYMERIC MATERIALS FOR PROPULSION ENVIRONMENTS

Major Property of Interest	Type of Polymer	Propulsion System Application
Ablative	Phenol-Formaldehyde	Charring resin for rocket nozzle
Chemically resistant	Fluorosilicone	Seals, gaskets, hose linings for liquid fuels
Cryogenic	Polyurethane	Insulative foam for cryogenic tankage
Adhesive	Epoxy	Bonding reinforcements on external surface of combustion chamber
Dielectric	Silicone	Wire and cable electrical insulation
Elastomeric	Polybutadiene acrylonitrile	Solid propellant binder
Power transmission	Diesters	Hydraulic fluid
Specific strength	Epoxy novolac	Resin matrix for Filament-Wound motor case
Thermally nonconductive	Polyamides	Resin modifier for plastic thrust chamber
Absorptivity: emissivity ratio	Alkyd-Silicone	Thermal control coating
Gelling agent	Polyvinyl chloride	Thixotropic liquid propellant

TABLE 2

ADVANTAGES AND LIMITATIONS OF ABLATIVE PLASTICS AND ELASTOMERS

ADVANTAGES
Accommodates intense heating
Thermally insulates substrate
No maximum service temperature
Passive in operation
Resistance to thermal shock
Large number of available materials
Lightweight
Low cost
Ease of fabrication
Design simplicity
Short Lead time
Nonstrategic materials
LIMITATIONS
Susceptible to mechanical damage
Efficiency decrease with long exposure times
Efficiency decrease in presence of very high temperature, chemically corrosive species
NOTE: Some data are from Reference 2.

TABLE 3

ENVIRONMENTAL VARIABLES WHICH INFLUENCE ABLATIVE PERFORMANCE

Thermal Parameters	Mechanical Parameters	Chemical Parameters
Temperature Gas enthalpy Mode of heat transfer Total heat load Shape of heat pulse Peak heating rate Heating time	Pressure Shear Abrasion Vibration Deceleration Acceleration	Reactivity Oxidation Reduction
NOTE: Some data are from Reference 7.		

TABLE 4

MATERIAL PROPERTIES AND CHARACTERISTICS WHICH INFLUENCE THE ABLATIVE PERFORMANCE

POLYMER	
Elemental composition	Glass transition temperature
Structure	Temperature of thermal decomposition
Molecular weight	Heat of decomposition
Degree of crosslinking	Thermophysical and thermodynamic properties
CURING AGENT OR CATALYST	
Elemental composition	Percent retained in polymer
REINFORCING AGENT AND FILLERS	
Elemental composition	Temperature of thermal decomposition
Physical form	Heats of Phase changes
Orientation in composite	Thermophysical and thermodynamic properties
FORMULATION AND COMPOUNDING	
Ratio of material components	Temperature, time, and pressure
COMPOSITE	
Uniformity of material distribution	Presence of defects, voids, extraneous matter
ABLATIVE PRODUCTS	
Solid residue	Gaseous products
Percent formed	Percent formed
Elemental composition	Elemental composition
Mechanical properties	Thermal diffusion coefficient
Porosity and pore distribution	Specific heat
Thermal conductivity	Residence time in residue

TABLE 5
POST-EXPOSURE MEASUREMENTS ON ABLATED MATERIALS

Type of Measurement	Technique	Information Obtained
<p>Profile changes Surface roughness</p>	<p>Silhouette photography micrometers Optical profilometer, and Brush analyzer</p>	<p>Total linear changes Possible localized spalling</p>
<p>Chemical composition</p>	<p>Elemental chemical analysis</p>	<p>Presence of newly formed compounds Composition of surface residue Secondary pyrolysis, evidence of Most volatile components in composites</p>
<p>Density</p>	<p>Volume displacement (beads) Mercury displacement</p>	<p>Mass per unit volume of discrete zones</p>
<p>Porosity and pore spectra</p>	<p>Mercury intrusion under pressure</p>	<p>Open and closed cell porosity Pore size and distribution</p>
<p>Surface area</p>	<p>Nitrogen adsorption</p>	<p>Degree of surface reactivity Presence of very small diameter pores</p>
<p>Microstructure</p>	<p>Resin impregnation and photomicrography</p>	<p>Cell wall structure Zones of reaction</p>
<p>Compressive strength</p>	<p>Micro-structural test</p>	<p>Stress-strain curve</p>
<p>Hardness</p>	<p>Rockwell hardness test</p>	<p>Resistance to ball indentation and recovery</p>
<p>X-Ray reflection</p>	<p>X-Ray reflection</p>	<p>Degree of crystallinity Identification of newly formed compounds</p>

NOTE: Most of the data are from Reference 7.

TABLE 6
THEORETICAL PERFORMANCE OF LIQUID PROPELLANTS

Oxidizer	Fuel	Mass Mixture Ratio, O/F	Specific Impulse, sec ^a	Bulk Density, gm/cc	Combustion Temperature, °F	Approximate Costs, \$/lb
<u>Cryogenic</u>						
O ₂	H ₂	4.50	456	0.31	5,012	0.26
O ₂	H ₂ -Be (50/50)	0.92	536	0.24	4,721	25.00
F ₂	H ₂	9.00	475	0.50	6,388	2.48
FLOX ^b	H ₂	5.38	461	0.35	5,331	1.00
<u>Earth Storable</u>						
O ₂	RP-1	2.67	354	1.02	5,682	0.02
O ₂	N ₂ H ₄	0.95	368	1.07	5,311	0.53
F ₂	RP-1	2.64	379	1.21	6,452	1.92
F ₂	N ₂ H ₄	2.34	424	1.31	7,298	2.15
F ₂	NH ₃	3.31	416	1.12	7,086	2.04
FLOX (30/70)	RP-1	3.80	399	1.20	7,172	0.90

TABLE 6 (Cont'd)
THEORETICAL PERFORMANCE OF LIQUID PROPELLANTS

Oxidizer	Fuel	Mass Mixture Ratio, O/F	Specific Impulse, sec	Bulk Density, gm/cc	Combustion Temperature °F	Approximate Costs, \$/lb
<u>Earth Storable</u>						
<u>Earth Storable</u>						
N_2O_4	N_2H_4 -UDMH (50/50) ^c	2.08	340	1.21	5,252	0.37
N_2O_4	N_2H_4	1.40	342	1.22	5,108	0.47
N_2O_4	MMH ^d	2.28	340	1.21	5,300	0.99
N_2O_4 -NO(75/25)	MMH	2.39	340	1.18	5,336	0.95
IRFNA ^e	MMH	2.63	324	1.24	4,904	0.91
H_2O_2	N_2H_4	2.09	337	1.26	4,598	0.75
H_2O_2	MMH	3.63	336	1.26	4,678	1.15
N_2H_4	B_5H_9	1.16	401	0.63	4,012	6.26
ClF_3	N_2H_4	2.90	338	1.51	6,108	0.92
ClF_3	MMH	3.00	331	1.44	5,579	2.63
<u>Space Storable^f</u>						
<u>Cryogenic</u>						
OF_2	H_2	7.00	465	0.43	5,774	7.03

TABLE 6 (Cont'd)
THEORETICAL PERFORMANCE OF LIQUID PROPELLANTS

Oxidizer	Fuel	Mass Mixture Ratio, O/F	Specific Impulse sec	Bulk Density, gm/cc	Combustion Temperature °F	Approximate Costs, \$/lb
<u>Space Storable</u>						
<u>Earth Storable</u>						
OF ₂	RP-1	3.80	396	1.28	7,114	6.01
OF ₂	N ₂ H ₄ -UDMH(50/50)	2.29	400	1.26	6,525	5.77
OF ₂	MMH	2.49	401	1.26	6,627	2.75
N ₂ F ₂	N ₂ H ₄	3.24	387	1.43	6,978	-
N ₂ F ₂	RP-1	3.63	352	1.34	6,139	-
<u>Space Storable</u>						
OF ₂	B ₂ H ₆	3.82	429	1.00	7,054	16.88

NOTE: Most data are from Reference 36.

CONDITIONS: a. 150 psia chamber pressure, vacuum 40:1 expansion, shifting equilibrium, b. Fluorine-Oxygen mixture, c. Unsymmetrical dimethyl hydrazine, d. Monomethyl hydrazine, e. Inhibited red fuming nitric acid, f. Normal boiling point above -238°F, and g. Stable at 77°F.

TABLE 7

ELASTOMERIC POLYMERS IN AN OXY-ACETYLENE FLAME

Composition	Ablation Rate mil/sec	Insulation Index $I_{200^{\circ}\text{C}}$, sec	Ablative Performance Index
Epoxy	14.0	11.0	284
Silicone	14.8	14.5	210
Chlorosulfonated, Polyethylene	21.7	9.0	482
Butadiene -Acrylonitrile, Polyvinyl chloride	22.3	9.7	501
Chloroprene	22.4	8.0	560
Vinylidene fluoride, hexafluoropropylene	23.6	8.7	554
Butadiene- acrylonitrile(NBR)	25.3	10.0	505
Urethane	28.2	8.0	709

NOTE: Data are from References 57, 64, 65.

CONDITIONS: Specimen 4 inches by 4 inches by 0.25 inch in a chemically neutral flame having a temperature of $5,500^{\circ}\text{F}$, with a surface heating rate of $550 \text{ Btu/ft}^2\text{-sec}$.

TABLE 8

BUTADIENE-NBR COMPOSITES IN AN OXY-ACETYLENE FLAME

Composition, parts by wt.	Ablation Rate, mil/sec	Insulation Index I _{200°C} sec	Ablative Performance Index
NBR-100	25.3	10.0	505
NBR-10, phenolic-90,	3.3	44.0	15
NBR-50, phenolic-50	4.3	39.1	22
NBR-10, phenolic-90, asbestos fiber-20	4.1	46.3	18
NBR-10, phenolic-90, aluminum silicate fiber-20	4.0	53.7	15
NBR-10, phenolic-90, silica fiber-20	4.2	60.9	14
NBR-100, fine silica-60	9.7	20.0	97
NBR-100, fine silica-45, boric oxide-15	5.3	51.4	21

NOTE: Data are from References 64 and 65.

CONDITIONS: Specimen 4 inches by 4 inches by 0.25 inch in a chemically neutral flame, a temperature of 5,500°F, and a surface heating rate of 550 Btu/ft²-sec.

TABLE 9
ELASTOMERIC COMPOSITES IN AN OXY-ACETYLENE FLAME

Major Polymer in Vulcanizate ^a	Vulcanizate Density, gm/cc	Oxidizing Flame ^b		Neutral Flame ^c Ablation Rate, mil/sec	Reducing Flame ^d Ablation Rate, mil/sec
		Weight Loss %	Ablation Rate, mil/sec		
Silicone	1.24	13.4	6.6	15.5	3.9
Cyanosilicone	-	5.8	7.1	-	-
Silicone-RTV	1.15	11.1	8.1	11.1	2.9
Polysulfide-ST	1.45	17.8	9.5	9.1	1.7
Polysulfide-FA	1.55	24.7	10.2	-	-
Vinyl pyridine-NBR	1.35	22.9	11.4	-	-
Isobutylene-isoprene (sulfur cure)	1.13	20.5	12.6	18.0	11.9
Tetrafluoroethylene	2.15	22.3	13.0	16.3	13.5
Chlorosulfonated polyethylene	1.33	28.8	13.5	11.1	14.0
Vinylidene fluoride- chlorotrifluoroethylene	2.02	25.9	13.7	-	-
Isobutylene-isoprene (resin cure)	1.12	26.0	13.9	18.8	13.7
Acrylonitrile-butadiene (NBR, high nitrile)	1.22	26.7	15.2	-	-

TABLE 9 (continued)

Major Polymer in Vulcanizate	Vulcanizate Density, gm/cc	Oxidizing Flame		Neutral Flame Ablation Rate, mil/sec	Reducing Flame Ablation Rate, mil/sec
		Weight Loss, %	Ablation Rate, mil/sec		
Chlorinated butyl	1.13	26.2	15.5	-	-
Brominated butyl	1.15	30.5	15.9	-	-
Ethylene propylene	1.03	26.6	15.9	-	-
Fluorinated silicone	1.42	21.0	16.1	-	-
Polyethylene	0.93	34.4	16.2	19.5	18.8
Urethane	1.29	26.3	16.5	-	-
Ethyl acrylate	1.36	25.1	16.6	-	-
NBR (medium nitrile)	1.17	24.6	16.7	18.2	16.0
Urethane	1.20	28.0	16.7	-	-
Styrene butadiene	1.12	29.7	16.7	7.9	15.4
Natural Rubber	1.13	32.5	17.6	-	-
Vinylidene fluoride hexafluoropropylene	1.93	37.5	19.2	19.8	19.3
Chloroprene	1.45	53.8	23.7	22.9	4.5

NOTE: Data are from Reference 66.

CONDITIONS: a. Specimen 2 inches by 2 inches by 0.50 inch. b. 5,700°F flame with a heating rate of 630 Btu/ft²-sec.
 c. 5,300°F flame with a heating rate of 390 Btu/ft²-sec. d. 5,000°F flame with a heating rate of 173 Btu/ft²-sec.

TABLE 10

THERMOPLASTIC POLYMERS IN AN OXY-ACETYLENE FLAME

Polymer	Ablation Rate mil/sec	Insulation Index $I_{200^{\circ}\text{C}}$ sec	Ablative Performance Index
Polyhexamethylene, adipamide	14.4	-	-
Methyl Methacrylate (acrylic)	17.6	11.6	303
Polyoxymethylene (acetal)	19.1	11.1	344
Polycarbonate	19.2	8.4	459
Ethyl Cellulose	20.5	10.8	379
Polystyrene	20.5	10.8	379
Polytetrafluoroethylene	20.6	11.8	352
Polypropylene	23.5	9.1	519
Polytrifluorochloroethylene	24.2	10.1	480
Polyethylene	26.5	9.4	565

NOTE: Data are from References 64 and 65.

CONDITIONS: Specimen 4 inches by 4 inches by 0.25 inch in a chemically neutral flame, a temperature of 5,500°F, and a surface heating rate of 550 Btu/ft²-sec.

TABLE 11

A PHENOLIC POLYMER AND COMPOSITES IN AN OXY-ACETYLENE FLAME

Composition, wt. %	Ablation Rate, mil/sec	Insulation Index I _{200°C} , sec	Ablative Performance Index
REFERENCE MATERIALS			
1010 Steel	13.2	6.0	440.0
ATJ Graphite	0.4	2.2	36.3
POWDER FILLED COMPOSITES			
Phenolic-100	4.4	39.6	22.2
Phenolic-40, zirconia-60	5.1	38.8	26.0
Phenolic-40, alumina-60	5.3	28.3	36.0
FIBER REINFORCED COMPOSITES			
Phenolic-40, graphite fabric-60	1.0	24.1	8.3
Phenolic-Amide copolymer-40, asbestos mat-60	2.5	90.5	6.0
Phenolic, silica fabric	2.7	59.0	9.2
Phenolic-Furfural-40, asbestos mat-60	3.1	80.4	8.0
Phenolic-40, asbestos mat-60	3.6	57.3	13.0
Phenolic, quartz fiber	5.7	22.0	51.8
Phenolic-39, glass fabric-60	7.6	21.8	70.0
Phenolic, nylon fabric	15.6	58.0	46.0

NOTE: Data are from References 64 and 65.

CONDITIONS: Specimen 4 inches by 4 inches by 0.25 inch in a chemically neutral flame having a temperature of 5,500°F, with a surface heating rate of 550 Btu/ft²-sec.

TABLE 12
 ABLATIVE PHENOLIC COMPOSITES IN OXY-HYDROGEN EXHAUST

Composition, wt. %	Density, lb/ft ³	Molding Pressure, psi	Exposure Time, sec	Mass Ablation Rate, gm/cc	Linear Ablation Rate, in/sec	Backface Temperature, °F
FABRIC LAMINATES						
Phenolic-33, silica-67	107	1,000	60	0.13	0.0012	425
Phenolic, glass, ceramic powder	-	1,000	23	-	0.0147	Burnthrough
Phenolic-39, carbon-61	76	15	20	0.50	0.0113	Burnthrough
Phenolic, carbon-69, ceramic powder	76	15	30	0.46	0.0100	Burnthrough
Phenolic-43, graphite-57	89	1,000	44	0.81	0.0070	Burnthrough
FABRIC-MOLDED COMPOSITES^a						
Phenolic-30, silica-70	103	100	60	0.33	0.0013	1,730
Phenolic-33, silica-67	108	1,000	60	0.29	0.0013	1,160
Phenolic-33, silica-67	108	1,000 ^b	60	0.22	0.0014	2,310

TABLE 12 (Cont'd)
 ABLATIVE PHENOLIC COMPOSITES IN OXY-HYDROGEN EXHAUST

Composition, wt. %	Density lb/ft ³	Molding Pressure, psi	Exposure Time, sec	Mass Ablation Rate, gm/sec	Linear Ablation Rate, in/sec	Backface Temperature, °F
Phenolic-Buna N-42, silica-58	97	100	60	0.31	0.0011	2,350
FIBER-FILLED COMPOSITES						
Phenolic-28, silica-72	93	100	60	0.32	0.0015	1,570
Phenolic-Buna N, silica	-	1,000	58	-	0.0044	Burnthrough
Phenolic, carbon	-	1,000	31	-	0.0085	Burnthrough
Phenolic, asbestos	-	1,000	29	-	0.0086	Burnthrough
Silicone-35 silica-65	-	100	60	0.08	0.0015	2,400

NOTE: Data are from References 68 and 69.

CONDITIONS: a. One-half inch squares. b. Post cured.

TABLE 13

ABLATIVE PLASTIC CONES IN OXY-HYDROGEN EXHAUST

Composition, wt. %	Reinforcement Orientation To Gas Stream	Material Density lb/ft ³	Linear Ablation Rate ^{a,b} in/sec	Mass Ablation Rate ^{a,c} gm/sec
Phenolic-25, silica fiber-75	Parallel	104	0.000	0.38
Phenolic-28, asbestos fiber-72	Random	115	0.018	2.84
Phenolic-42, asbestos fiber-58	Random	104	0.020	3.70
Phenolic-21, silica fabric-79	Perpendicular	116	0.021	1.21
Phenolic-42, asbestos fiber-38, glass frit-20	Random	102	0.025	3.30
Phenolic-38, glass fabric squares-62	Perpendicular	114	0.029	4.03
Phenyl Silane-36, glass fabric-64	Perpendicular	121	0.057	3.24
Phenolic-53, nylon fabric squares-47	Perpendicular	74	0.058	5.61
Polytetrafluoroethylene-75, alumino silicate fiber-25	Parallel	132	0.061	9.77
Phenolic-48, cotton fabric squares-52	Perpendicular	84	0.073	6.00

NOTES: Data are from Reference 70.

a. Based on six firings of two seconds duration each.

b. Stagnation point value.

c. Based on entire model

TABLE 14
 ABLATIVE PLASTICS IN OXY-HYDROGEN EXHAUST

Composition ^a , wt. %	Throat Density, lb/ft ³	Firing Time, sec	Linear Ablation Rate ^c , in./sec	Mass Ablation Rate ^d , gm/sec	Char Depth ^c , in.	Relative Performance Index ^e
HOMOGENEOUS PLASTICS						
Polyethylene-100	60	1.4	0.104	18.8	0.0	9.38
Epoxy-100	77	1.6	0.091	10.9	-	10.45
Phenolic-100	-	2.7	0.054	-	-	-
POWDER-FILLED COMPOSITES						
Polytetrafluoro- ethylene-15, magnesia-85	-	0.8	0.181	47.5	-	14.9
Phenolic-20, alumina-80	-	2.0	0.073	37.8	-	7.02
FIBER-REINFORCED COMPOSITES						
Phenolic-41, asbestos-59	109	3.8	0.038	4.17	0.050	2.93
Phenolic-49, silica 0.5 inch-51	92	8.9	0.016	3.28	0.125	1.46
Phenolic-30, silica, 0.5 inch-70	95	9.9	0.015	3.00	0.098	1.17

TABLE 14 (Cont'd)
 ABLATIVE PLASTICS IN OXY-HYDROGEN EXHAUST

Composition wt. %	Throat Density, lb/ft ³	Firing Time, sec	Linear Ablation Rate, in/sec	Mass Ablation Rate, gm/sec	Char Depth, in	Relative Performance Index
Phenolic-34, silica, 1 inch-66	95	11.2	0.013	3.33	0.093	1.03
Phenyl silane-35, quartz-65	99	10.9	0.013	2.84	0.125	1.06
FABRIC-REINFORCED COMPOSITES						
Reference Standard, phenolic-30 silica-70	100	11.2	0.013	3.15	0.093	1.00
Phenyl silane-27, silica-73	106	12.8	0.011	3.21	0.125	0.84
Phenolic-38, glass-62	100	5.2	0.028	10.4	-	2.70
Phenolic-35, graphite-65	81	7.8	0.019	2.59	0.300	1.41
Phenolic-40, graphite squares-60	85	7.7	0.019	2.66	0.200	1.43
Phenolic-40, carbon fabric-60	85	8.8	0.017	6.99	0.270	1.37
Phenolic-30, nylon-70	72	4.1	0.035	16.3	0.0	2.75

TABLE 14 (Cont'd)

ABLATIVE PLASTICS IN OXY-HYDROGEN EXHAUST

Composition wt. %	Throat Density, lb/ft ³	Firing Time, sec	Linear Ablation Rate, inch/sec	Mass Ablation Rate, gm/sec	Char Depth, Inch	Relative Performance Index
Epoxy novolac-25, silica-75	106	11.2	0.013	4.73	0.125	1.00
Furfuraldehyde-41, graphite-squares-59	82	6.3	0.023	3.15	0.200	1.75
Phenolic-35, graphite-31, silica-34	92	9.9	0.015	2.24	0.200	1.11
Phenolic-35, graphite-57, zirconia powder-8%	91	9.8	0.015	2.74	0.250	1.11

NOTE: Data are from References 74 and 75.

- a. Fibers oriented normal to the gas stream.
- b. Time for a radial throat erosion of 0.145 inch, which drops the chamber pressure from 500 to 200 psia.
- c. Throat region.
- d. Average specimen ablation per unit time,
- e. Specimen firing time divided by reference specimen (silica-fabric-reinforced phenolic) firing time.

TABLE 15

ABLATIVE PERFORMANCE OF MATERIALS IN OXY-KEROSENE EXHAUST

Composition	Linear Ablation Rate, mil/sec ^b	Mass Ablation Rate, gm/sec ^b
PLASTICS^a		
Phenolic Resin	35.6	1.105
Phenolic, graphite fabric	14.2	0.520
Phenolic silica fabric	16.4	1.254
Phenolic, silica fabric, zirconia powder	18.4	1.184
Phenolic, aluminum silicate fiber, graphite powder	23.7	1.083
Phenolic, quartz fiber	24.3	0.398
Epoxy, silica fabric	24.7	1.535
Phenolic, glass fabric	37.4	1.352
Phenolic, asbestos fiber	38.1	1.401
Phenolic, aluminum silicate fiber	40.0	1.302
Epoxy, glass fabric	-	2.320
ELASTOMERS		
Acrylonitrile butadiene, phenolic powder	35.6	0.990

TABLE 15 (continued)

ABLATIVE PERFORMANCE OF MATERIALS IN OXY-KEROSENE EXHAUST

Composition	Linear Ablation Rate, mil/sec	Mass Ablation Rate, gm/sec
Acrylonitrile-butadiene, silica fibers	31.7	0.461
CERAMICS		
Graphite-ATJ	10.3	0.059
Magnesia	6.0	0.080
Magnesia, stainless steel honeycomb	29.2	1.820
<p>NOTE: Data are from Reference 77.</p> <p>a. Nominal 35% resin content. b. Five second exposure.</p>		

TABLE 16
ABLATION OF REINFORCED PLASTICS IN SUPERSONIC OXY-ETHYL ALCOHOL EXHAUST

Resin ^a	Reinforcement	Specific Gravity	Calorimetric Heating Rate, Btu/ft ² -sec	Surface Brightness Temperature, °F _b	Stagnation Point Ablation Rate, inch/sec	Effective Heat of Ablation Btu/lb	Effective Thermal Diffusivity ft ² /hr x 10 ⁻⁶
Melamine	Glass fabric	1.81	1,085	2,290	0.053	2,200	-
Phenolic	Glass Fiber	1.86	988	2,560	0.041	2,500	-
Phenolic	Asbestos Mat	1.78	962	2,630	0.042	2,500	0.98
Phenolic	Aluminum silicate fiber	1.83	898	2,810	0.048	1,900	1.64
Phenolic	Silica fabric	1.63	908	2,790	0.017	6,400	1.47
Phenolic	Glass fabric, 0.5-inch squares	1.84	1,085	2,290	0.042	2,700	2.52
Silicone	Glass fiber	1.93	755	3,210	0.039	1,900	2.68
Silicone	Asbestos mat	1.88	877	2,870	0.077	3,310	3.31
Silicone	Aluminum silicate fiber	1.80	782	3,140	0.042	2,000	0.92
Silicone	Silica fabric	1.65	782	3,140	0.015	6,300	-
Silicone	Glass fabric 0.5 in. squares	1.88	860	2,920	0.044	2,000	1.25

NOTE: Data are from Reference 80

a. 33% resin,

b. Optical pyrometric measurement.

TABLE 17

ABLATIVE PLASTICS IN OXY-GASOLINE COMBUSTION PRODUCTS

Resin, wt %	Filler, wt %	Ablative Surface Temperature, °F	Mass Ablation Rate, gm/sec
Phenolic-35 ^a	Silica fabric-65	3,300	0.020
Phenolic-35	Quartz fabric-65	3,200	0.030
Phenolic 35 ^a	Glass fabric-65	1,650	0.04
Phenolic-30	Aluminum silicate fiber-70	1,900	0.04
Phenolic-35 ^a	Quartz fiber-65	3,400	0.07
Polytetra- fluoroethylene-30	Asbestos fiber-70	-	0.19
Phenolic-50 ^a	Nylon fabric-50	2,100	0.19
Polytetra- fluoroethylene-100		-	0.21
Epoxy-100		-	0.40
Polystyrene-100		-	0.43
Epoxy-41	Zirconia powder-59	-	0.45
Epoxy-30	Alumina powder-70	-	0.53
Epoxy-10	Alumina powder-90	-	0.53
Nylon-100		-	0.62
Epoxy-67	Silicon carbide powder-33	-	0.65

NOTE: Data are from Reference 81.

a. Estimated values.

TABLE 18

ABLATIVE PERFORMANCE OF PLASTIC NOZZLES IN A $N_2O_4-N_2H_4$ -UDM¹ PROPELLANT ENVIRONMENT

Composition, Fiber Orientation ^a	Firing Duration, sec	Throat Ablation, mil/sec ^b	Throat Char Depth, Inch	Throat Area Change, %	Chamber Pressure Ratio ^c
Phenolic, silica fabric, 60° volcanic ash	303	-	0.42	-4	1.00
Phenolic, silica fabric, 90°	300	-	0.60	-4	1.00
Phenolic, silica fabric, 60°	301	-	0.55	-14	0.86
Phenolic, silica fabric squares, 90° volcanic ash	301	-	0.57	-7	0.98
Phenolic, silica fabric squares, 90°	301	-	0.66	-12	0.92
Phenolic silica fiber, 90°	251	0.05	0.41	+7	1.05
Phenolic, graphite fabric, 60°	117	0.41	0.70	+23	1.29
Phenolic, zirconia fiber	114	0.39	0.34	+24	-
Phenolic, graphite fabric, 90°	82	0.49	0.60	+21	1.24
Phenolic, graphite fabric squares, 90°	42	1.00	0.39	+22	1.29
Phenolic, asbestos fiber, 60°	30	1.3	0.09	+20	1.26
Pyrolytic graphite- ATJ graphite	300	0.3	-	+5	1.05
Graphite-ATJ	160	0.26	-	+22	1.24

NOTE: Data are from Reference 81.

- a. Angle between major fiber axis and nozzle axis. b. Based on radius change.
c. Initial chamber pressure divided by final chamber pressure.

TABLE 19
 PERFORMANCE OF ABLATIVE PLASTIC THRUST CHAMBERS IN $N_2O_4-N_2H_4$ -UDMH

Materials Composition		Firing Duration, sec	Chamber Region		Throat Region	
Chamber	Throat		Mass Ablation Rate gm/sec	Char Constant ^a (in^2/sec) ^{1/2}	Linear Ablation Rate mil/sec	Char Depth inch
Phenolic-polyamide-25% silica roving-75%	Tantalum carbide coated graphite	152.0	1.18	0.0439	0.715	0.52
Phenolic-polyamide-25% silica roving-75%	Pyrolytic graphite washers	147.0	1.42	0.0494	0.729	0.57
Silicone, silica tape	Graphite	113.5	1.17	0.0300	0.925	0.31
Phenolic-33% magnesia fiber-57% asbestos fiber-10%	Graphite	108.0	1.67	0.0187	0.885	0.19
Phenolic-polyamide-25% silica roving-75%	Tantalum-90 tungsten-10	107.0	2.08	0.0488	1.120	0.55
Phenolic-50% asbestos felt-50%	Graphite	81.0	2.61	0.0200	1.315	0.27
Phenolic-polyamide-25% silica roving-75%	AIJ-graphite	49.0	5.25	0.0513	1.155	0.35
Phenolic-polyamide-20% silica tape-80%	Same	86.7	0.80	0.0472	1.405	0.35

TABLE 19 (Cont'd)
 PERFORMANCE OF ABLATIVE PLASTIC THRUST CHAMBERS IN $N_2O_4-N_2H_4$ -UDMH

Material Composition		Firing Duration, sec	Chamber Region		Throat Region	
Chamber	Throat		Mass Ablation Rate, gm/sec	Char Constant, (inch ² /sec) ^{1/2}	Linear Ablation Rate, mil/sec	Char Depth, inch
Phenolic-30% silica tape-70%	Same	78.0	0.82	0.0458	1.480	0.39
Phenolic-polyamide-40%, silica tape-60%	Same	75.2	1.04	0.0379	1.485	0.28
Phenylaldehyde-25%, silica roving-75%	Same	60.5	-	0.0470	2.040	0.32
Phenyl silane-elastomer-35%, silica tape-65%	Same	52.0	0.98	0.0353	1.915	0.30
Phenolic-40%, graphite tape-60%	Same	48.5	2.08	0.0733	2.750	0.62
Phenolic-35%, carbon fiber-65%	Same	36.0	2.14	0.0575	3.500	0.35
Phenolic-50%, asbestos felt-50%	Same	20.0	1.80	0.0234	6.95	0.04

NOTE: Data are from Reference 83.

- a. The square root of the thermal diffusivity times a constant.
- b. Measured at end of firing period.

TABLE 20

ABLATIVE PERFORMANCE OF PHENOLIC-SILICA THRUST CHAMBERS
IN N_2O_4 - N_2H_4 -UDMH EXHAUST PRODUCTS

<u>Engine Performance</u>					
Chamber pressure, psia.	150	150	150	100	100
Thrust, lb.	150	150	150	3,000	3,000
Oxidizer: fuel ratio	2.0	2.0	2.0	2.1	1.8
Firing duration, sec.	40	60	195	260	420
Combustion efficiency, %	94	96	100	99	99
<u>Materials Performance (inches)</u>					
Chamber char depth	0.24	0.32	0.55	0.30	0.64
Chamber erosion	0.0	0.0	0.0	0.0	0.0
Throat char depth	0.2	0.23	-	0.50	0.48
Throat erosion	0.12	0.17	-	0.33	0.84
NOTE: Data are from Reference 23.					

TABLE 21

ABLATIVE PERFORMANCE OF PLASTIC THRUST CHAMBERS IN A FLUORINE-HYDRAZINE
EXHAUST

Materials Compositions, wt.%	Firing Time, sec	Char Rate, mil/sec ^a		Erosion Rate, mil/sec ^b	
		Station A	Station B	Station A	Station B
Phenolic-31, silica fabric-69	45.5	11.0	9.2	7.0	4.8
Modified phenolic-30, silica fabric-70	45.5	14.9	10.3	8.8	5.9
Phenolic-30, carbon fabric-70	45.5	13.8	12.1	0.4	0.0
Phenolic-30, asbestos-70	44.5	7.0	6.3	0.4	0.0
Furfuryl-31, asbestos-69	54.5	7.5	5.7	0.3	0.2

NOTE: Data are from Reference 84.

- a. Based on a thickness measurement from the original contour to the char depth.
b. Actual erosion depth divided by the firing time.

TABLE 22
 ABLATIVE PERFORMANCE OF PLASTIC THRUST CHAMBERS IN OE_2 - B_2H_6 PROPELLANT EXHAUST

Materials Composition		Firing Time, sec	Throat Erosion		Near Injector	Char Depth, inch	
Chamber	Nozzle		Inch	%		Near Nozzle	Throat
Phenolic, graphite fabric	Same	43.6	0.08	40	0.46	0.44	0.36
Precharred epoxy novolac, graphite fabric	Same	34.7	0.07	30	0.43	0.48	0.40
Phenolic, graphite fabric	Phenolic, silica fabric	15.4	0.16	75	0.20	0.19	0.10
Phenolic, silica fabric	Same	10.3	-	52	0.08	0.11	0.09
Phenolic, silica fabric	90-W, 2-Mo	7.6	0.0	0	-	-	-

NOTE: Data are from Reference 45.

TABLE 23
SOLID ROCKET APPLICATIONS

Application	Firing Duration, sec	Thrust, lb	Chamber Pressure, psia	Mass ratio ^a
Control, retro, ullage	0.03-40	1-8000	500-1700	0.3-0.9
Aircraft/launch escape	0.5-1.2	1500-33,000	1300-2500	0.3-0.47
Sounding rockets	3-50	1400-8000	550-1150	0.67-0.75
Antisubmarine	1-25	600-16,000	900-2300	0.3-0.65
Upper stage	1.6-43	470-21,000	34-580	0.86-0.94
Air-to-Surface				
Guided	2.9	7700	1150	0.6
Unguided	0.8-1.0	6000-8000	1400-1700	0.25-0.54
Air-to-air				
Guided	2.1-5.2	2700-7700	750-1150	0.6-0.70
Unguided	1.8	31,000	1000	0.66
Surface-to-air				
Homing	0.06-32	800-490,000	760-2600	0.6-0.84
Beam-riding	3.2-5.4	15,000-110,000	1000-2000	0.66-0.73
Launch	110-155	1,150,000	750	0.89
Surface-to-surface				
Guided	1.4-60	950-185,000	540-1000	0.44-0.91
Unguided	1.5-3.3	33,000-110,000	1100-1250	0.54-0.58

NOTE: Most data are from Reference 137.

a. Ratio of burnout weight to launch weight.

TABLE 24

PROPERTIES DESIRED IN SOLID PROPELLANTS

Physico-Chemical	Mechanical	Permanence
<p>High density</p> <p>Compatible ingredients</p> <p>Noncorrosive</p> <p>Bondability to motor cases</p> <p>High strength</p> <p>Insensitive to impurities and processing variables</p> <p>Radiation opaque</p> <p>Low glass transition temperature</p>	<p>Maintain structural integrity</p> <p>Deform 30-40% during motor firing</p> <p>Accommodate thermal and mechanical stresses</p> <p>Low sensitivity to thermal and mechanical shock</p>	<p>High resistance to natural and induced environmental extremes</p> <p>Long age life</p>

TABLE 25
TYPICAL PROPERTIES OF SOLID PROPELLANTS

Propellant Type	Double Base, Cast	Composite, Metallized	Composite, Cast	Composite, Molded	Asphalt Base, Thermoplastic
Composition, %	Cellulose nitrate, 45-55 Glycerol nitrate, 25-40 Plasticizer, 12-22 Additive, 1-2	Elastomer, 13 Ammonium perchlorate, 68 Modifier, 3 Aluminum, 16	Elastomer, 15-50 Ammonium perchlorate, 50-85	Elastomer, 10 Ammonium picrate, 40-70 Potassium nitrate, 20-50	Asphalt, 22-30 Potassium perchlorate, 70-78
Adiabatic flame temperature, °F	2,600 - 4,000	5,500	2,800 - 4,500	3,200	3,300 - 3,800
Specific impulse, sea level, sec	160 - 220	250	175 - 240	160 - 200	180 - 200
Density, lb/ft ³	98	107	102	105	109
Burning rate 1000 psi at 70°F, in/sec	0.22 - 0.37	0.30	0.1 - 0.5	0.24 - 1.0	1.3 - 1.7
Molecular wt., lb/mole	22-28	25	22 - 25	30	30
Storability	Fair	Good	Good	Good	Good
Mechanical Properties	Hard and tough	Hard and tough	Soft and resilient to hard and tough	Hard and brittle	Variable, poor when warm

NOTE: Most data are from Reference 95.

TABLE 26
TYPICAL EXHAUST PRODUCTS (%) FROM SOLID PROPELLANTS

Propellant Composition	Nitrocellulose, Nitroglycerin, Plasticizer	Polyurethane, Ammonium Perchlorate	Polyurethane, Ammonium Perchlorate, Aluminum	Polysulfide, Ammonium Perchlorate	Elastomer, Ammonium Nitrate	Asphalt, Potassium Perchlorate
CO ₂	27.7	27.9	1.3	16.7	15.6	3.3
CO	23.4	9.6	28.7	3.9	2.5	44.0
H ₂	7.6	0.8	38.4	4.0	28.6	27.4
H ₂ O	26.2	24.9	6.6	41.5	31.5	9.9
N ₂	15.1	8.6	6.4	9.2	21.8	0.1
HCl	-	-	12.0	18.4	-	-
Al ₂ O ₃ (s)	-	-	6.5	-	-	-
KCl	-	6.6	-	-	-	15.1
H ₂ S	-	-	-	2.6	-	-
S ₂	-	-	-	2.0	-	-
SO ₂	-	-	-	1.6	-	0.2
Others	0.0	21.6	0.1	0.1	0.0	0.0

NOTE: Products % exhausted to 14.7 psi.

From Handbook of Astronautical Engineering by R. Geckler and K. Klager. Copyrighted 1961. Used by permission of the McGraw-Hill Book Co.

TABLE 27

IMPORTANT COMBUSTION PRODUCTS FROM SOLID PROPELLANTS

Gaseous Species	Maximum Concentration, Vol. %
H ₂	56.8
CO	40.8
HF	28.0
N ₂	25.3
H ₂ O	23.9
BeF ₂	20.0
HCl	13.4
F	10.5
CO ₂	10.2
BF ₃	7.1
H	5.9
BF	5.3
Cl	4.2
CH	3.9
BF ₂	3.3
AlCl	2.5
BOF	2.4
BeOH	2.3
HBO ₂	2.2
BeF	1.9
AlF	1.4
BeCl ₂	1.2
Be	1.1

NOTE: Data are from Reference 103.

TABLE 28

EROSION RATES OF ELASTOMERIC LINERS AND AFT CLOSURES

Elastomeric Binder	Motor Position	Erosion Rate, mil/sec
Ethylene-Propylene	Case liner	3.1
Nitrile-Type A	" "	3.3
Butyl	" "	3.5
Nitrile-Type B	" "	3.6
Nitrile-Type C	" "	3.8
Styrene-Butadiene	" "	4.2
Butyl	Aft closure	3.2
Ethylene-Propylene	" "	11.9
Nitrile-Type A	" "	12.3
Nitrile-Type B	" "	12.5
Nitrile-Type C	" "	12.5
Styrene-Butadiene	" "	12.5

NOTE: Data are from Reference 123.

Materials were evaluated in a composite form, but exact composition of the commercially available materials has not been disclosed.

Polyurethane-60%, asbestos-40%	+35	1.9	30	+312	4.8	40	+71	1.8	30
Melamine-60% asbestos-40%	+3	3.0	37	+2	4.4	44	-83	4.0	5
Silicone-58% asbestos-42%	+55	5.0	13	+206	5.5	54	+32	4.9	25
Epoxy-60% asbestos-40%	+39	3.1	33	+86	4.7	50	+23	5.1	25
Phenolic-59% asbestos-41%	0	4.7	22	+118	4.4	9	-26	5.9	0
Buna N-38% silica powder-62%	-94	5.2	15	-121	3.9	0	-131	3.7	10
Epoxy-39% castor oil-20% asbestos-41%	+39	2.7	33	+357	2.7	81	+57	3.8	30

NOTE: Data are from Reference 124.

- a. Temperature-4,700°F, cold-wall heat flux-55 Btu/ft² sec, duration-15 to 18 sec.
- b. Temperature-5,600°F, cold-wall heat flux-190 Btu/ft² sec, duration-30 sec.
- c. Temperature-6,640°F, cold-wall heat flux-140 Btu/ft² sec, duration-30 sec.

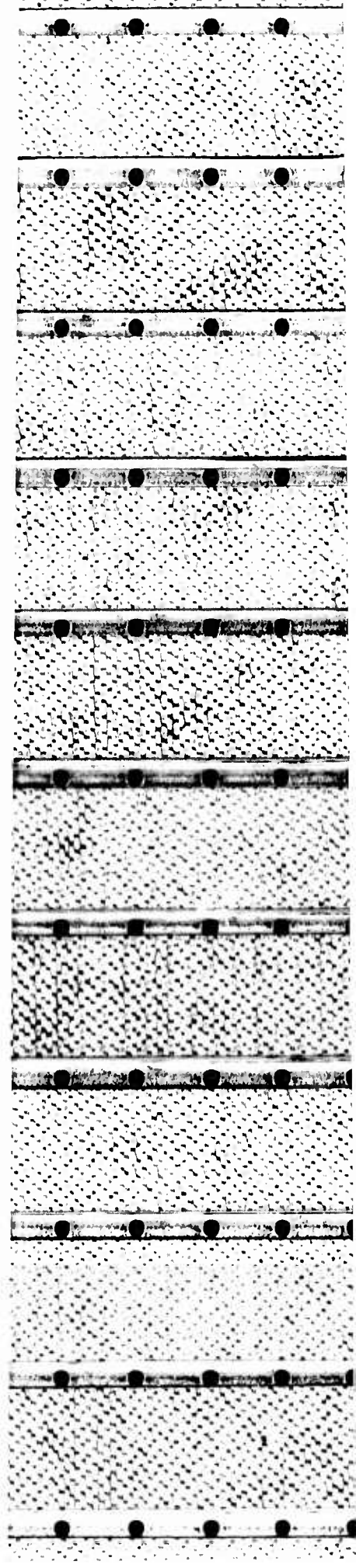


TABLE 30
THERMOCHEMICAL EFFECTS OF ALUMINIZED EXHAUST PRODUCTS ON PHENOLIC-SILICA ABLATION

Propellant Type ^g	Aluminum Content, %	Chamber Pressure, psia	Flame Temperature ^b , °F	Water Content, mole %	Heat Flux ^c , Btu/ft ² -sec	Throat Ablation Rate ^d , mils/sec
Polysulfide	2	438	4,780	36.7	290	3.50
Polysulfide	2	528	4,780	36.7	337	5.10
Nitrile	12	530	5,190	14.0	590	11.90
Nitrile	12	607	5,190	14.0	643	12.30
Polybutadiene acrylic acid	16	605	5,290	9.3	801	17.90
Polybutadiene acrylic acid	16	700	5,290	9.3	880	19.80
Petrin acrylate	18	461	6,260	16.7	1,167	29.30

NOTE: Data are from Reference 125.

a. Ammonium perchlorate oxidizer.
b. Based on a 1,000 psi chamber pressure.
c. Based on convective and radiative flux.
d. One inch diameter throat.

**THIS REPORT HAS BEEN DELIMITED
AND CLEARED FOR PUBLIC RELEASE
UNDER DOD DIRECTIVE 5200.20 AND
NO RESTRICTIONS ARE IMPOSED UPON
ITS USE AND DISCLOSURE.**

DISTRIBUTION STATEMENT A

**APPROVED FOR PUBLIC RELEASE;
DISTRIBUTION UNLIMITED.**

TABLE 31

PARTICLE EROSION OF DUCTING MATERIAL IN AN
ALUMINIZED SOLID PROPELLANT EXHAUST

Type of Material	Average Recession Rate, mils/sec
Reinforced Plastics	
Phenolic-Graphite (end-grain fabric)	61
Phenolic-Silica (shingle-grain fabric)	120
Phenolic-Silica (end-grain fabric)	155
Ceramics	
Pyrolytic graphite (PG)	17
ZTA Graphite	31
ATJ Graphite (PG-coated)	31
ATJ Graphite (silicon-carbide-coated)	55
Fuse silica	155
Refractory Metals	
Tungsten (graphite backup)	6
Carburized tantalum- 10 tungsten ^a	11

NOTE: Data are from Reference 128.

a. Evaluated in a higher aluminized propellant exhaust.

TABLE 32
THEORETICAL PERFORMANCE OF HYBRID PROPELLANTS

Oxidizer (liquid)	Fuel (solid)	Mass Mixture Ratio, O/F	Specific Impulse, sec ^a	Bulk Density, gm/cc	Combustion Temperature °F ^a
O ₂	(CH ₂) _n	2.70	300	1.07	6,169
H ₂ O ₂	(CH ₂) _n	6.70	277	1.34	4,938
N ₂ O ₄	(CH ₂) _n	4.00	276	1.29	5,739
F ₂	(CH ₂) _n	2.70	325	1.78	7,428
ClF ₃	(CH ₂) _n	3.34	257	1.48	5,914
ClO ₃ F	(CH ₂) _n	4.26	280	1.29	6,239
O ₂	AlH ₃	0.72	318	1.42	7,278
H ₂ O ₂	AlH ₃	0.92	326	1.58	6,600
F ₂	AlH ₃	2.85	353	1.56	9,110
ClF ₃	AlH ₃	3.35	291	1.79	7,807

TABLE 32
THEORETICAL PERFORMANCE OF HYBRID PROPELLANTS (Con't)

Oxidizer (liquid)	Fuel (solid)	Mass Mixture Ratio, O/F	Specific Impulse, sec	Bulk Density, gm/cc	Combustion Temperature, °F
O ₂	BeH ₂	1.22	371	1.31	6,988
H ₂ O ₂	BeH ₂	1.33	375	1.51	5,973
F ₂	BeH ₂	4.26	395	1.53	9,136
ClF ₃	BeH ₂	4.55	329	1.77	7,640
O ₂	LiH	2.70	300	1.07	6,169
H ₂ O ₂	LiH	6.70	277	1.34	4,938
F ₂	LiH	2.70	325	1.78	7,428
ClF ₃	LiH	3.34	257	1.48	5,914

a. Based on 1,000 psia chamber pressure and sea level expansion.

From Handbook of Astronautical Engineering by R. Geckler and K. Klazer. Copyrighted 1961. Used by permission of the McGraw-Hill Book Co.

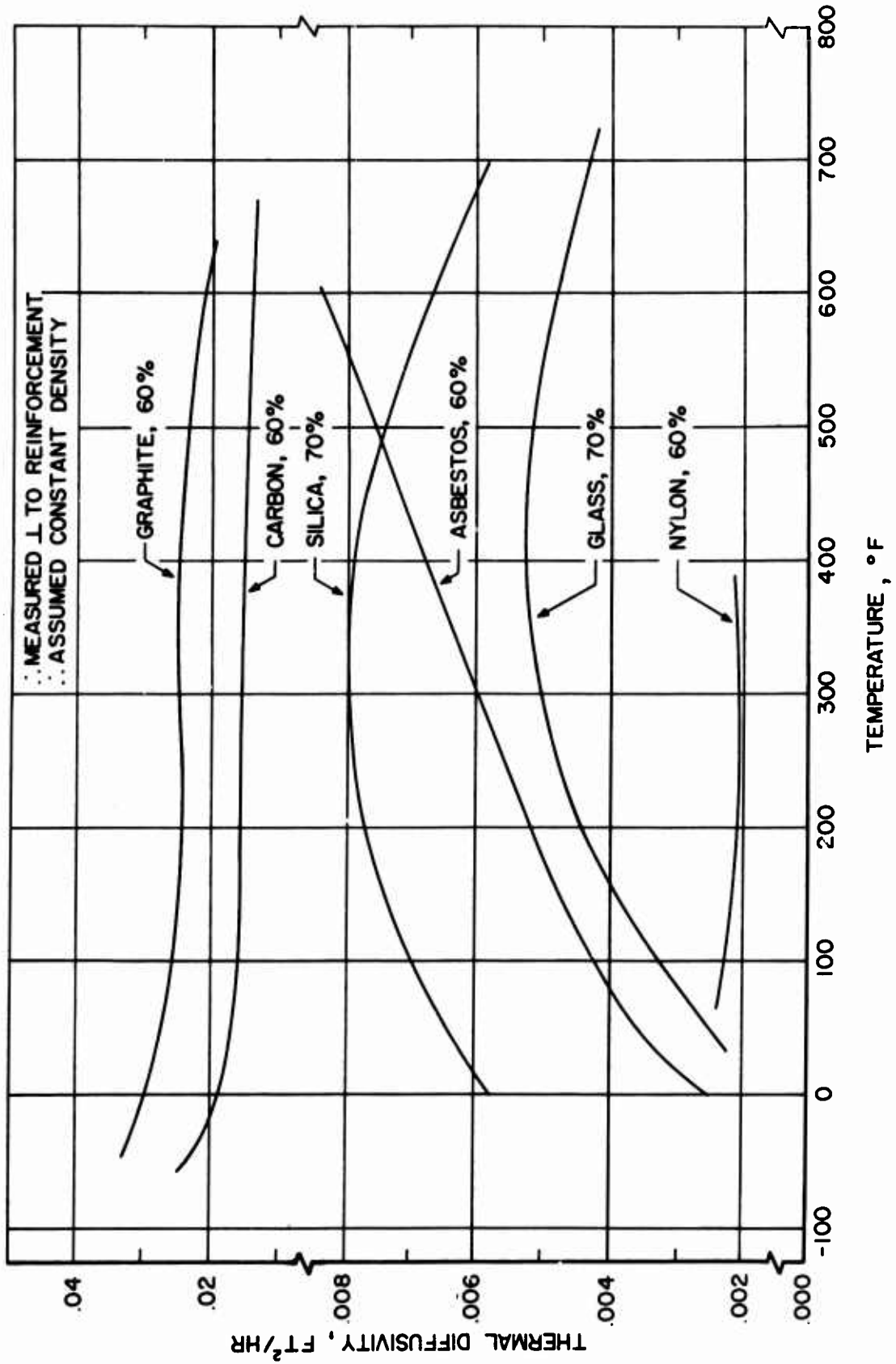


Figure 1. Thermal Diffusivities of Various Fiber Reinforced Phenolic Composites

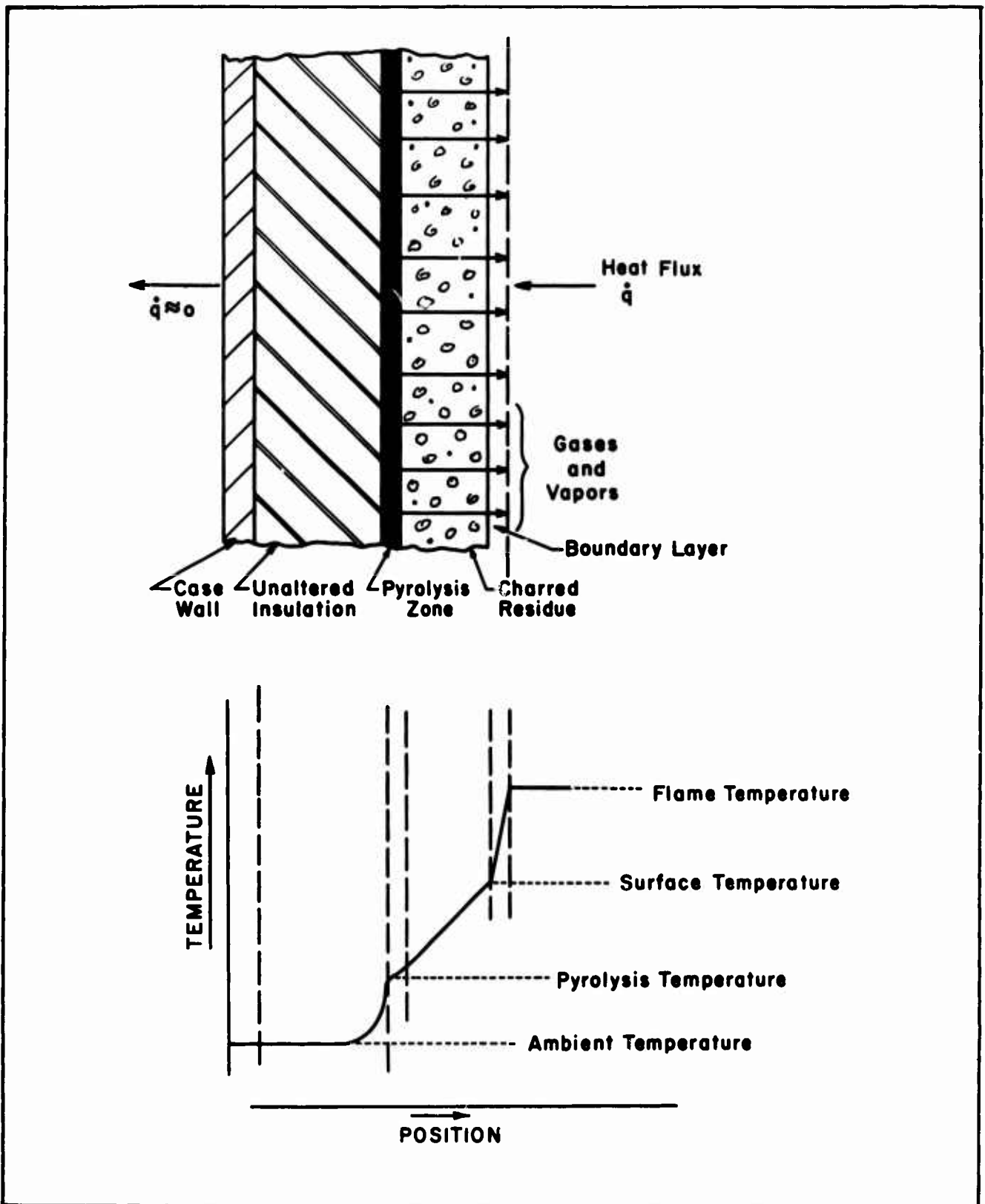
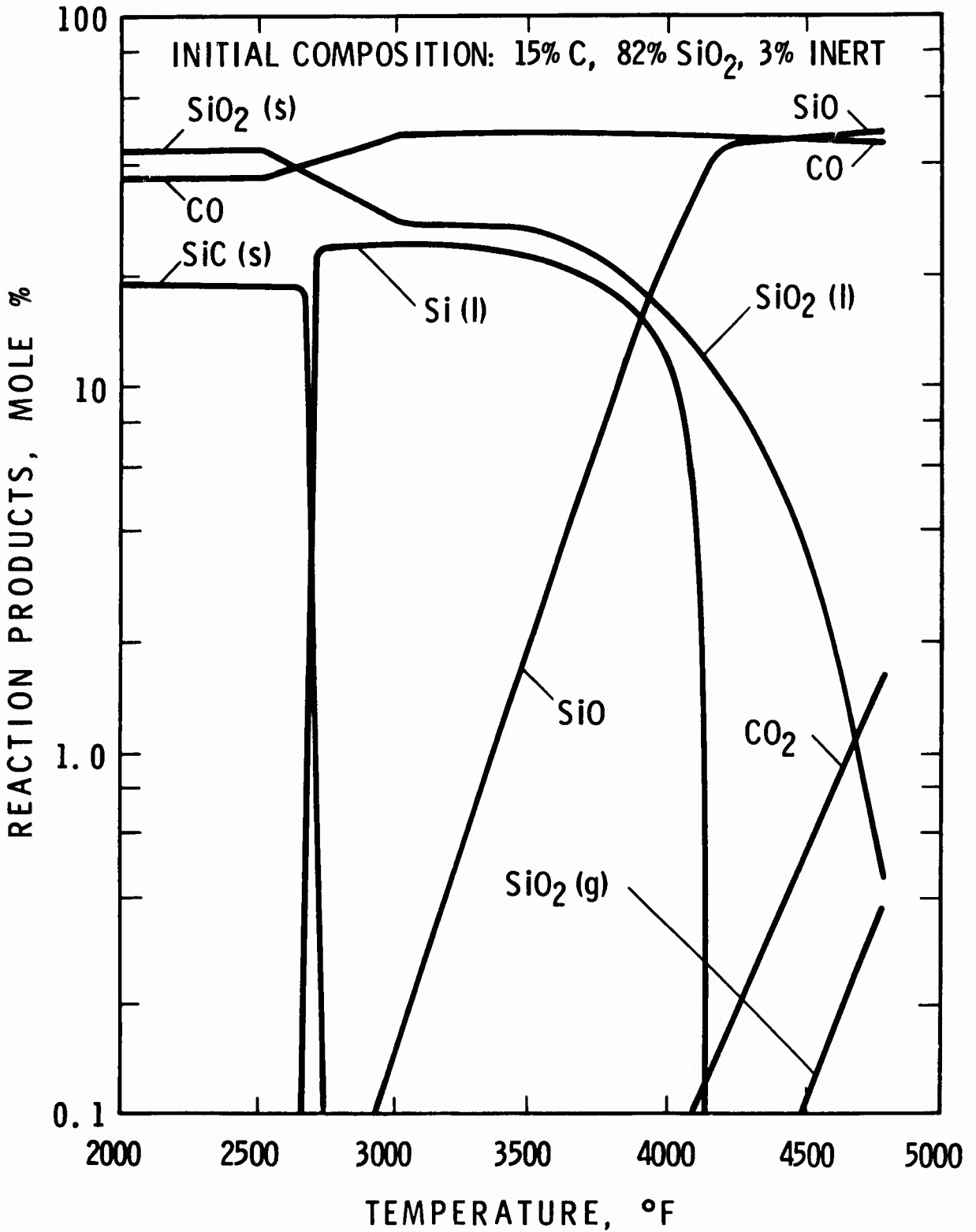
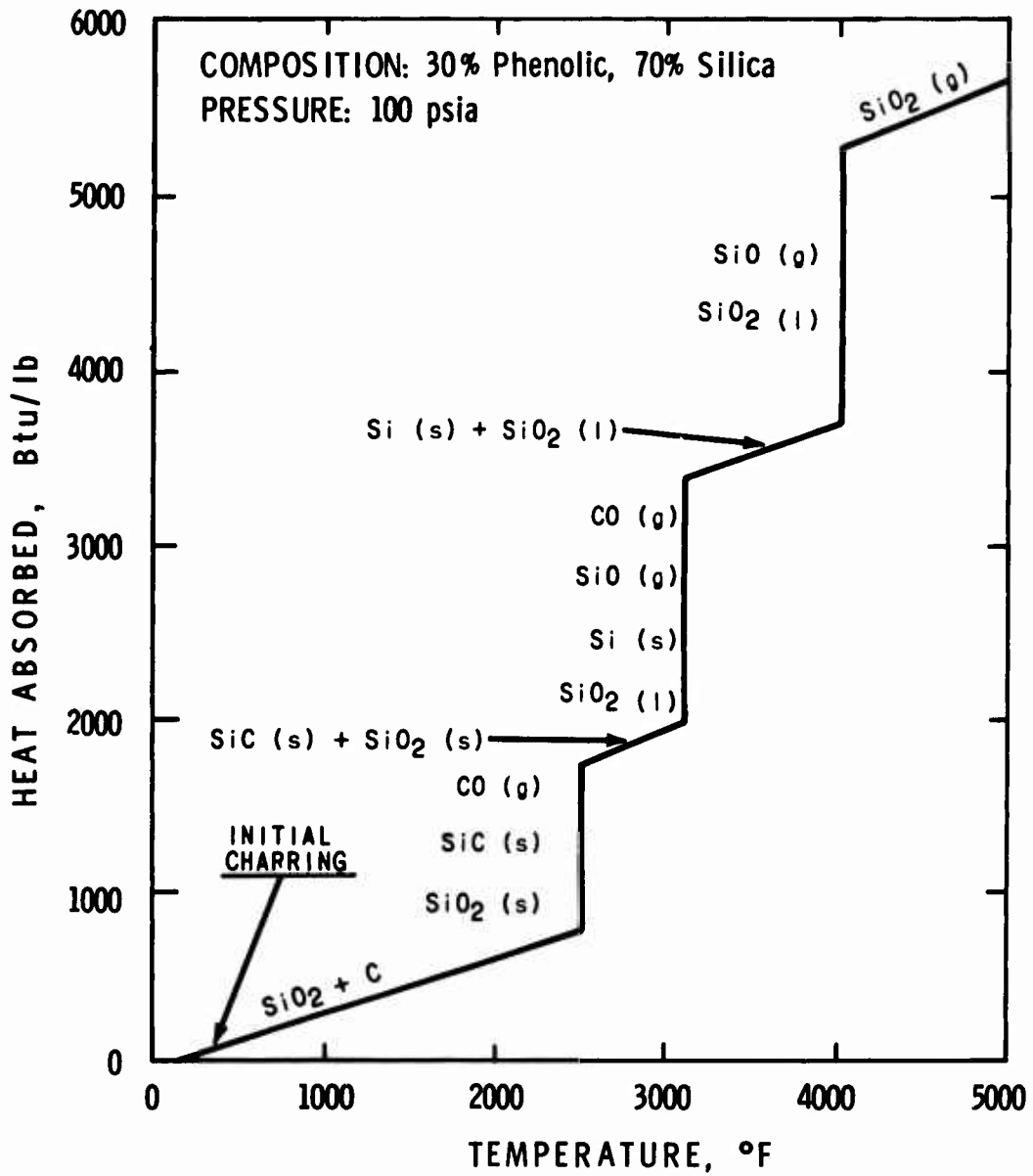


Figure 2. Cross-Sectional Schematic and Temperature Distribution in an Ablating Charring Polymer



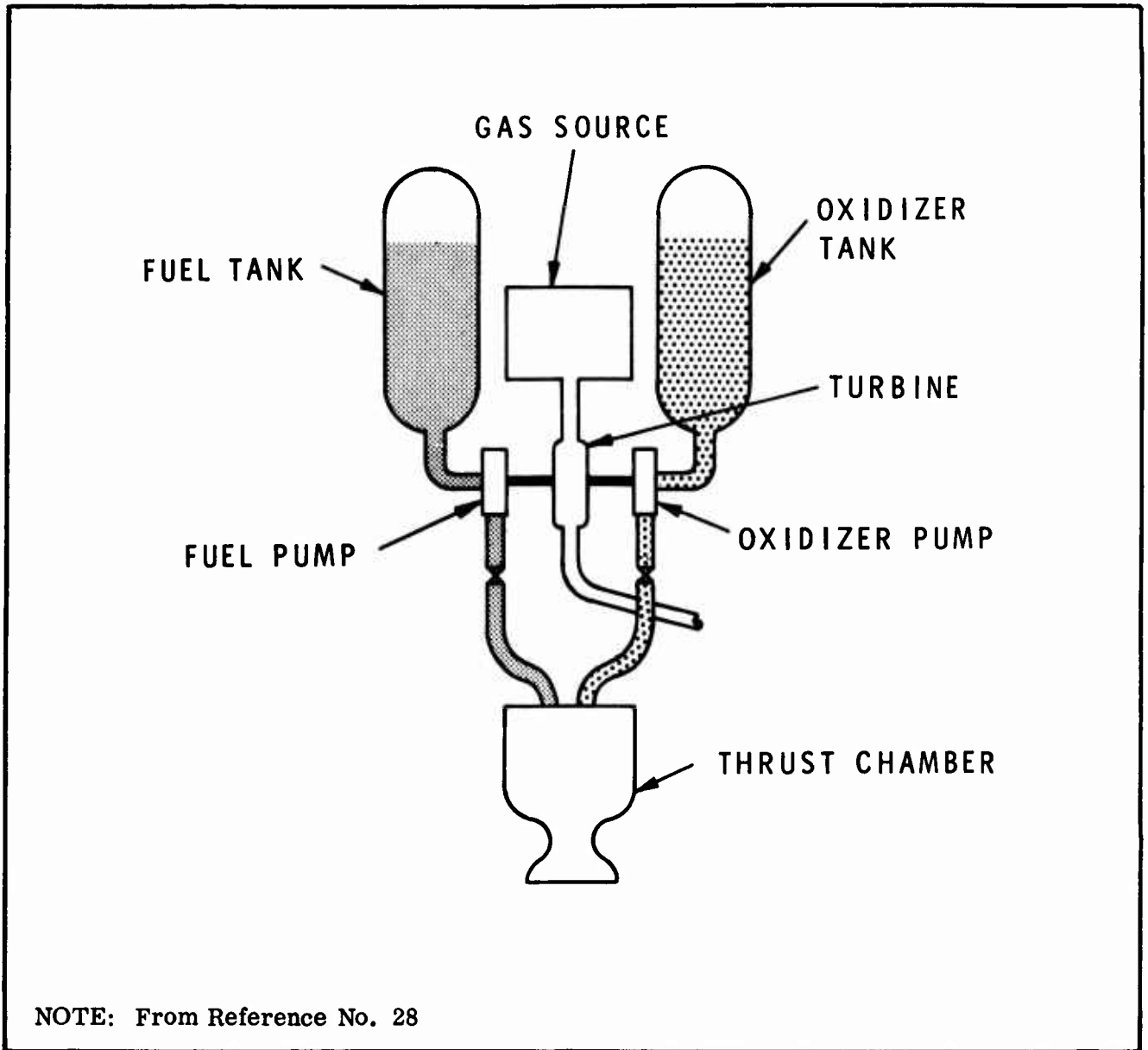
NOTE: From Reference No. 18

Figure 3. Equilibrium Chemical Reactions of Silica and Carbon at Elevated Temperatures



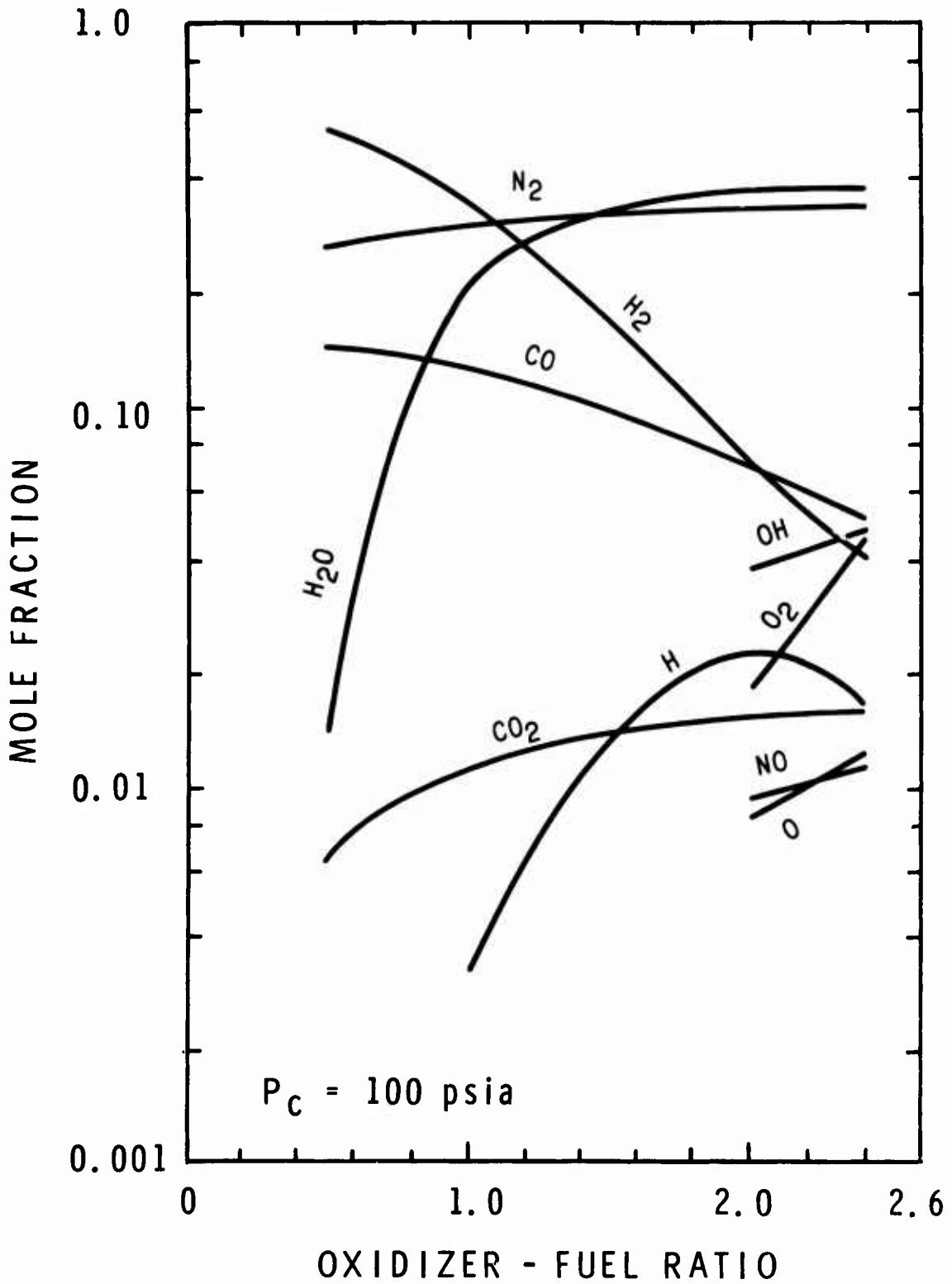
NOTE: From Reference No. 18

Figure 4. Potential Heat Absorbing Capability of an Ablative Phenolic-Silica Composite



NOTE: From Reference No. 28

Figure 5. Schematic of a Liquid Propellant Engine System



NOTE: From Reference No. 37

Figure 6. Variation in Combustion Products From $N_2O_4 - N_2H_4 - UDMH$ as a Function of Oxidizer: Fuel Ratios

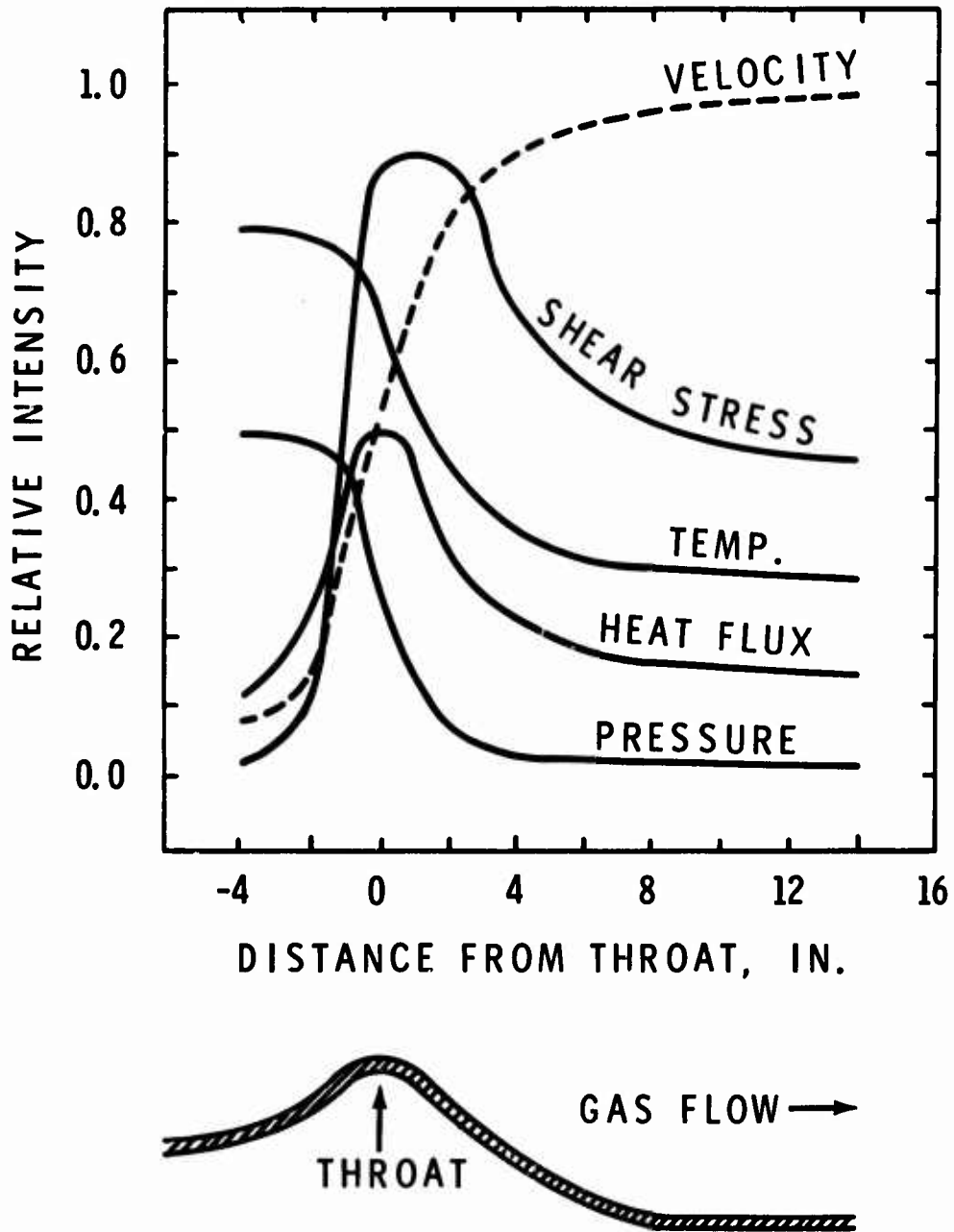
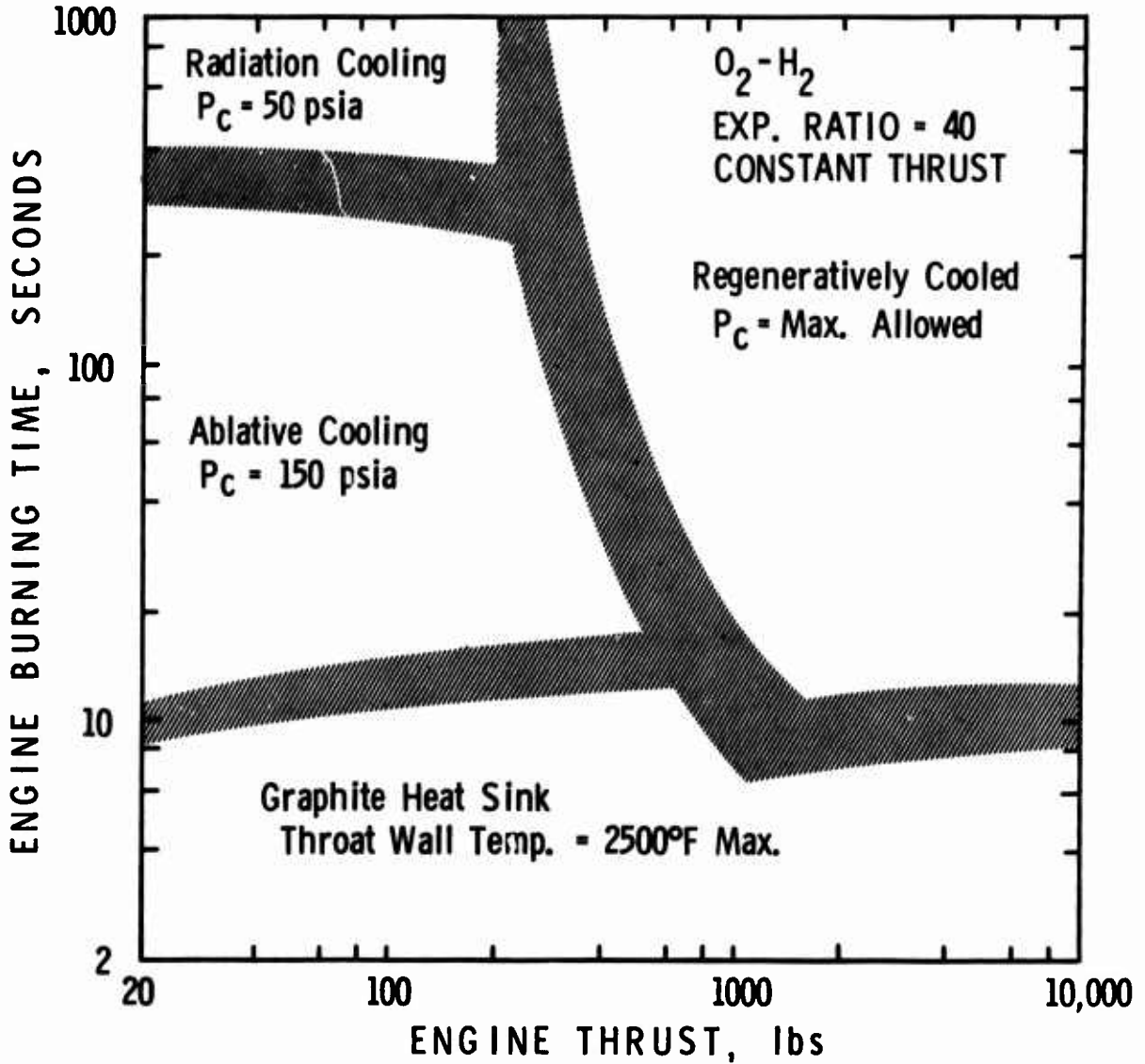


Figure 7. Environment and Partial Schematic of Liquid Propellant Rocket Engine Nozzle



NOTE: From Reference No. 30

Figure 8. Applicability of Cooling Techniques for Minimum Weight Space Engines

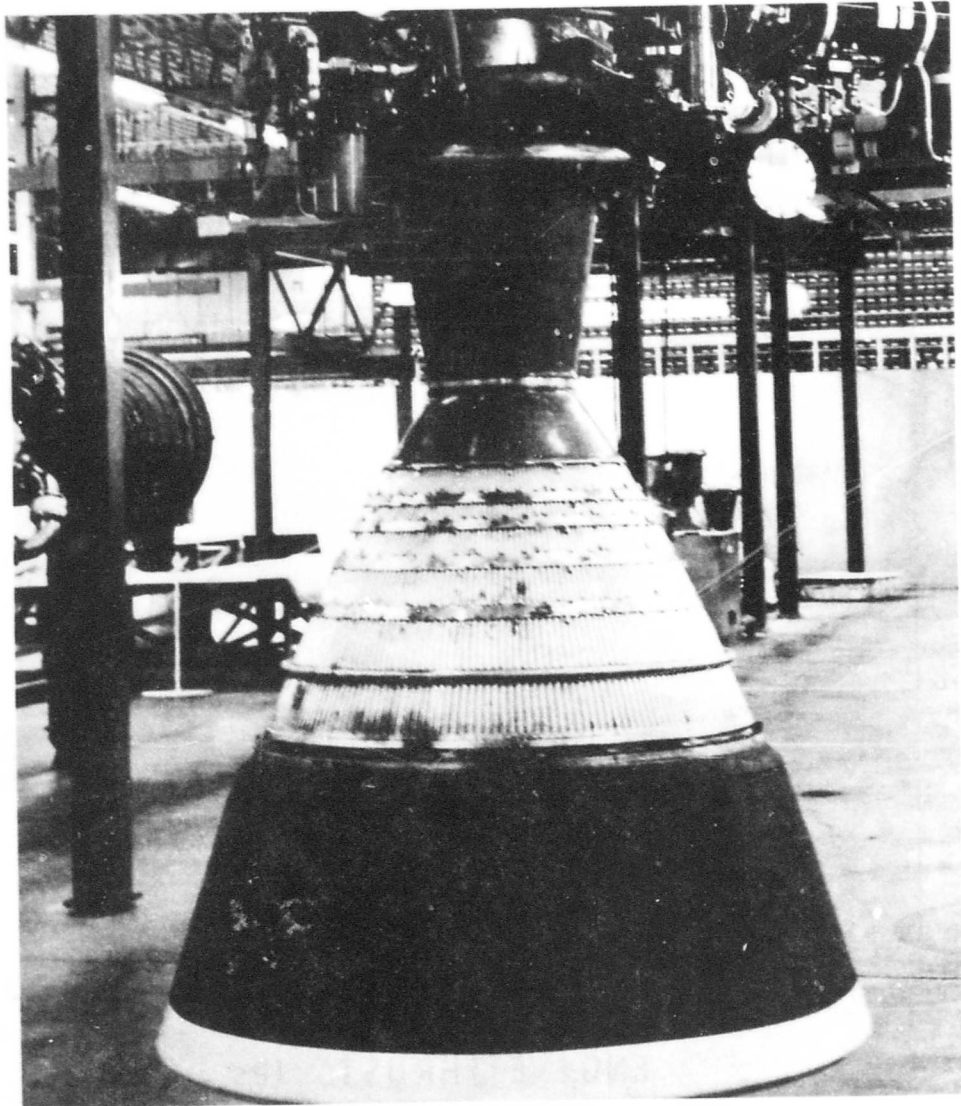


Figure 9. Ablative Plastic Skirt on a Nozzle of a Liquid Propellant Engine

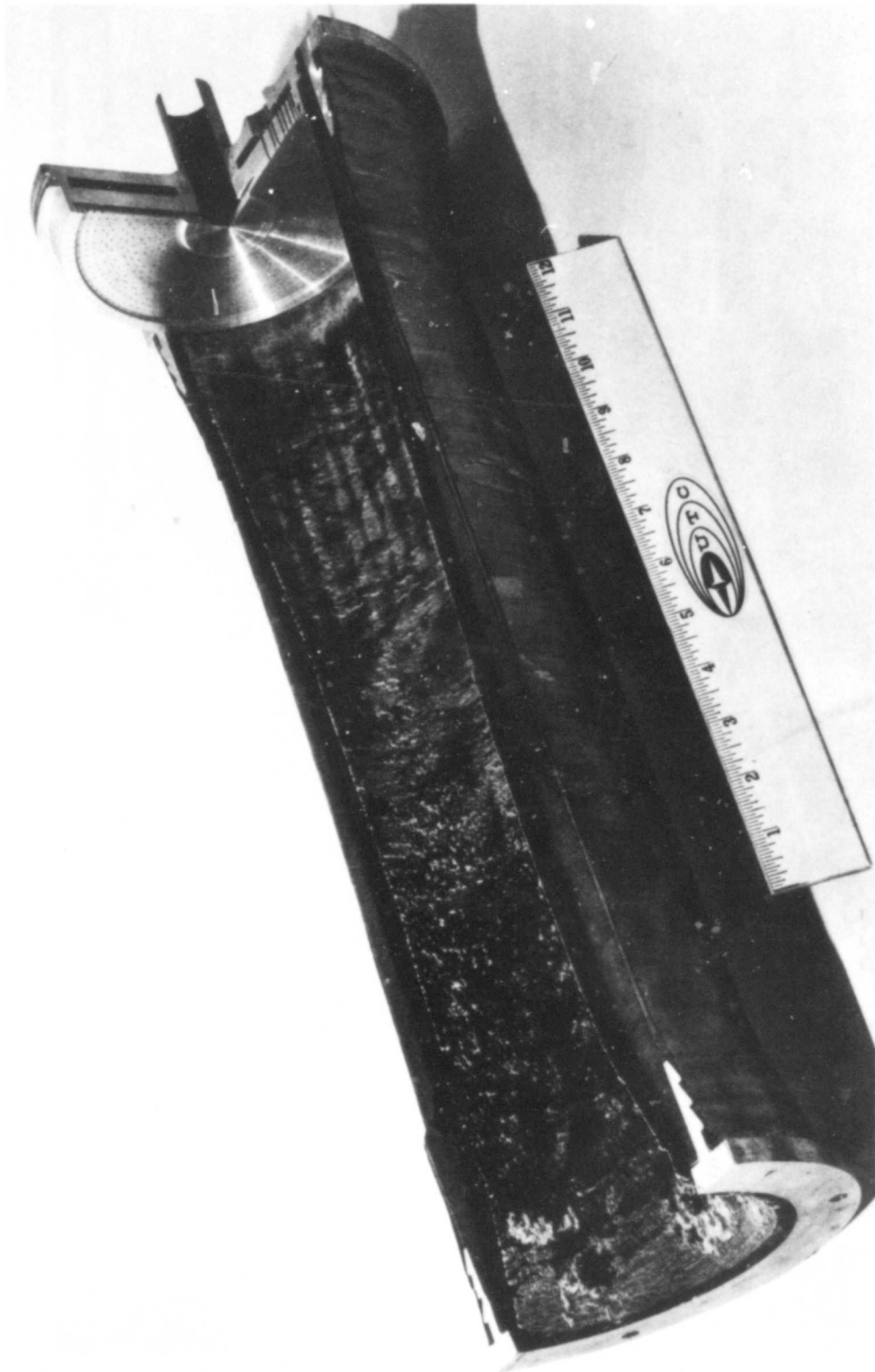


Figure 10. Ablative Plastic Thrust Chamber for a 4,000 Pound Thrust Liquid Propellant Engine

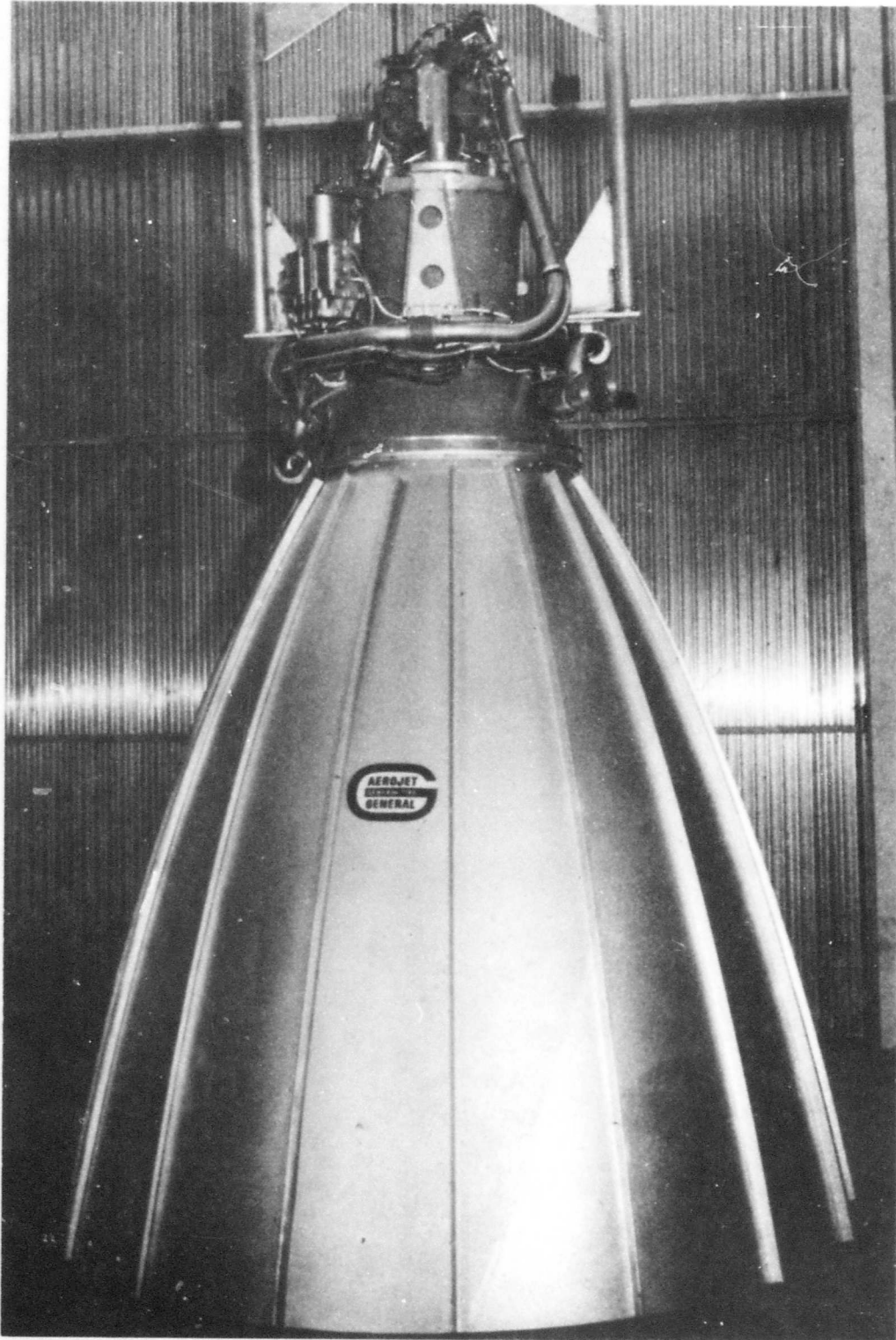
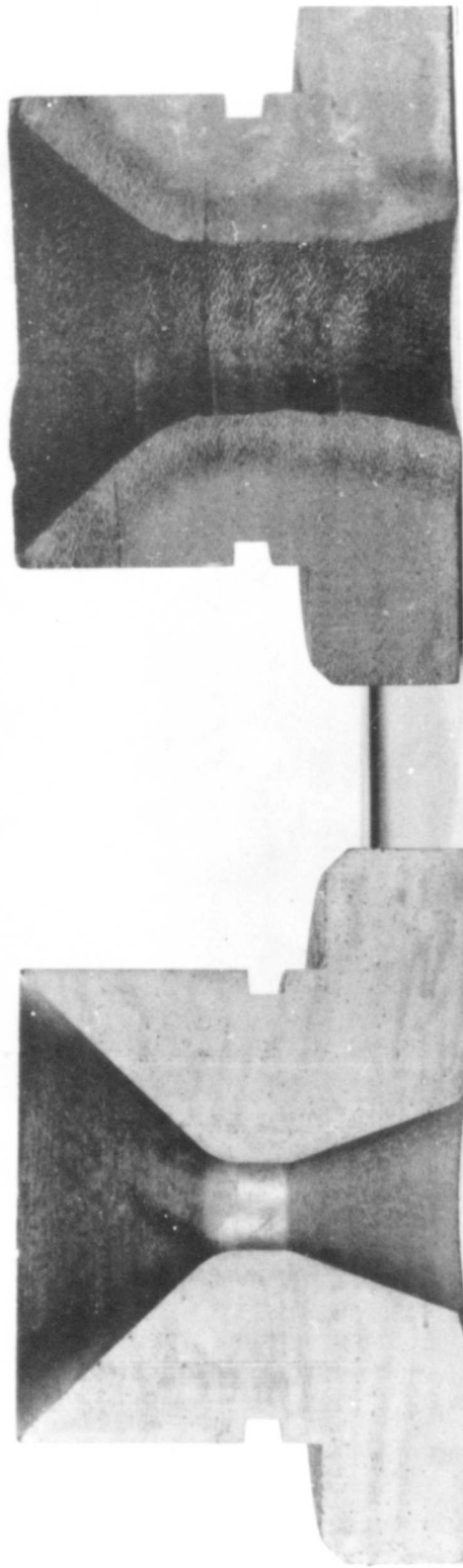


Figure 11. Ablative Plastic Thrust Chamber and Radiative Expansion Skirt for the Apollo Lunar Service Module



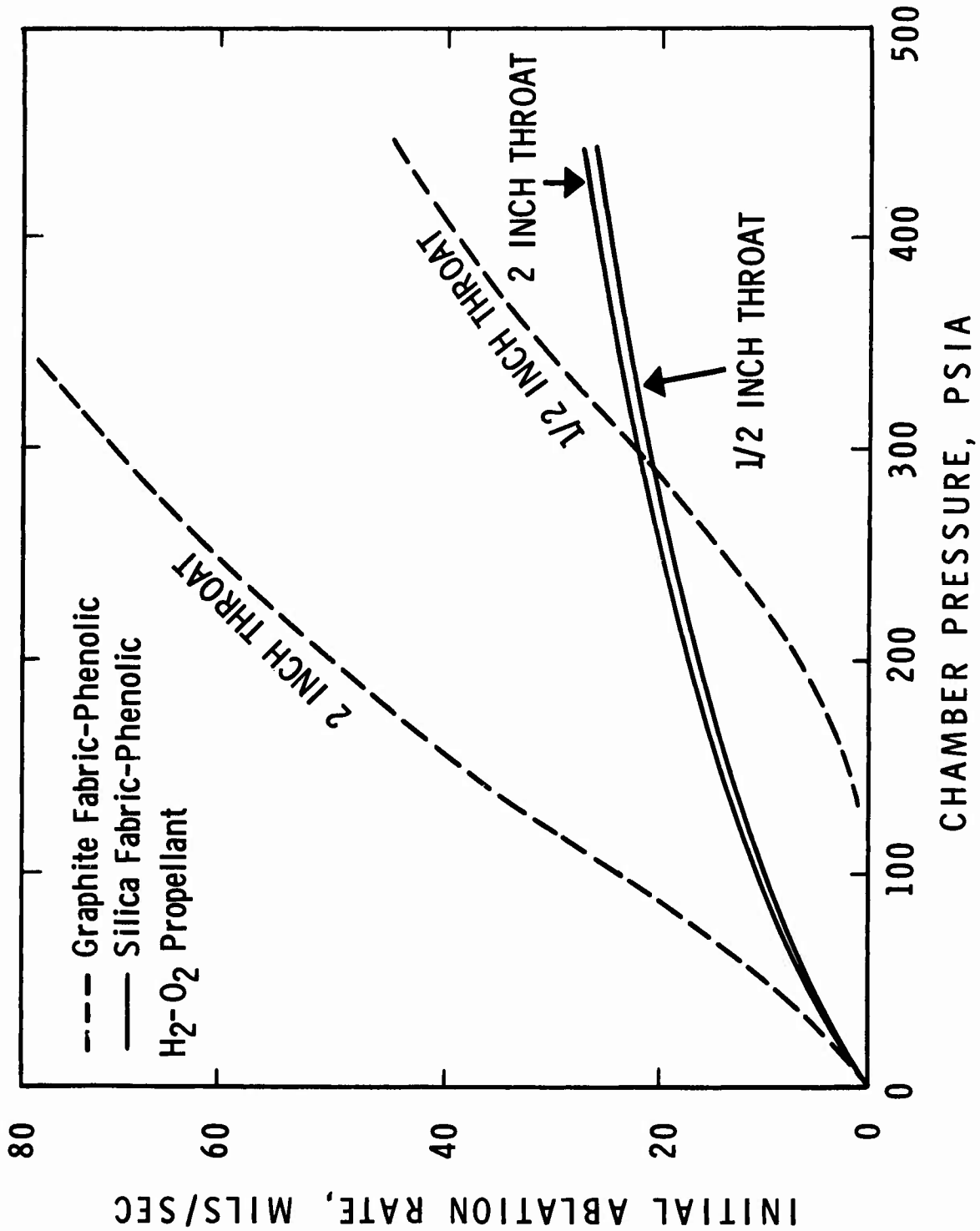
Figure 12. Experimental Arrangement for Exposing Ablative Panels in Oxy-Acetylene Combustion Products



AFTER EXPOSURE

ORIGINAL CONFIGURATION

Figure 13. Cross-Sectional View of a Nozzle Specimen Before and After Exposure



NOTE: From Reference No. 75

Figure 14. Effect of Chamber Pressure on the Ablation Rate of Several Fabric Reinforced Phenolics

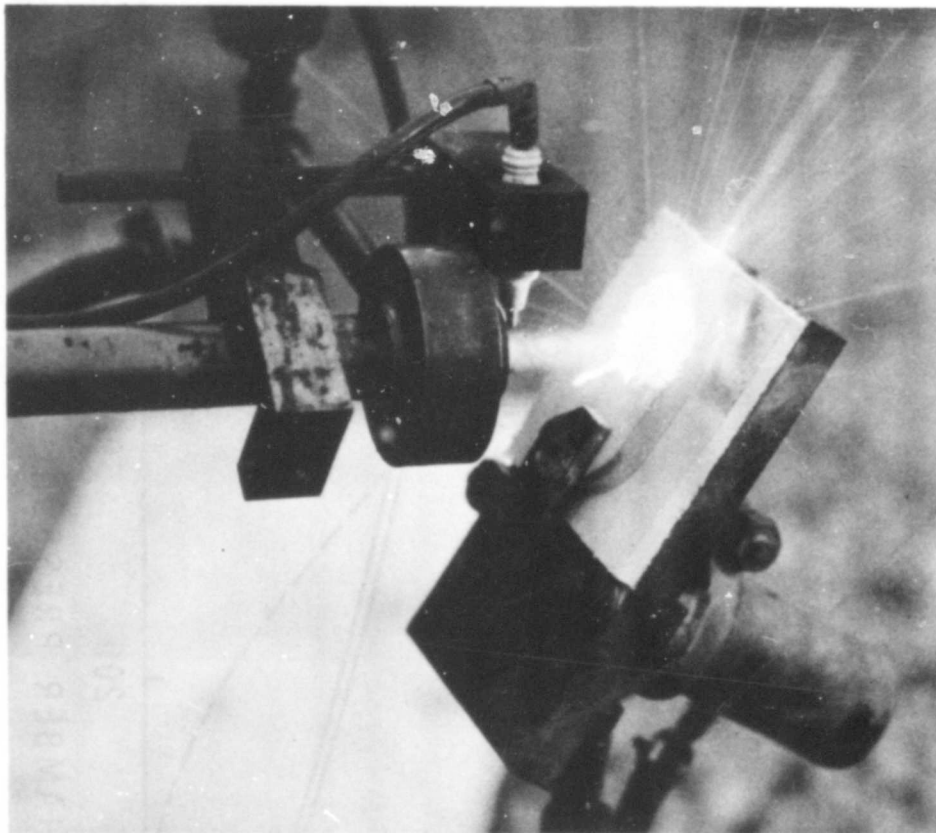


Figure 15. Ablative Specimens Being Exposed to Supersonic Oxy-Kerosene Exhaust



Figure 16. Ablative Plastic Thrust Chamber for N_2O_4 -UDMH Engine

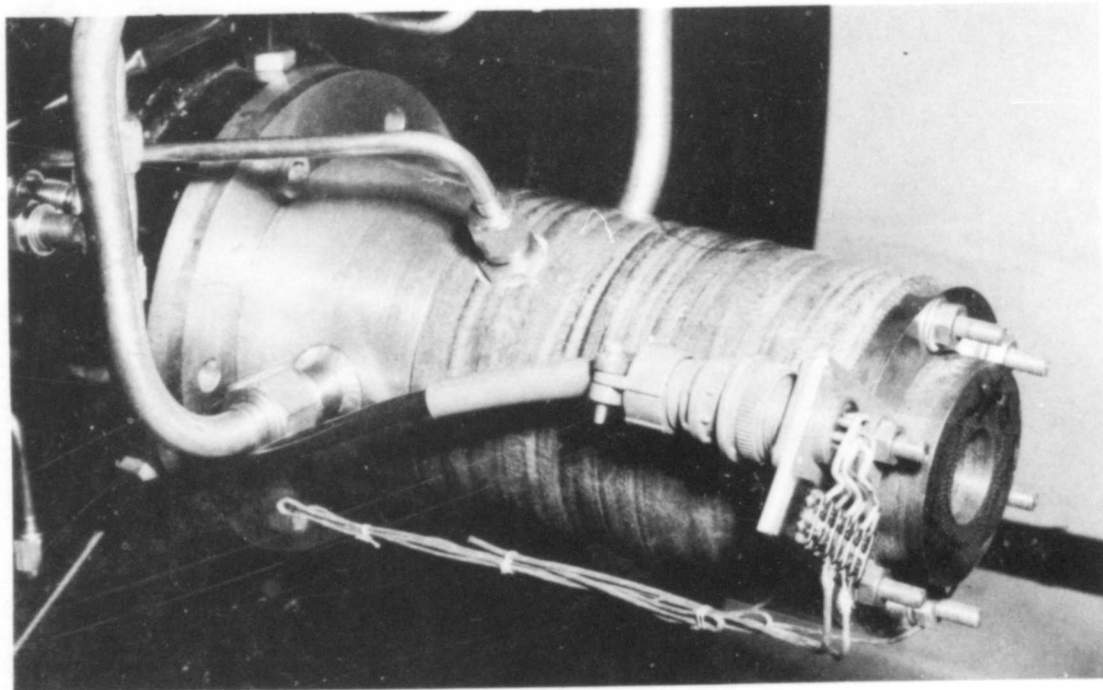


Figure 17. Ablative Plastic Thrust Chamber Installed on a $N_2O_4 - N_2H_4 - UDMH$ Micromotor

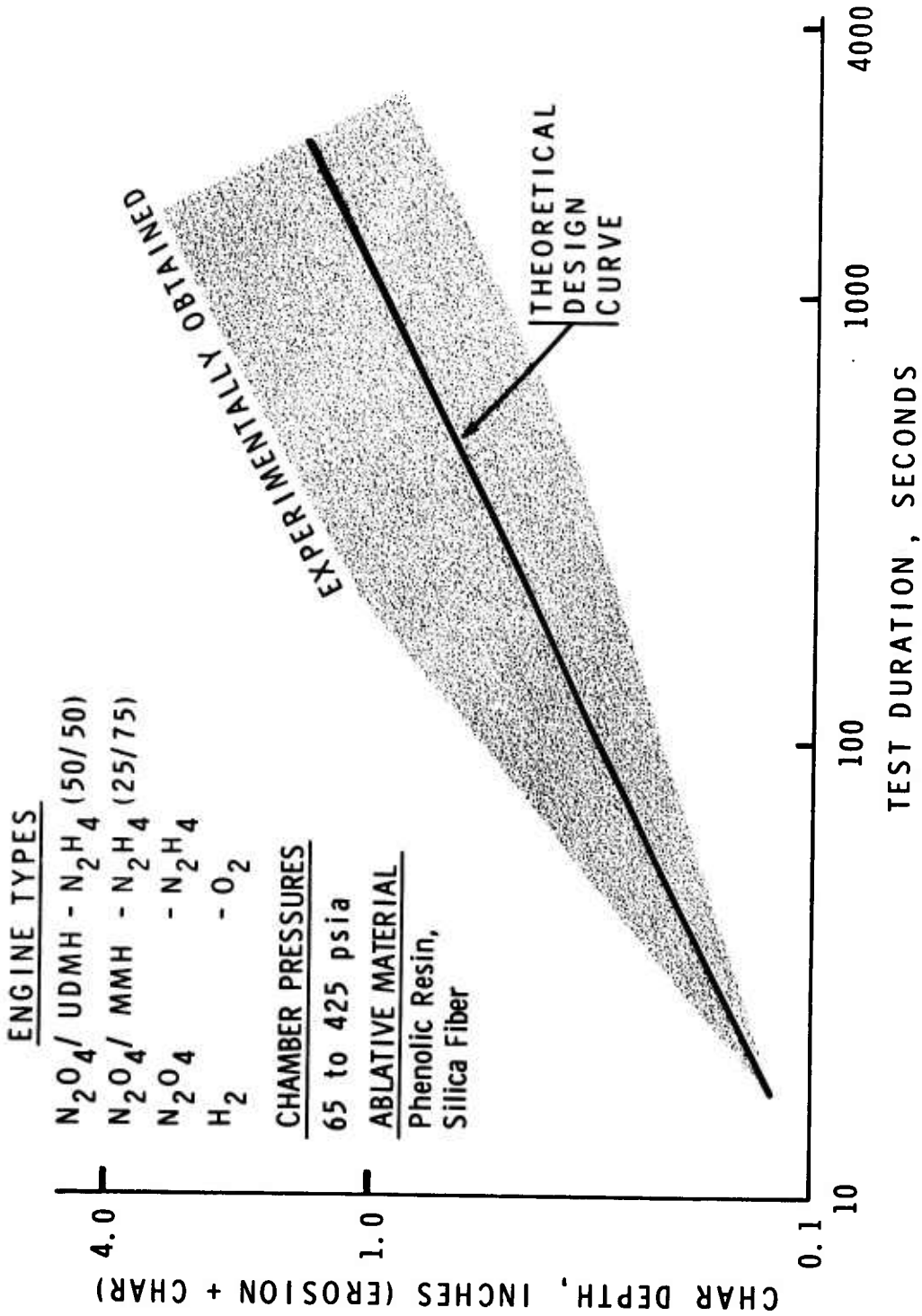


Figure 18. Charring Performance of Ablative Plastic (Phenolic-Silica Fiber) Thrust Chambers Using Various Liquid Propellants



Figure 19. Ablative Phenolic-Graphite Thrust Chamber After Exposure to $OF_2 - B_2H_6$ Exhaust

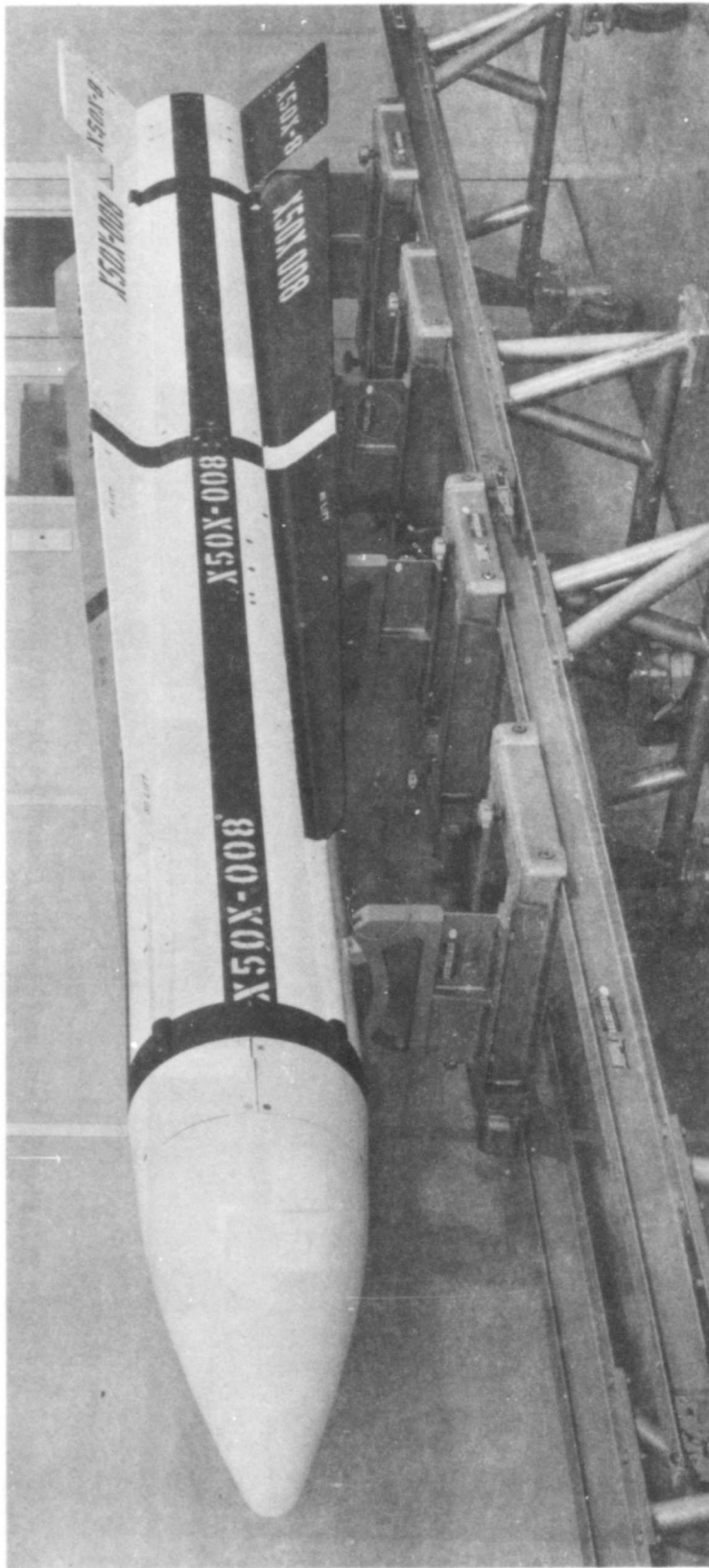


Figure 20. Advanced Guided Air-To-Air Rocket Containing Plastic Wings and Fuselage

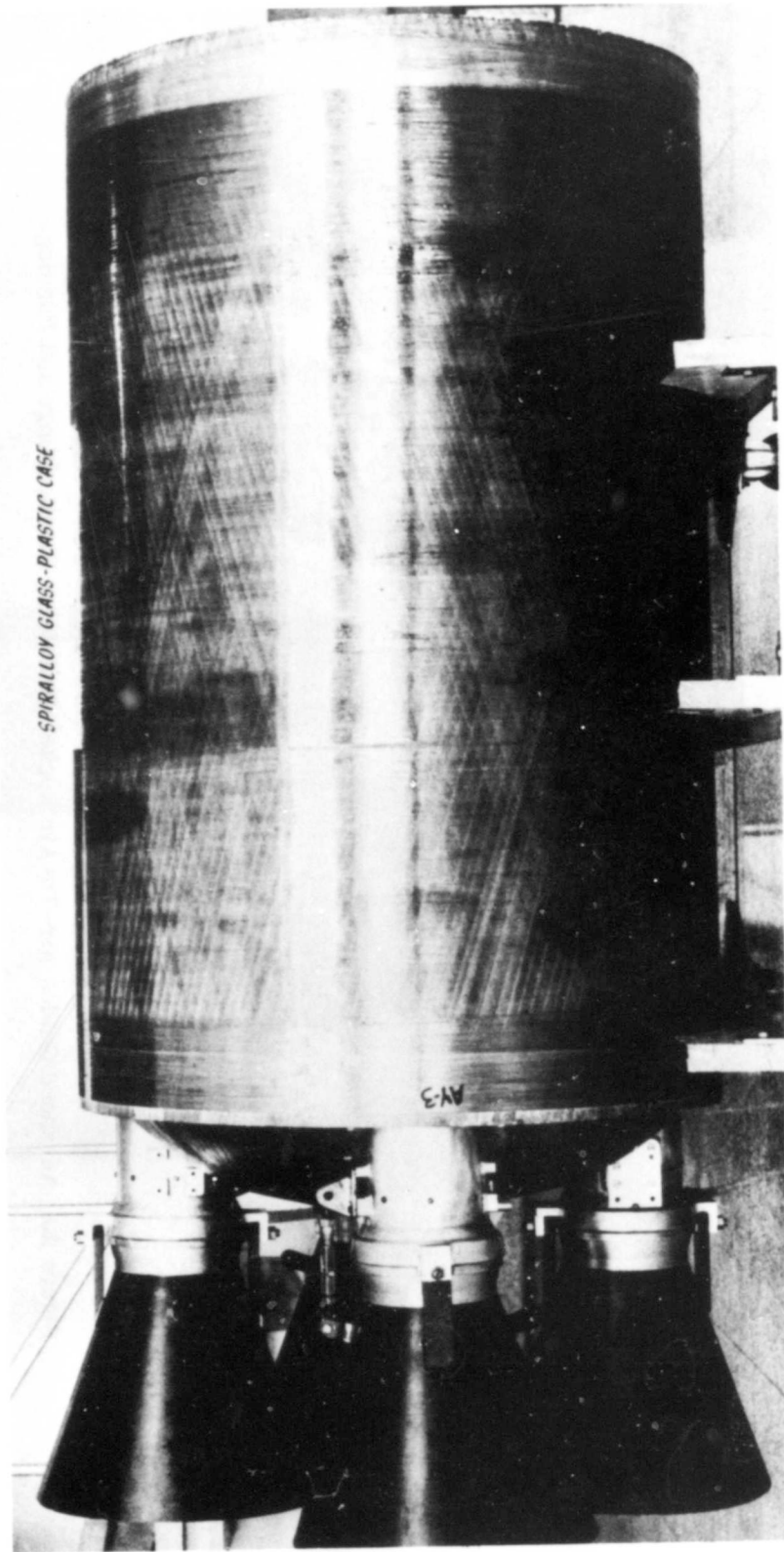


Figure 21. Plastic Case and Nozzles Comprise the Third Stage Motor of the Minuteman ICBM



Figure 22. Plastic Retro-Rocket for the Ranger Lunar Spacecraft

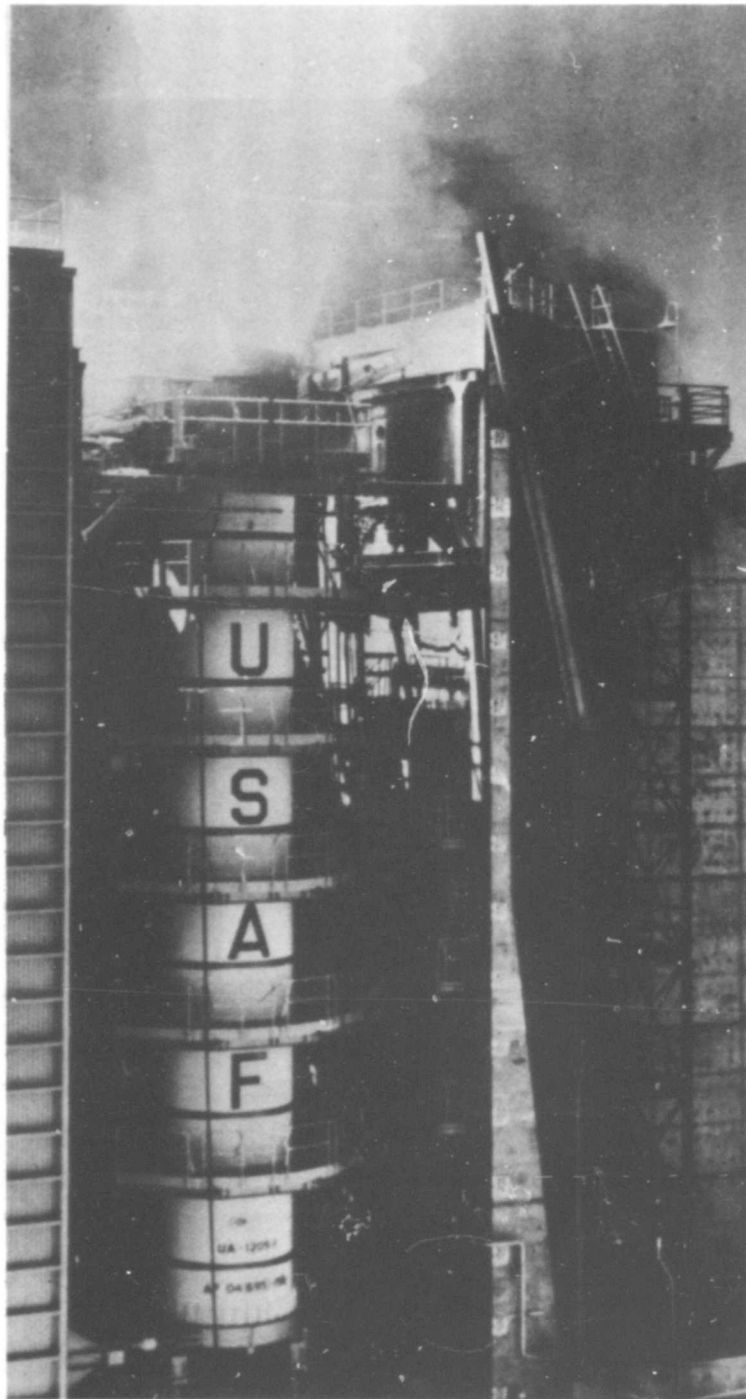
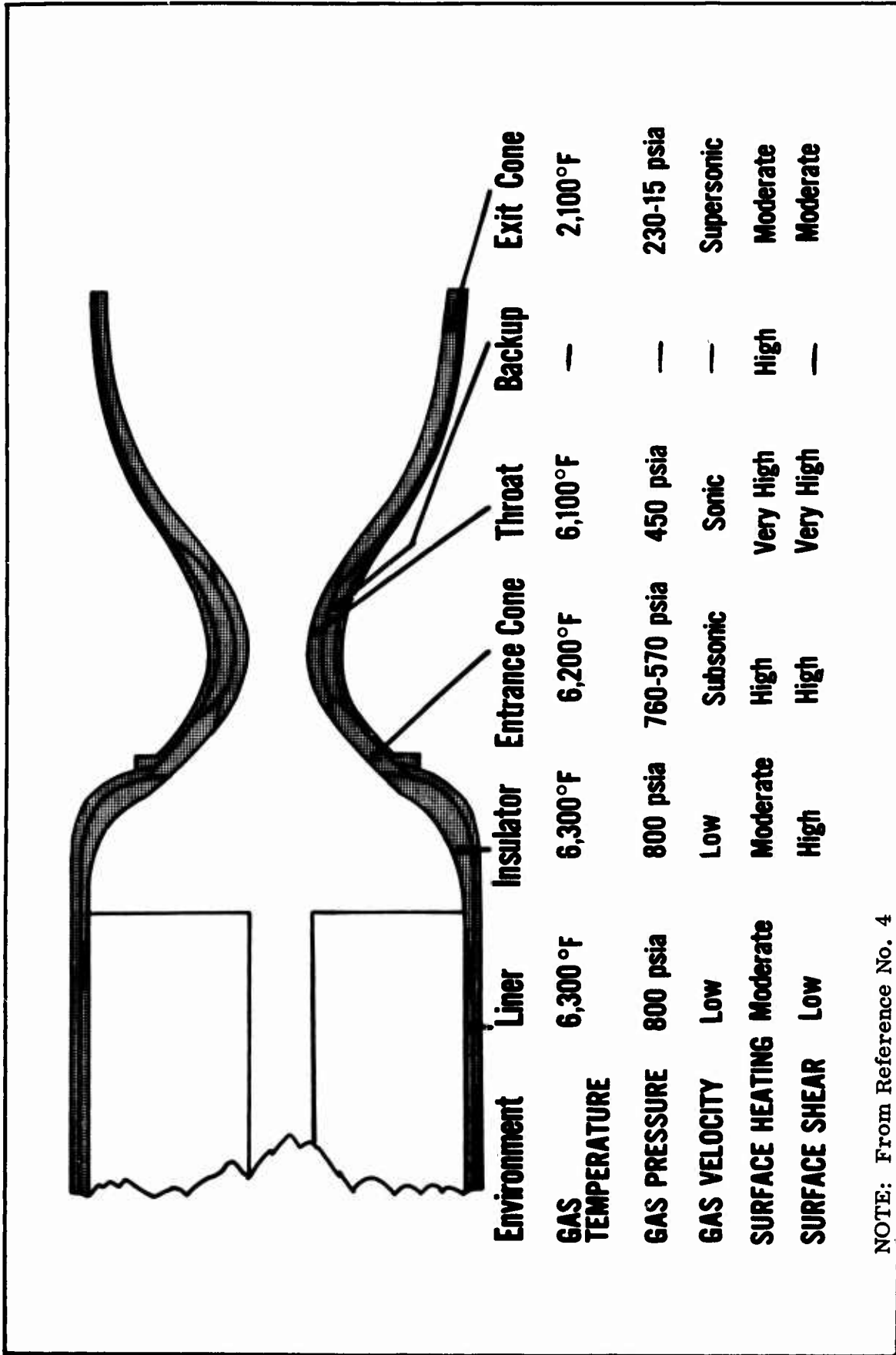
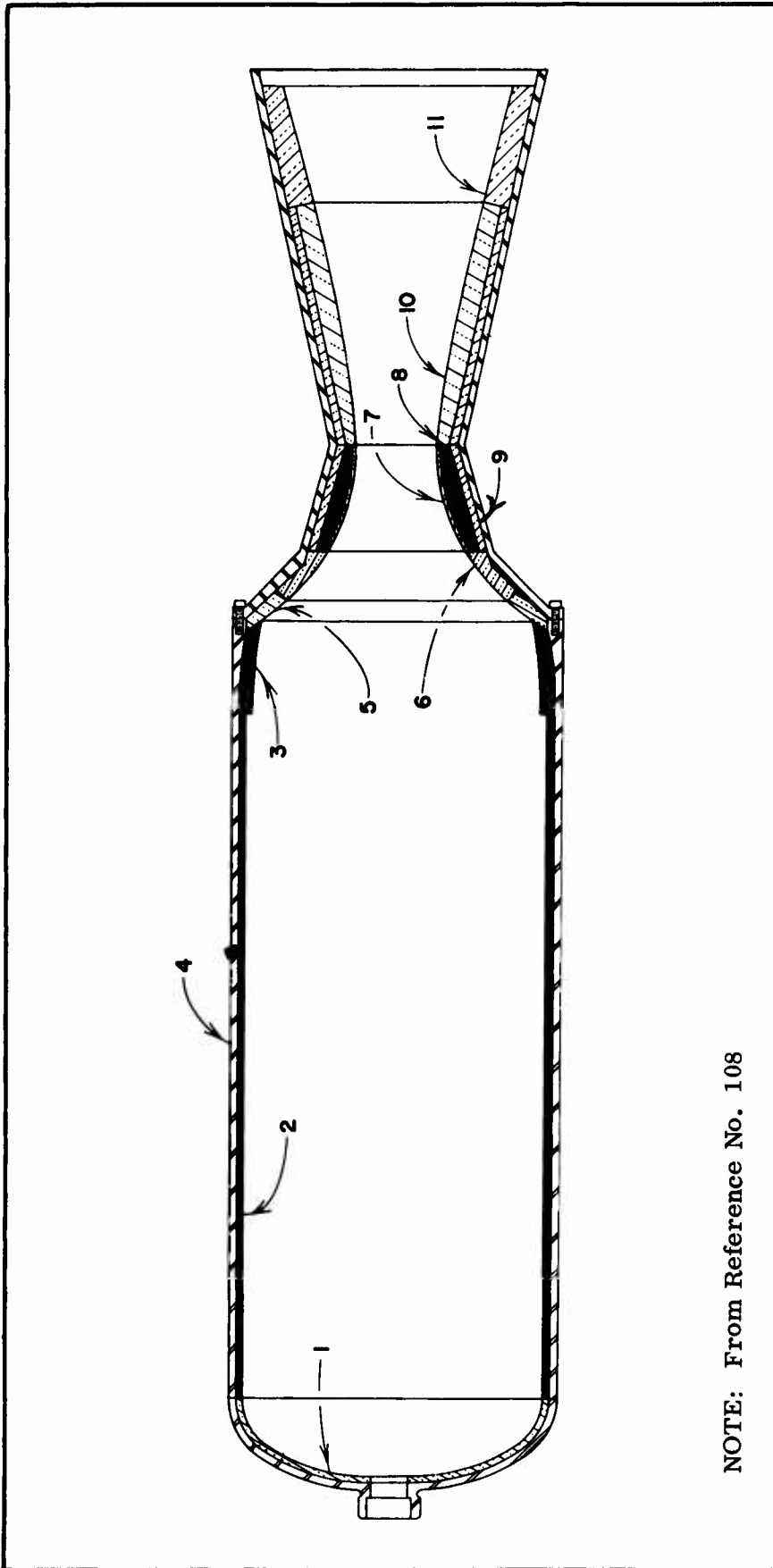


Figure 23. Five Segment, 120-inch Diameter, Megapound Thrust Solid Propellant Motor During Test Firing



NOTE: From Reference No. 4

Figure 24. Environmental Parameters of an Advanced Solid Propellant Motor



NOTE: From Reference No. 108

Figure 25. Schematic of a Solid Propellant Motor

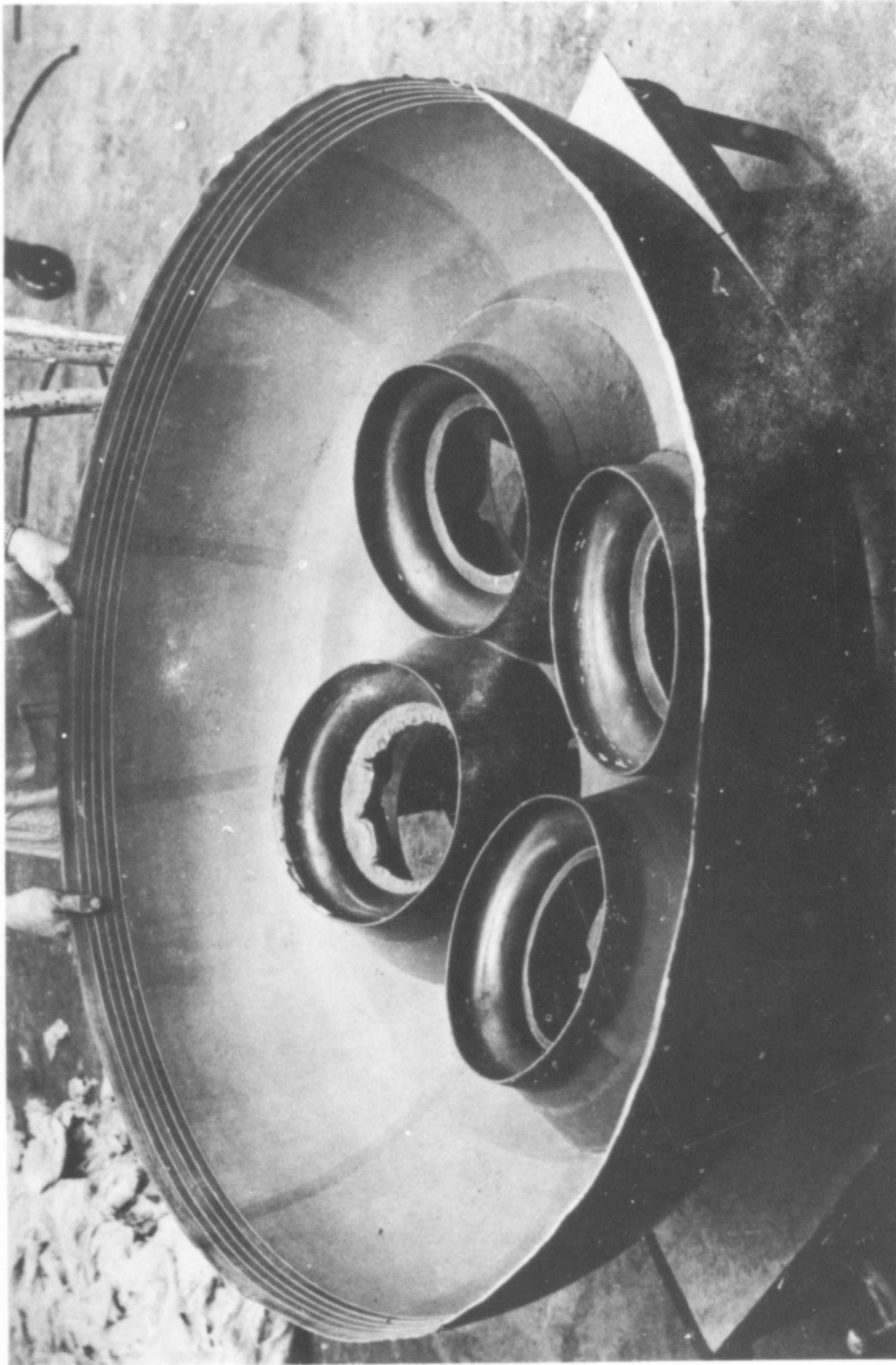


Figure 26. Elastomeric Aft Bulkhead Insulator for a Multiple Nozzle Solid Propellant Motor



Figure 27. A Phenolic-Asbestos Fiber Insulative Backup for a Graphite Nozzle Throat

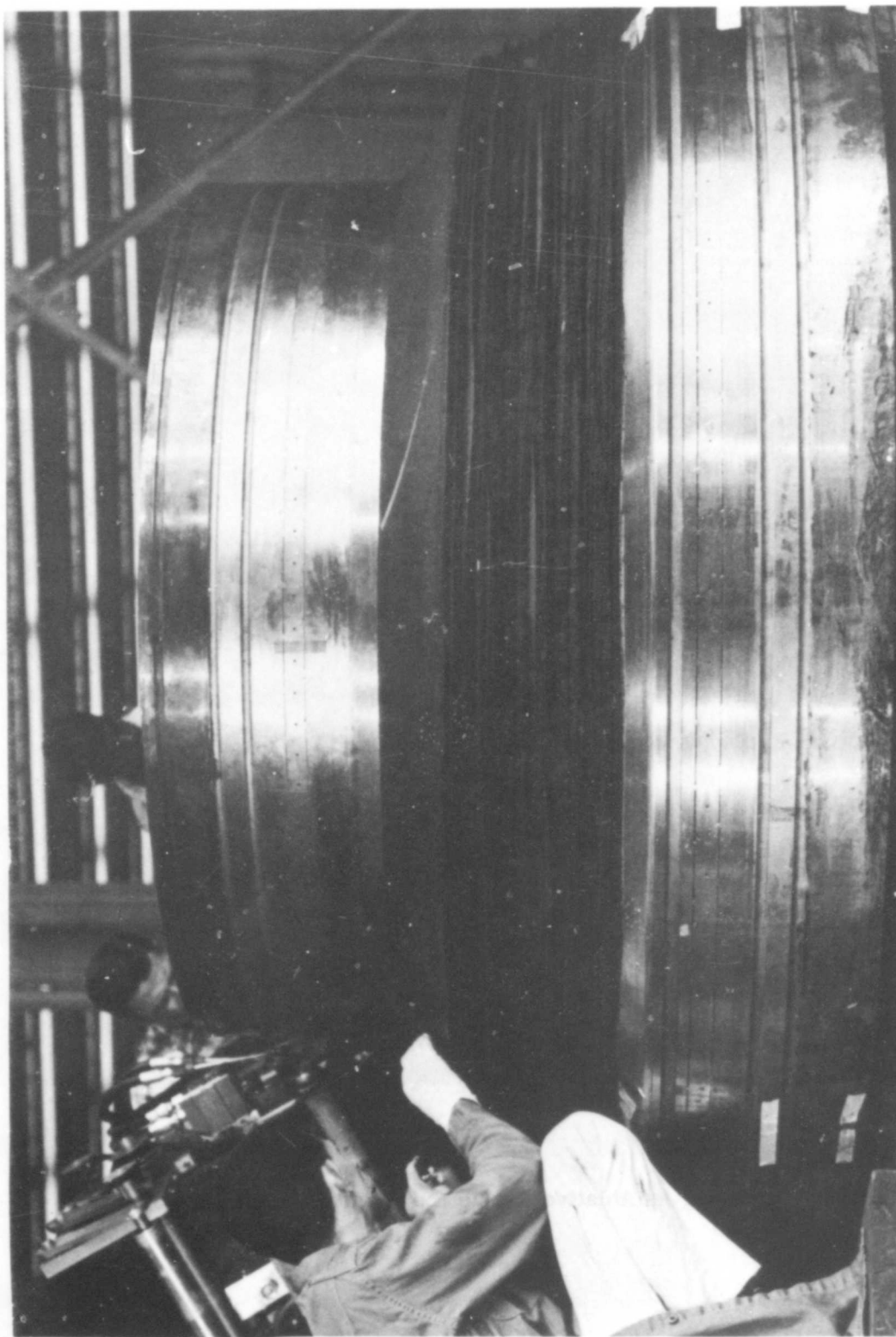


Figure 28. An Ablative Nozzle Throat of Phenolic-Graphite Tape for the 156-inch Diameter Solid Propellant Motor

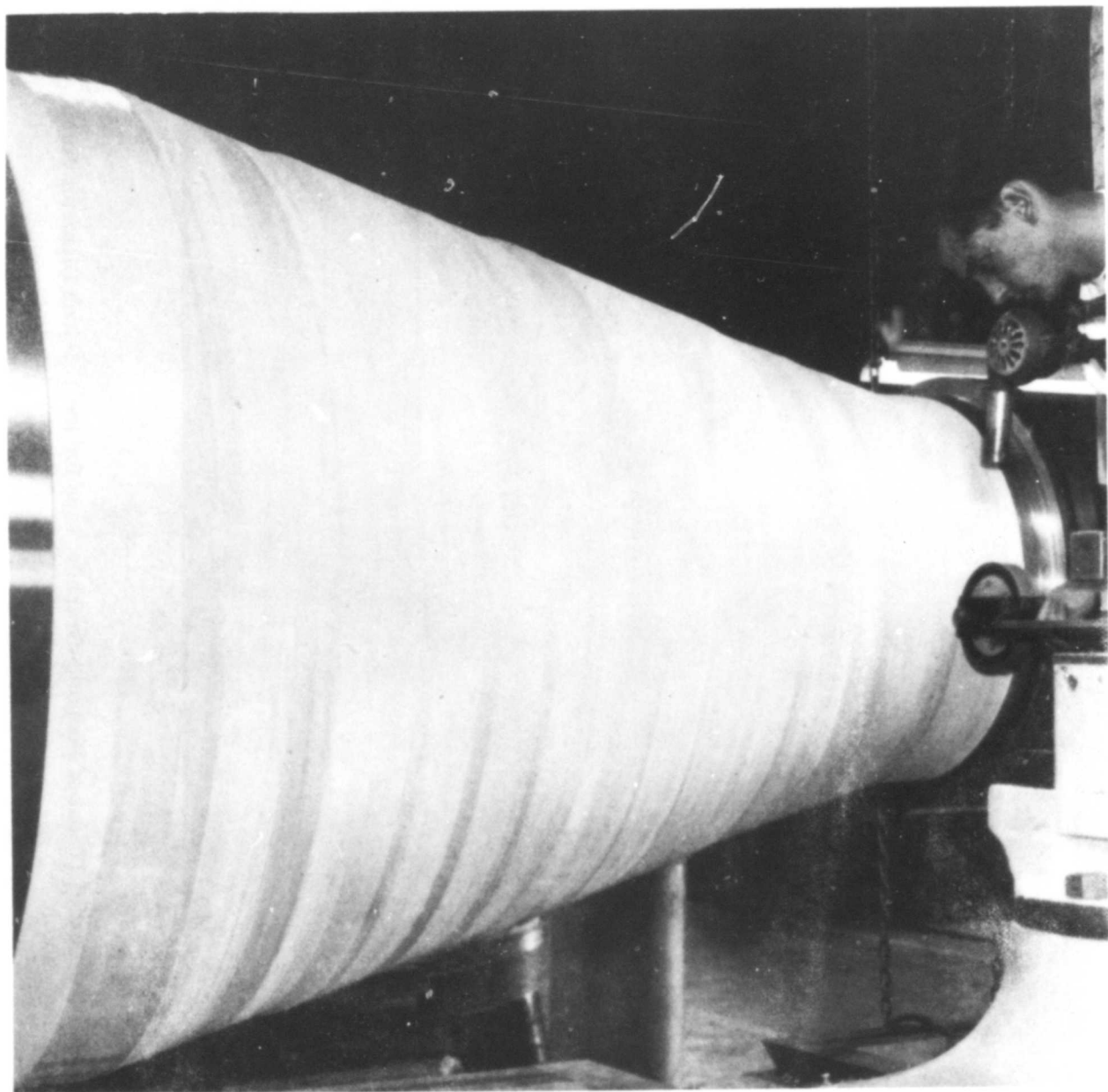


Figure 29. Tape Wrapping An Ablative Nozzle Exit Cone with Phenolic-Silica

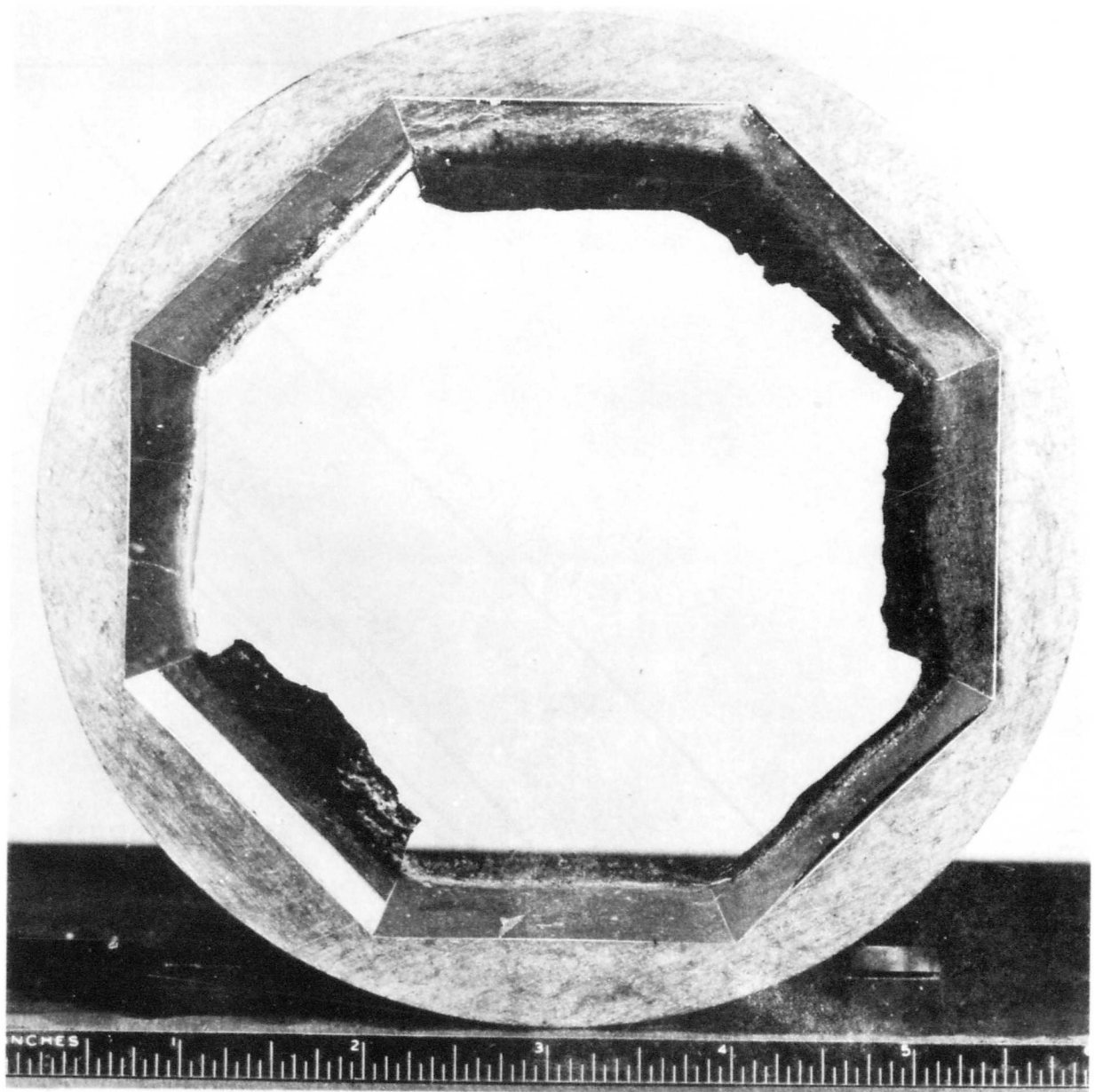
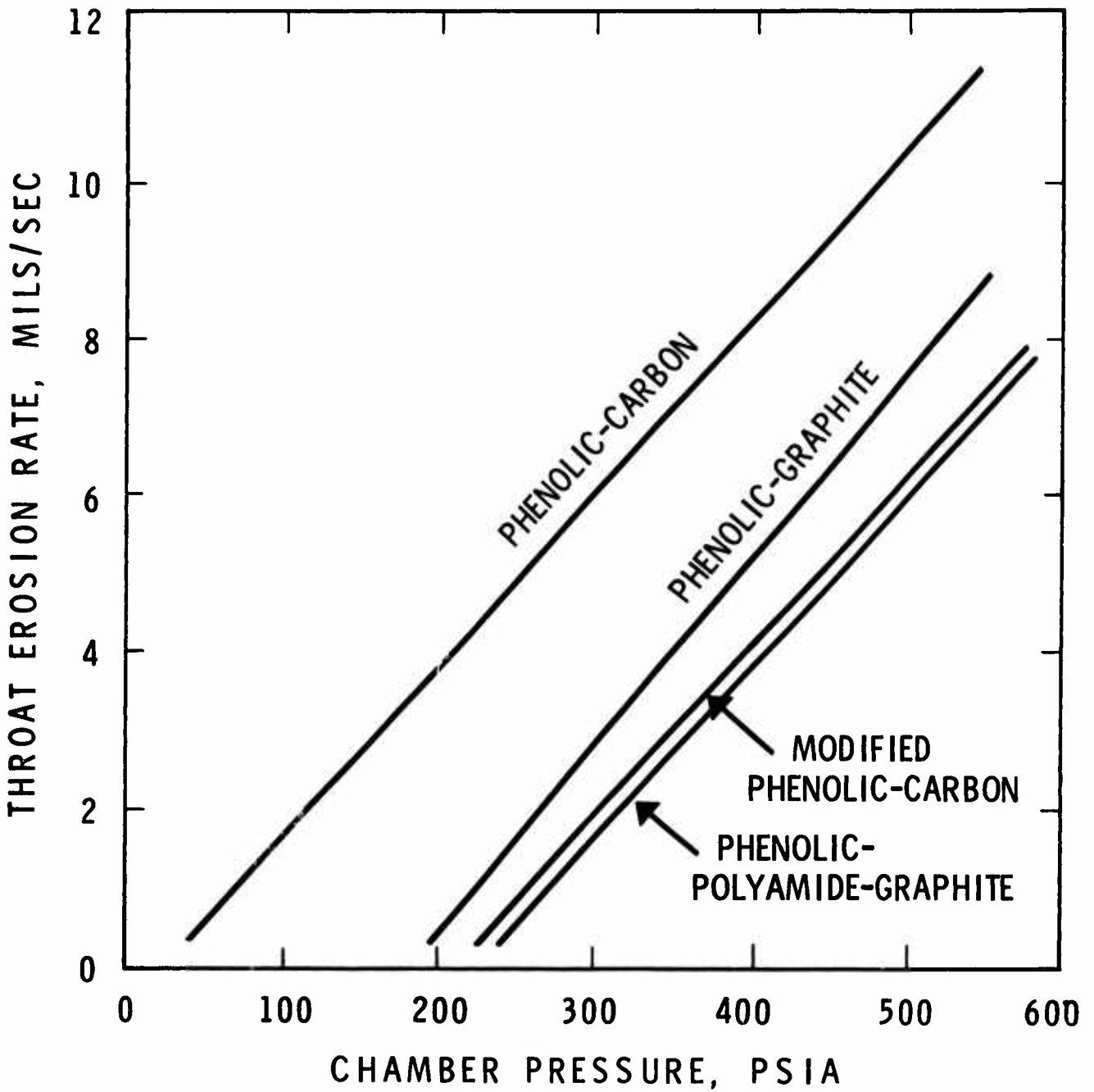


Figure 30. Eight Insulative Test Specimens After Exposure to a Solid Propellant Firing



NOTE: From Reference No. 123

Figure 31. Ablation of Reinforced Plastic Throats in a Solid Propellant Motor

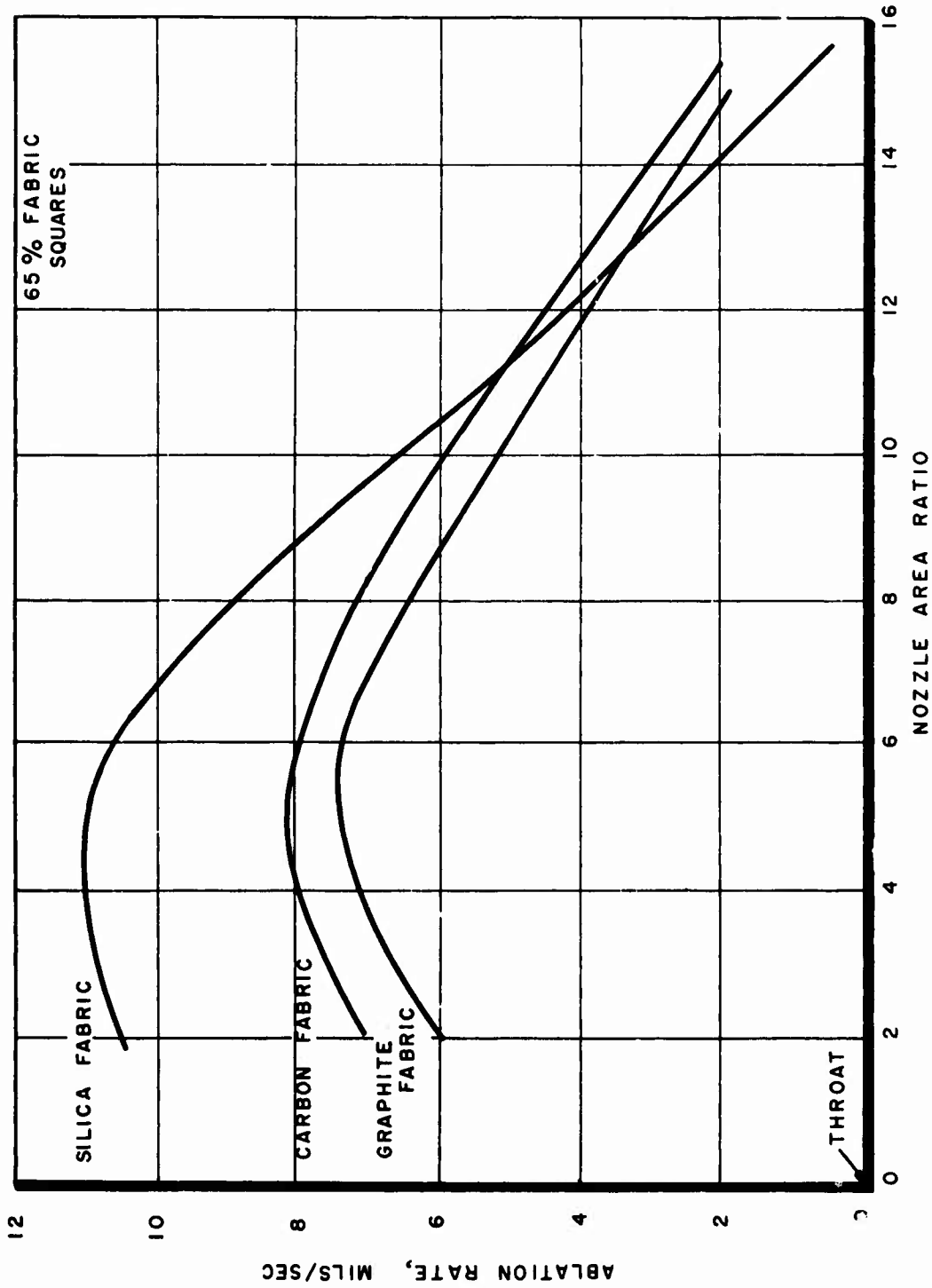
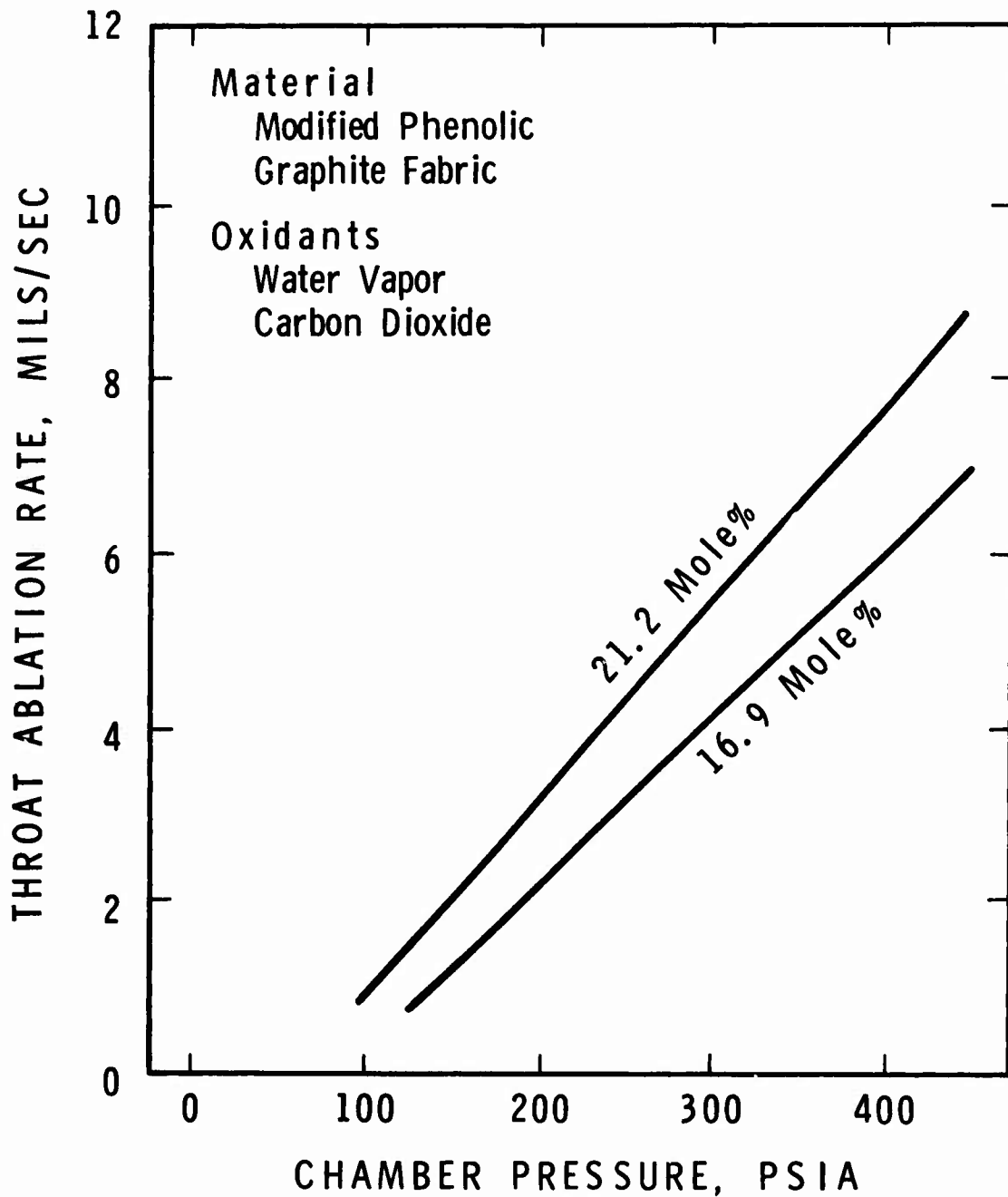


Figure 32. The Ablation Rate of Phenolic Molding Materials as a Function of the Nozzle Exit Cone Position



NOTE: From Reference No. 123

Figure 33. Influence of Exhaust Stream Oxidants on the Ablation Rate of a Charring Ablative Plastic

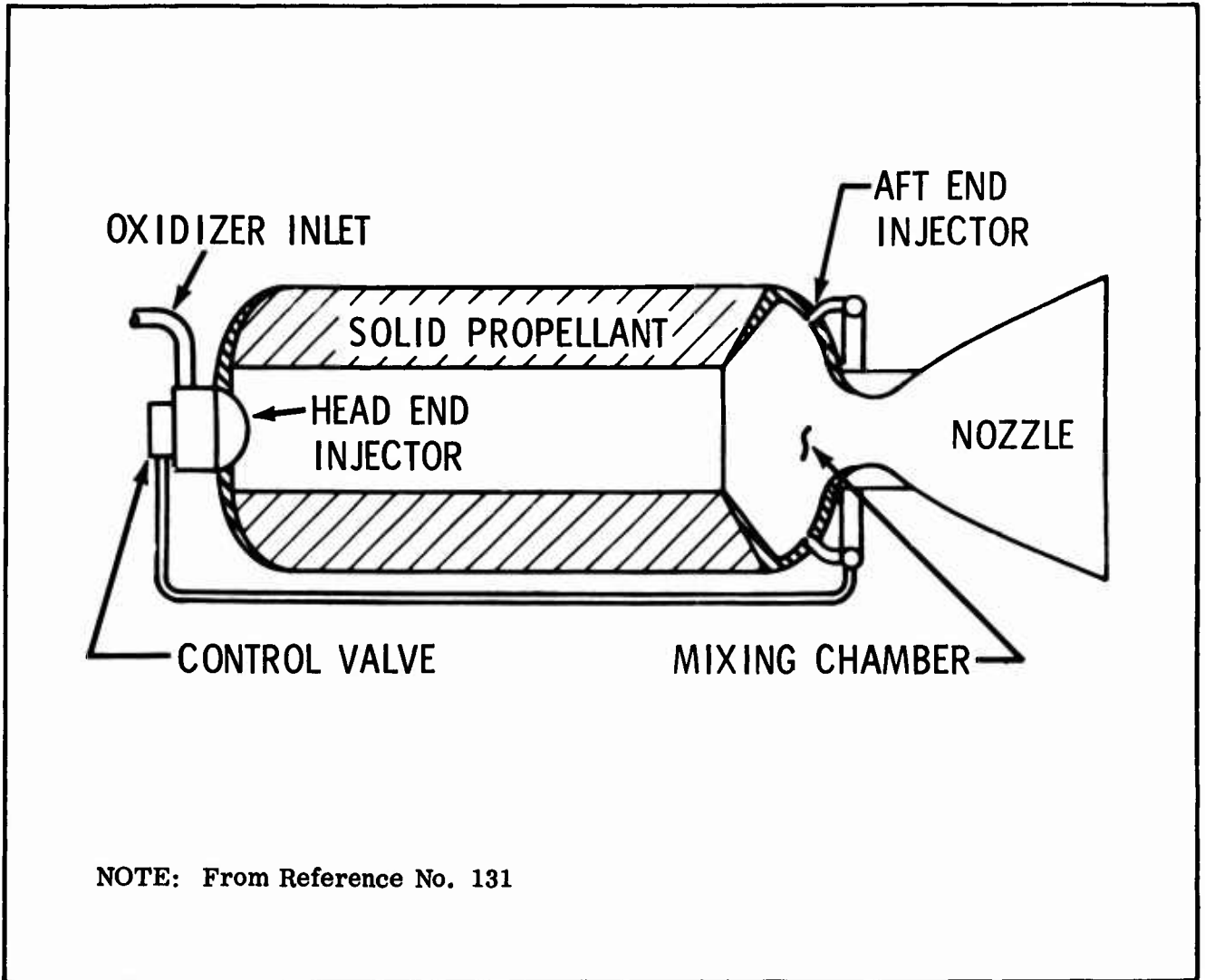


Figure 34. Schematic of a Hybrid Rocket Motor

Unclassified

Security Classification

DOCUMENT CONTROL DATA - R&D

(Security classification of title, body of abstract and indexing annotation must be entered when the overall report is classified)

1. ORIGINATING ACTIVITY <i>(Corporate author)</i> Plastics and Composites Branch Nonmetallic Materials Division Air Force Materials Laboratory		2a. REPORT SECURITY CLASSIFICATION Unclassified	
		2b. GROUP	
3. REPORT TITLE Ablative Plastics and Elastomers in Chemical Propulsion Environments			
4. DESCRIPTIVE NOTES <i>(Type of report and inclusive dates)</i> Summary report			
5. AUTHOR(S) <i>(Last name, first name, initial)</i> Schmidt, D. L.			
6. REPORT DATE		7a. TOTAL NO. OF PAGES 126	7b. NO. OF REFS 137
8a. CONTRACT OR GRANT NO.		9a. ORIGINATOR'S REPORT NUMBER(S) AFML-TR-65-4	
b. PROJECT NO. 7340			
c. Task No. 734001		9b. OTHER REPORT NO(S) <i>(Any other numbers that may be assigned this report)</i>	
d.			
10. AVAILABILITY/LIMITATION NOTICES Qualified requesters may obtain copies of this report from DDC. This report contains comparative data on different manufacturers' specifically named materials.			
11. SUPPLEMENTARY NOTES		12. SPONSORING MILITARY ACTIVITY Research and Technology Division Air Force Systems Command Wright-Patterson Air Force Base, Ohio	
13. ABSTRACT : Ablative plastics and elastomers have been used successfully in a variety of primary and secondary liquid propellant engines. The ablators have provided a minimum-weight design when the engine thrust levels were low to moderately high (up to 20,000 pounds), firing times were short to relatively long (up to 2,000 sec), chamber pressures were low (several hundred psia or less), or when the engine involved throttling, restarting, multiple pulses, or low propellant flow rates. The attractiveness of ablators for cooling tends to decrease with a nonoptimum propellant injector, high gasdynamic shear forces, or extremely corrosive combustion products. Ablative organics have scored even more impressive gains in the thermal protection of solid and hybrid propellant motors. Virtually the entire motor contains ablative polymers in one form or another, including the propellant case, head-end insulator, case liner, entrance cone, nozzle, exit cone, external insulator, propellant grain supports, igniter basket, and jet vanes, as well as the ground launch equipment which is immersed in the hot exhaust for several seconds. The interaction of propellant combustion products with plastics and elastomers results in thermal, chemical, and mechanical degradation of surface material. Thermal effects are due to the temperature level of the energetic combustion process. They are generally discernible as pyrolysis, gasification, vaporization, sublimation, melting, and thermal stress failure. The chemical corrosive effects are a function of the chemical composition, reactant concentrations and the temperature level of the exhaust species coming in contact with the ablating material surfaces. They usually result in increased surface vaporization or fluxing (lowered viscosity) of melted components. Mechanical effects involve gasdynamic shear erosion, particle impact, and material spallation. Results are well-documented herein			

DD FORM 1 JAN 64 1473

Unclassified

Security Classification

14. KEY WORDS	LINK A		LINK B		LINK C	
	ROLE	WT	ROLE	WT	ROLE	WT
Ablation, Thermal Protection Ablative Resins, Ablative Composites, Propulsion Heating Plastics						

INSTRUCTIONS

1. ORIGINATING ACTIVITY: Enter the name and address of the contractor, subcontractor, grantee, Department of Defense activity or other organization (*corporate author*) issuing the report.

2a. REPORT SECURITY CLASSIFICATION: Enter the overall security classification of the report. Indicate whether "Restricted Data" is included. Marking is to be in accordance with appropriate security regulations.

2b. GROUP: Automatic downgrading is specified in DoD Directive 5200.10 and Armed Forces Industrial Manual. Enter the group number. Also, when applicable, show that optional markings have been used for Group 3 and Group 4 as authorized.

3. REPORT TITLE: Enter the complete report title in all capital letters. Titles in all cases should be unclassified. If a meaningful title cannot be selected without classification, show title classification in all capitals in parenthesis immediately following the title.

4. DESCRIPTIVE NOTES: If appropriate, enter the type of report, e.g., interim, progress, summary, annual, or final. Give the inclusive dates when a specific reporting period is covered.

5. AUTHOR(S): Enter the name(s) of author(s) as shown on or in the report. Enter last name, first name, middle initial. If military, show rank and branch of service. The name of the principal author is an absolute minimum requirement.

6. REPORT DATE: Enter the date of the report as day, month, year, or month, year. If more than one date appears on the report, use date of publication.

7a. TOTAL NUMBER OF PAGES: The total page count should follow normal pagination procedures, i.e., enter the number of pages containing information.

7b. NUMBER OF REFERENCES: Enter the total number of references cited in the report.

8a. CONTRACT OR GRANT NUMBER: If appropriate, enter the applicable number of the contract or grant under which the report was written.

8b, 8c, & 8d. PROJECT NUMBER: Enter the appropriate military department identification, such as project number, subproject number, system numbers, task number, etc.

9a. ORIGINATOR'S REPORT NUMBER(S): Enter the official report number by which the document will be identified and controlled by the originating activity. This number must be unique to this report.

9b. OTHER REPORT NUMBER(S): If the report has been assigned any other report numbers (*either by the originator or by the sponsor*), also enter this number(s).

10. AVAILABILITY/LIMITATION NOTICES: Enter any limitations on further dissemination of the report, other than those

imposed by security classification, using standard statements such as:

- (1) "Qualified requesters may obtain copies of this report from DDC."
- (2) "Foreign announcement and dissemination of this report by DDC is not authorized."
- (3) "U. S. Government agencies may obtain copies of this report directly from DDC. Other qualified DDC users shall request through _____."
- (4) "U. S. military agencies may obtain copies of this report directly from DDC. Other qualified users shall request through _____."
- (5) "All distribution of this report is controlled. Qualified DDC users shall request through _____."

If the report has been furnished to the Office of Technical Services, Department of Commerce, for sale to the public, indicate this fact and enter the price, if known.

11. SUPPLEMENTARY NOTES: Use for additional explanatory notes.

12. SPONSORING MILITARY ACTIVITY: Enter the name of the departmental project office or laboratory sponsoring (*paying for*) the research and development. Include address.

13. ABSTRACT: Enter an abstract giving a brief and factual summary of the document indicative of the report, even though it may also appear elsewhere in the body of the technical report. If additional space is required, a continuation sheet shall be attached.

It is highly desirable that the abstract of classified reports be unclassified. Each paragraph of the abstract shall end with an indication of the military security classification of the information in the paragraph, represented as (TS), (S), (C), or (U).

There is no limitation on the length of the abstract. However, the suggested length is from 150 to 225 words.

14. KEY WORDS: Key words are technically meaningful terms or short phrases that characterize a report and may be used as index entries for cataloging the report. Key words must be selected so that no security classification is required. Identifiers, such as equipment model designation, trade name, military project code name, geographic location, may be used as key words but will be followed by an indication of technical context. The assignment of links, rules, and weights is optional.